# Hypercapnia impairs ENaC cell surface expression and function by promoting phosphorylation and polyubiquitination of ENaC β-subunit in alveolar epithelial cells

Inaugural Dissertation
submitted to the
Faculty of Medicine
in partial fulfillment of the requirements
for the PhD-Degree
of the Faculties of Veterinary Medicine and Medicine
of the Justus Liebig University Giessen

by
Gwozdzinska, Paulina
of
Lodz, Poland

Giessen 2018

From the Institute of Department of Internal Medicine II
Director: Prof. Dr. Werner Seeger
of the Faculty of Medicine of the Justus Liebig University Giessen

| | |
|---|---|
| First Supervisor and Committee Member: | Prof. Dr. Werner Seeger |
| Second Supervisor and Committee Member: | Prof. Dr. Martin Diener |
| Committee Members: | Prof. Dr. Christine Wrenzycki |
| | Prof. Dr. Wolfgang M. Kübler |

Date of Doctoral Defense: 19.06.2018

## Table of contents

**Abstract**

An elevation of $CO_2$ concentration in the blood (hypercapnia) may occur as a result of poor alveolar gas exchange and is frequently detected in patients with respiratory diseases including those with acute respiratory distress syndrome (ARDS). Hypercapnia may be further exacerbated as a consequence of lung-protective mechanical ventilation with low tidal volumes, which is necessary in patients with ARDS. The vectorial $Na^+$ transport across the alveolar epithelium mediated by the epithelial $Na^+$ channel (ENaC) and the Na,K-ATPase provides the driving force for alveolar fluid clearance (AFC). Persistent alveolar edema is a hallmark of ARDS and can be attributed in part to impaired $Na^+$ and fluid reabsorption, which leads to worse outcomes. Thus, the effects of hypercapnia on ENaC function in the alveolar epithelium and understanding of the signaling pathways that may via downregulation of ENaC impair edema clearance in hypercapnic patients with ARDS are of high clinical relevance.

The current work describes the molecular mechanisms by which hypercapnia reduces cell surface expression of ENaC in alveolar epithelial cells (AECs) and thus impairs ENaC-driven transepithelial $Na^+$ transport. We found that acute hypercapnia independently of pH ($pCO_2$ ~120 mmHg, pH 7.4 for 30 min) led to polyubiquitination of β-ENaC and subsequent endocytosis of the α/β-ENaC complex from the cell surface of primary rat ATII and human alveolar epithelial A549 cells, as assessed by cell surface biotinylation and fluorescent microscopy. In contrast, hypercapnia altered neither mRNA nor intracellular levels of ENaC proteins, indicating that acutely elevated $CO_2$ levels affect the trafficking of the channel rather than its transcription or degradation. Furthermore, our data established that hypercapnia by decreasing ENaC cell surface expression reduced both total ($I_{sc}$) and amiloride-sensitive ($I_{amil\text{-}sens}$) $Na^+$ current in H441 human airway epithelial cells. Moreover, the hypercapnia-induced increase in polyubiquitination of β-ENaC and endocytosis of the α/β-ENaC complex were prevented by silencing the E3 ubiquitin ligase, Nedd4-2. Co-immunoprecipitation studies confirmed the direct interaction of Nedd4-2 with the β-subunit of ENaC. Most importantly, the $CO_2$-induced β-ENaC ubiquitination and α/β-ENaC retrieval from the cell surface were strongly dependent on the extracellular signal regulated kinase (ERK)1/2 that directly phosphorylated β-ENaC at the T615 residue. In line with these findings, transfection of A549 cells with a β-ENaC mutant lacking T615, normalized cell surface density of α/β-ENaC upon hypercapnic exposure. Activation of ERK1/2 caused subsequent activation of AMP-activated

protein kinase (AMPK) and c-Jun N-terminal kinase (JNK)1/2 that in turn phosphorylated Nedd4-2 at the T899 residue. Replacement of the T899 residue by an alanine (T899A), which prevented JNK-mediated phosphorylation of Nedd4-2 significantly inhibited polyubiquitination of β-ENaC and improved cell surface expression of the α/β-ENaC complex upon $CO_2$ treatment. Similarly, pharmacological inhibition of JNK rescued the abundance of ENaC at the cell surface upon hypercapnia. Additionally, chemical inhibition or genetic ablation of AMPK prevented the hypercapnia-induced β-ENaC polyubiquitination and internalization of the α/β-ENaC complex. A comparable reduction of ENaC endocytosis upon hypercapnia treatment was observed when an upstream kinase of AMPK, the $Ca^{2+}$/calmodulin-dependent protein kinase kinase-β (CaMKK-β) was inhibited, confirming that the activation of AMPK was required for ENaC downregulation during acute hypercapnia. Thus, we describe a novel $CO_2$-induced signaling pattern in alveolar epithelial cells, which by activation of the ERK/AMPK/JNK axis impairs cell surface expression and function of ENaC via promoting ubiquitination of β-ENaC and driving subsequent internalization of the channel. This signaling cascade may further impair alveolar fluid balance therefore leading to worse outcomes in patients with ARDS and thus also represent a potentially targetable pathway that might lead to discovery of novel therapies against alveolar edema in patients with hypercapnic respiratory failure.

## Zusammenfassung

Ein verminderter alveolärer Gasaustausch, welcher häufig bei Patienten mit Atemwegserkrankungen auftritt, einschließlich solchen mit einem akuten Lungenversagen (auch bekannt als acute respiratotry distress syndrome (ARDS)) führt oft zu einer Erhöhung der $CO_2$ Konzentration im Blut (Hyperkapnie). Hyperkapnie kann als Folge einer lungenschonenden Beatmung mit niedrigen Tidalvolumina, die bei Patienten mit ARDS notwendig ist, exazerbiert werden. Der vektorielle $Na^+$-Transport über das Alveolarepithel, der durch den epithelialen $Na^+$-Kanal (ENaC) und die Na,K-ATPase vermittelt wird, liefert die treibende Kraft für die Alveolarfluid-Clearance (AFC). Das persistierende alveoläre Ödem ist ein typisches Merkmal des ARDS und kann teilweise auf eine gestörte $Na^+$ und Flüssigkeitsreabsorption zurückgeführt werden, was mit einem schlechteren Outcome assoziiert ist. Daher sind die Auswirkungen von Hyperkapnie auf die alveolarepitheliale ENaC-Funktion und die Identifikation der Signalwege, die durch eine Herunterregulierung von ENaC die Ödem-Clearance bei hyperkapnischen Patienten mit ARDS beeinträchtigen können, von hoher klinischer Relevanz.

Die vorliegende Arbeit beschreibt die molekularen Mechanismen, durch die Hyperkapnie die Expression von ENaC auf der Zelloberfläche in Alveolarepithelzellen (AECs) reduziert und somit den ENaC-getriebenen transepithelialen $Na^+$-Transport beeinträchtigt. Wir beschreiben, dass eine akute Hyperkapnie, unabhängig vom pH-Wert ($pCO_2$ ~ 120 mmHg, pH 7,4 für 30 min), zur Polyubiquitinierung des β-ENaC und anschließender Endozytose des α/β-ENaC-Komplexes von der Zelloberfläche von primären Ratten-ATII- und menschlichen A549 Alveolarepithelzellen führte, wie durch Zelloberflächen-Biotinylierung und Fluoreszenzmikroskopie bestimmt wurde. Im Gegensatz dazu veränderte Hyperkapnie weder die mRNA noch die intrazellulären Konzentrationen von ENaC-Proteinen, was darauf hindeutet, dass akut erhöhte $CO_2$-Werte eher der zellulären Lokalisation des Kanals als dessen Transkription oder Abbau beeinflussen. Des Weiteren zeigten unsere Daten, dass Hyperkapnie durch Verringerung der ENaC-Zelloberflächenexpression sowohl den gesamten ($I_{sc}$) als auch den amilorid-sensitiven ($I_{amil\text{-}sens}$) $Na^+$-Strom in humanen H441 Atemwegsepithelzellen reduziert. Ferner führte Hyperkapnie zu einer Polyubiquitinierung des β-ENaC und der Endozytose des α/β-ENaC-Komplexes, welches durch eine genetische Ablation der E3-Ubiquitin-Ligase, Nedd4-2, gehemmt werden konnte. Co-Immunpräzipitationsstudien bestätigten die direkte Interaktion von Nedd4-2 mit der β-Untereinheit

von ENaC. Vordergründig war, dass die $CO_2$-induzierte β-ENaC-Ubiquitinierung und die Endozytose des α/β-ENaC von der Zelloberfläche stark von der extrazellulären Signal-regulierten Kinase (ERK)1/2, welche β-ENaC direkt am T615 phosphoryliert, abhängig waren. Im Einklang mit diesen Erkenntnissen, normalisierte die Transfektion von A549-Zellen mit einer β-ENaC-Mutante, mit fehlendem T615, die Zelloberflächendichte von α/β-ENaC bei hyperkapnischer Exposition. Die Aktivierung von ERK1/2 führte zu einer nachfolgenden Aktivierung der AMP-aktivierten Proteinkinase (AMPK) und c-Jun-N-terminalen Kinase (JNK)1/2, die wiederum Nedd4-2 am T899 phosphorylierte. Der Ersatz des T899 durch ein Alanin (T899A), das die JNK-vermittelte Phosphorylierung von Nedd4-2 verhinderte, inhibierte signifikant die Polyubiquitinierung von β-ENaC und erhöhte die Zelloberflächenexpression des α/β-ENaC-Komplexes bei der $CO_2$-Behandlung. Die pharmakologische Hemmung von JNK führte ebenso zur ENaC-Stabilisierung auf der Zelloberfläche nach Hyperkapnie. Zusätzlich verhinderte die chemische Inhibierung oder die genetische Ablation von AMPK die, durch Hyperkapnie induzierte, β-ENaC-Polyubiquitinierung und Internalisierung des α/β-ENaC-Komplexes. Eine vergleichbare Reduktion der ENaC-Endozytose nach Behandlung mit Hyperkapnie wurde beobachtet, wenn eine Upstream-gelegene Kinase von AMPK, die $Ca^{2+}$/Calmodulin-abhängige Proteinkinase-β (CaMKK-β), inhibiert wurde. Dies bestätigt, dass die Aktivierung von AMPK benötigt wurde, um ENaC während einer akuten Hyperkapnie herunterzuregulieren. Folglich beschreiben wir ein neuartiges $CO_2$-induziertes Signalmuster in Alveolarepithelzellen, das durch Aktivierung der ERK/AM/JNK-Achse die Expression und Funktion von ENaC auf der Zelloberfläche beeinflusst, indem es die Ubiquitinierung von β-ENaC fördert und die anschließende Internalisierung des Kanals vorantreibt. Diese Signalkaskade kann den alveolären Flüssigkeitshaushalt weiter beeinträchtigen und somit zu schlechteren Outcomes bei Patienten mit ARDS führen und einen potenziell adressierbaren Signalweg darstellen, der zur Entdeckung neuer Therapien gegen Alveolarödem bei Patienten mit hyperkapnischem respiratorischem Versagen führen könnte.

## Abbreviations

| | |
|---|---|
| A | Alanine |
| A549 | Human adenocarcinoma alveolar epithelial cell |
| A6 | *Xenopus laevis* kidney cell |
| AEC | Alveolar epithelial cell |
| AECC | American-European consensus conference |
| AFC | Alveolar fluid clearance |
| ALF | Alveolar lining fluid |
| ALI | Acute lung injury |
| ALTA | Albuterol to Treat Acute Lung Injury |
| AMP | Adenosine monophosphate |
| AMPK | AMP-activated protein kinase |
| AQP5 | Aquaporin 5 |
| AP-2 | Adaptor protein 2 |
| ARDS | Acute respiratory distress syndrome |
| ATI | Alveolar epithelial type I cell |
| ATII | Alveolar epithelial type II cell |
| BSA | Bovine serum albumin |
| C2 | Calcium binding domain of Nedd4-2 |
| $Ca^{2+}$ | Calcium ion |
| Calu-3 | Human airway epithelial cell line |
| CAP | Channel activating protease |
| CaMKK-β | $Ca^{2+}$/calmodulin-dependent kinase kinase β |
| cAMP | Cyclic adenosine monophosphate |
| cDNA | Complementary deoxyribonucleic acid |
| CF | Cystic fibrosis |
| CFTR | Cystic fibrosis transmembrane conductance regulator |
| CHO | Chinese hamster ovary cell |
| CNG | Cyclic nucleotide gated channel |
| $CO_2$ | Carbon dioxide |

| | |
|---|---|
| Co-IP | Co-immunoprecipitation |
| COOH | C-terminus of protein with free carboxyl group |
| COPD | Chronic obstructive pulmonary disease |
| Ctrl | Control |
| DAPI | 4',6-diamidino-2-phenylindole |
| Deg | Degenerin |
| DMEM | Dulbecco's modified Eagle's medium |
| DMSO | Dimethyl sulfoxide |
| DNA | Deoxyribonucleic acid |
| DTT | Dithiothreitol |
| DUB | Deubiquitinating enzyme |
| E1 | Ubiquitin-activating enzyme |
| E2 | Ubiquitin-conjugating enzyme |
| E3 | Ubiquitin ligase |
| E. coli | Escherichia coli |
| EGF | Epithermal growth factor |
| ENaC | Epithelial sodium channel |
| ER | Endoplasmic reticulum |
| ERK | Extracellular signal-regulated kinase |
| FBS | Fetal bovine serum |
| $FiO_2$ | Fraction of inspired oxygen |
| GAPDH | Glyceraldehyde 3-phosphate dehydrogenase |
| GFP | Green fluorescence protein |
| GILZ1 | Glucocorticoid-induced leucine zipper protein-1 |
| h | Hour |
| H441 | Human airway epithelial cell |
| HA | Hemagglutinin |
| HECT | Homologous to the E6-AP carboxyl terminus |
| HRP | Horseradish peroxidase |
| HSC | Highly selective channel |
| $I_{amil\text{-}sens}$ | Amiloride-sensitive current |

| | |
|---|---|
| ICU | Intensive care unit |
| IgG | Immunoglobulin G |
| IL | Interleukin |
| $I_{sc}$ | Short-circuit current |
| ITS | Insulin-transferrin sodium selenite |
| JNK | c-Jun N-terminal kinase |
| kb | Kilo base |
| KGF | Keratinocyte growth factor |
| $K_{Ca}$ | Calcium-activated potassium channel |
| $K_v$ | Voltage-gated potassium channel |
| LB | Luria-Bertani |
| LPS | Lipopolysaccharide |
| M1, M2 | Transmembrane domains of ENaC |
| MAPK | Mitogen-activated protein kinase |
| MARCKS | Myristoylated alanine-rich C-kinase substrate |
| mCT1 | Murine collecting duct epithelial cells |
| MSC | Mesenchymal stem (stromal) cells |
| MDCK | Madin-Darby canine kidney |
| mmHg | Millimeters of mercury |
| mRNA | Messenger RNA |
| n | Number of independent experiments |
| NCBI | National Center for Biotechnology Information |
| Nedd4-2 | Neural precursor cell expressed developmentally down-regulated protein 4-2 |
| $NH_2$ | N- terminus of the protein with free amine group |
| Na,K-ATPase | Sodium-potassium adenosine triphosphatase |
| NO | Nitric oxide |
| ns | Not significant |
| NSC | Non-selective channel |
| $PaO_2$ | Arterial partial pressure of oxygen |
| PBS | Phosphate-buffered saline |
| PCR | Polymerase chain reaction |

| | |
|---|---|
| PEEP | Positive end-expiratory pressure |
| $pH_e$ | Extracellular pH |
| $pH_i$ | Intracellular pH |
| PHA | Pseudohypoaldosteronism |
| PIP2 | Phosphatidylinositol biphosphate |
| PKA | Protein kinase A |
| PKC | Protein kinase C |
| $P_o$ | Open probability |
| PM | Plasma membrane |
| PY | PPPXY, P-proline, X-any amino acid and Y-tyrosine |
| RNA | Ribonucleic acid |
| ROS | Reactive oxygen species |
| RPMI 1640 | Roswell Park Memorial Institute 1640 medium |
| rpm | Rounds per minute |
| rtPCR | Reverse transcription polymerase chain reaction |
| SCNN1 | Sodium channel non-neuronal 1 |
| SDS-PAGE | Sodium dodecyl sulfate-polyacrylamide gel electrophoresis |
| SEM | Standard error of mean |
| SGK1 | Serum- and glucocorticoid- induced protein kinase-1 |
| siRNA | Small interfering RNA |
| SOC | Medium salt-optimized with carbon (glucose)-medium |
| T | Threonine |
| TEER | Transepithelial electrical resistance |
| TGF-β | Transforming growth factor-β |
| TIP | Lectin-like domain of TNF-α |
| TNF | Tumor necrosis factor |
| TfR | Transferrin receptor |
| T-TBS | Tween 20-tris-buffer saline |
| Ub | Ubiquitin |
| UCH-L3 | Ubiquitin carboxyl-terminal hydrolase isozyme L3 |
| V5 | Epitope tag derived from paramyxovirus of simian virus 5 |

| | |
|---|---|
| VILI | Ventilator-induced lung injury |
| $V_t$ | Tidal volume |
| WNK1 | With no lysine 2 |
| WW | Tryptophan rich domain of Nedd4-2 |
| WT | Wild-type |

# 1. Introduction

## 1.1 Overview of acute respiratory distress syndrome (ARDS)

Acute respiratory distress syndrome (ARDS) remains one of the most common clinical problems encountered in intensive care units (ICU). The syndrome has a high incidence, in the United States approximately 200,000 patients present annually with a lethal outcome in up to 40% of these patients (Rubenfeld and Herridge 2007). Globally, 5.5 millions of patients per year need an ICU admission and mechanical ventilation (Adhikari et al. 2010). ARDS is a life-threatening condition that is associated with formation of pulmonary edema that disturbs gas exchange leading to hypoxemia and impaired carbon dioxide elimination (Matthay and Zemans 2011). Based on the current definition of ARDS, the so called Berlin Definition from 2012, the syndrome is characterized by acute onset of bilateral airspace infiltrates with arterial hypoxemia without left arterial hypertension and can be classified as mild, moderate or severe depending on the extent of hypoxemia (Ranieri et al. 2012). This new definition of ARDS improved and simplified the previous one proposed in 1994 at an American-European consensus conference on ARDS (AECC) (Bernard et al. 1994). The severity of ARDS is classified by the ratio of arterial partial pressure of oxygen ($PaO_2$) to the fraction of inspired oxygen ($FiO_2$). Patients with $PaO_2/FiO_2$ of 300, 200 or ≤ 100 mmHg suffer from mild moderate or severe ARDS, respectively, whereas per definition patients with ARDS require mechanical ventilation with a positive end-expiratory pressure (PEEP) of 5 cm $H_2O$ or higher (Ranieri et al. 2012).

There are numerous clinical conditions that may lead to ARDS, some of which directly affect the lung, such as viral or bacterial pneumonia, aspiration of gastric contents, pulmonary contusions or near-drowning, whereas other noxae are primarily extra-pulmonary including non-pulmonary sepsis, pancreatitis, severe poly-trauma or drug overdose (Ware and Matthay 2001; Ranieri et al. 2012). During ARDS the injured lungs undergo pathogenic changes in three major phases: exudative, proliferative and fibrotic. The destruction of vascular endothelium, epithelium, recruitment and accumulation of neutrophils, macrophages and blood cells in the alveolar compartment together with the presence of alveolar edema are key features of the exudative phase of ARDS. The proliferative stage of ARDS is characterized by pneumocyte hyperplasia and myofibroblast proliferation, whereas collagen deposition and fibroproliferation are hallmarks of the fibrotic phase (Bachofen and Weibel 1982; Meyrick 1986). The injuries of the lung endothelial

and epithelial barriers caused predominantly by neutrophil- and platelet-dependent damage are detected in ARDS patients however, an endothelial injury *per se* is not sufficient to cause ARDS. Early studies in sheep clearly demonstrated that alveolar fluid clearance (AFC) remained normal in the presence of lung vascular permeability enhancement as long as the alveolar epithelial barrier was intact. In contrast, when live bacteria impaired the integrity of the epithelium, AFC markedly decreased (Wiener-Kronish et al. 1991). This study established that persistence of excess fluid in the alveolar space occurs only when endothelial injuries are accompanied by an impairment of epithelial barrier function. These data are in line with the notion that lung biopsies from patients with ARDS show diffuse alveolar epithelial and endothelial damage (Bachofen and Weibel 1977).

The mechanisms of epithelial and endothelial damage during ARDS are complex and dependent on the cause of ARDS. Several studies suggested that active neutrophils by secreting toxic mediators such as proteases or reactive oxygen species (ROS) may cause disruption of cell junctions and death of alveolar epithelial and endothelial cells leading to accumulation of protein-rich alveolar edema (Herold et al. 2013). Integrity of the alveolar-capillary barrier function is crucial to prevent alveolar flooding but also to actively remove excess alveolar liquid thus allowing optimal gas exchange. In contrast, impairment of epithelial barrier integrity leads to formation and persistence of alveolar edema, which are the hallmarks of ARDS (Bachofen and Weibel 1977).

Currently, there is a lack of effective pharmacological therapies for patients with ARDS. While various agents showed promise in preclinical trials, unfortunately so far these have not translated into therapeutic modalities in the clinical setting. For example, inhaled synthetic surfactant, antibodies against bacterial endotoxins or corticosteroids have been tested in clinical trials but none of them were effective (Raghavendran et al. 2008; Raghavendran et al. 2011). Moreover, the use of nitric oxide (NO), a potent pulmonary vasodilator improved oxygenation but did not improve outcomes (Taylor et al. 2004). Also, stimulation of $\beta_2$-adrenergic receptors increases vectorial sodium transport and improves edema clearance in various animal models and alveolar epithelial cells (Sznajder 2001; Mutlu et al. 2004). However, the use of $\beta_2$-agonist in the treatment of ARDS was not beneficial in the recent "Albuterol to Treat Acute Lung Injury (ALTA)" study in which no difference in the primary outcome of ventilator-free days between the placebo and albuterol groups was evident (Matthay et al. 2011). Similarly, promising findings in a human lung injury model were the basis for clinical trials applying keratinocyte growth factor (KGF) for the treatment of

ARDS. KGF has been presented as a modulator of several mechanisms potentially important for alveolar epithelial repair however, the results of a most recent clinical trials showed no improvement in outcomes of patients with ARDS (Shyamsundar et al. 2014; McAuley et al. 2017). An attractive therapeutic option for ARDS is cell-based therapy with bone marrow–derived mesenchymal stem (stromal) cells (MSCs). Based on various preclinical studies the beneficial effects of MSCs are mediated by paracrine secretion of anti-inflammatory cytokines, keratinocyte growth factor, angiopoietin-1and anti-microbial peptides that decrease inflammation and promote repair of the injured alveolar epithelium. Interestingly, treatment with human MSCs re-establishes alveolar fluid clearance in endotoxin-induced acute lung injury in *ex vivo* perfused human lungs partly by restoring amiloride-dependent sodium transport, suggesting that MSC-derived factors may have beneficial effects on apical sodium absorption mediated by ENaC (Matthay 2015). Because of the promising preclinical data in studies performed in mice, studies in large animal models of ARDS and *ex vivo* perfused human lungs, some clinical trials are now on-going. Currently, mechanical ventilation, fluid management and prone positioning are the supportive therapeutic possibilities used for reestablishing oxygenation in patients with ARDS (Wiedemann et al. 2006; Johnson and Matthay 2010; Guérin et al. 2013). Importantly, mechanical ventilation *per se* is harmful for lungs even if low tidal volumes ($V_t$) are used, a condition that is termed ventilator-induced lung injury (VILI) (Biehl et al. 2013). It has been reported that PEEP may be beneficial due to prevention of alveolar collapse in mechanically-ventilated patients with ARDS (Briel et al. 2010; Chikhani et al. 2016). PEEP improves arterial oxygenation but also leads to the impairment of oxygen delivery to tissues that may explain the ambiguous effects of various PEEP levels on survival. Another ventilator setting that clearly affects outcome is the $V_t$. Until the late 1990s a high $V_t$ of 10 to 12 ml/kg ideal body weight was widely used. However, it became increasingly evident that while initially improving oxygenation such large tidal volumes caused lung inflammation and disruption of the alveolar-capillary barrier, ultimately hypoxemia and further deterioration of patients with ARDS (Cheng et al. 2005). A landmark study of the ARDS Network in 2000 showed that ventilation with lower tidal volumes (~6 ml/kg) decreases harmful stretch of the lung, release of inflammatory mediators and markedly reduces mortality. This ventilation strategy is clearly beneficial for patients with ARDS (when compared to ventilation with high $V_t$) however, it may lead to retention of carbon dioxide and thus respiratory acidosis (ARDSNetwork 2000).

## 1.2 Hypercapnia

Carbon dioxide is generated as a waste product during cellular respiration and its removal from the blood occurs during ventilation. Normal partial pressure of arterial blood $CO_2$ ($Pa_{CO2}$) is 35-45 mmHg in healthy individuals but patients with lung diseases such as chronic obstructive lung disease (COPD), cystic fibrosis (CF) and ARDS develop aberrations in gas exchange that lead to the accumulation of $CO_2$ in the blood and tissue, a condition termed hypercapnia (Laffey and Kavanagh 1999; Mutlu et al. 2002; Belkin et al. 2006). Moreover, patients who are mechanically ventilated with low tidal volumes may have a further $CO_2$ retention due to alveolar hypoventilation (Vadász et al. 2012; Bellani et al. 2016).

Increased concentrations of carbon dioxide decrease pH levels in the blood, leading to respiratory acidosis that may have anti-inflammatory effects (Curley et al. 2010). Since excessive inflammation is a hallmark of ARDS, it has been proposed that hypercapnia may improve outcomes in patients with ARDS (Ryu et al. 2012). In this regard, some investigators suggested that hypercapnia may be tolerated (the concept of "permissive" hypercapnia) or even induced ("therapeutic" hypercapnia) to limit inflammation. Although elevated $CO_2$ levels have been shown to impair neutrophils function, reduce pro-inflammatory cytokines and inhibit ROS production, these effects are most likely due to the hypercapnia-associated acidosis rather than hypercapnia itself (Curley et al. 20010). Furthermore, it has been reported that buffering hypercapnic acidosis fails to improve ALI secondary to infections (Higgins et al. 2009; Nichol et al. 2009). Indeed, most recent clinical trials suggest that an elevated $CO_2$ level is an independent risk factor and is associated with worse outcomes in critically ill patients, particularly in patients with ARDS (Nin et al. 2017; Tiruvoipati et al. 2017).

There are several factors that may contribute to the decreased survival of hypercapnic patients with ARDS. For instant, hypercapnia independently of changes in pH impairs innate immunity and lung host defense, leading to a decreased resistance of patients to bacterial infections (Helenius et al. 2009; Wang et al. 2010). In lipopolysaccharide-stimulated human and mouse macrophages exposed to elevated $CO_2$ concentrations, expression levels of cytokines directly implicated in antimicrobial host defense such as tumor necrosis factor-α (TNF-α) and interleukin-6 (IL-6) were significantly reduced (Wang et al. 2010). Moreover, an immunosuppressive effect of hypercapnia has been reported in a study that investigated *Pseudomonas aeruginosa*-infected mice (Gates et

al. 2013). In these experiments, elevated $CO_2$ levels reduced bacterial clearance from the lungs and allowed dissemination of *Pseudomonas aeruginosa* to other organs leading to increased mortality. Additionally, several reports showed that hypercapnia independently of changes in pH, ROS or carbonic anhydrases alters reabsorption of alveolar fluid by a mechanism that leads to Na,K-ATPase downregulation (Briva et al. 2007; Chen et al. 2008; Vadász et al. 2008). Interestingly, hypercapnia induces phosphorylation of the cellular energy sensor AMP-activated protein kinase (AMPK). Activated AMPK drives protein kinase C (PKC)-ζ translocation to the cellular surface, where PKC-ζ phosphorylates the α-subunit of the Na,K-ATPase leading to its internalization and thus inhibition of lung fluid clearance (Vadász et al. 2008). Moreover, a member of the mitogen-activated protein kinases (MAPK) family, c-Jun N-terminal kinase (JNK)1/2 is also involved in the hypercapnia-induced endocytosis of Na,K-ATPase in humans, mice, rats and in *Drosophila melanogaster* (Vadász et al. 2012). It has been described that hypercapnia-induced activation of JNK promotes internalization of Na,K-ATPase via phosphorylation of LMO7b (a scaffolding protein) at the Ser1295 residue (Dada et al. 2015). Moreover, long-term hypercapnia induces the activation of miR183 that downregulates isocitrate dehydrogenese 2 leading to mitochondrial dysfunction and inhibited proliferation of AEC (Vohwinkel et al. 2011).

Notably, $CO_2$ has been presented as a signaling molecule that impacts the level of important cellular second messengers such as intracellular calcium $[Ca^{2+}]_i$ or cyclic adenosine monophosphate (cAMP). For example, increased $[Ca^{2+}]_i$ levels were demonstrated in alveolar epithelial type II cells exposed to hypercapnia (Vadász et al. 2008). It has been shown that the elevated $[Ca^{2+}]_i$ levels secondary to hypercapnia and independently of pH led to rapid CaMKK-β-dependent activation of AMPK and subsequent inhibition of Na,K-ATPase thus impairing alveolar epithelial function. In contrast, human endothelial cells treated with hypercapnia present only a minor increase in $[Ca^{2+}]_i$, suggesting that epithelial cells probably exhibit different $CO_2$ sensing mechanisms compared to endothelial cells (Nishio et al. 2001). Moreover, hypercapnia has been shown to inhibit the cAMP-dependent cystic fibrosis transmembrane conductance regulator (CFTR) in primary human airway epithelia (Calu-3) (Turner 2014).

Although the $CO_2$ sensor remains unidentified, recent scientific reports suggest that the level of $CO_2$ is sensed in lung cells. It has been well characterized that hypercapnia is sensed by excitable cells such as the glomus cells of the carotid body (Putnam et al. 2004). In these cells, elevated $CO_2$

levels lead to depolarization causing an increase in alveolar ventilation in order to maintain regular $CO_2$ levels in the body. In contrast to neuronal cells, the impact of elevated $CO_2$ levels on non-excitable mammalian cells has been less investigated however, recent studies suggest that hypercapnia initiates specific signaling patterns in the alveolar epithelium leading to downregulation of ion transport proteins and thus has potential deleterious effects on lung function (Briva et al. 2007; Chen et al. 2008; Vadász et al. 2008).

### 1.3 Alveolar epithelial $Na^+$ and fluid transport

The surface of the lung is formed by numerous epithelial cells that provide a continuous layer and represent a physical barrier against environment insults (Jeffery and Reid 1975; Denker and Nigam 1998). The structural integrity of pulmonary epithelial cells that are sealed together via tight junctions allows ions transport and gas exchange. The human lungs have a total surface area of approximately 130 $m^2$ and a major part of this area is represented by the alveolar region, which shows an asymmetric distribution of apically- and basolaterally-located ion transporters (Hollenhorst et al. 2011) (Figure 1.1).

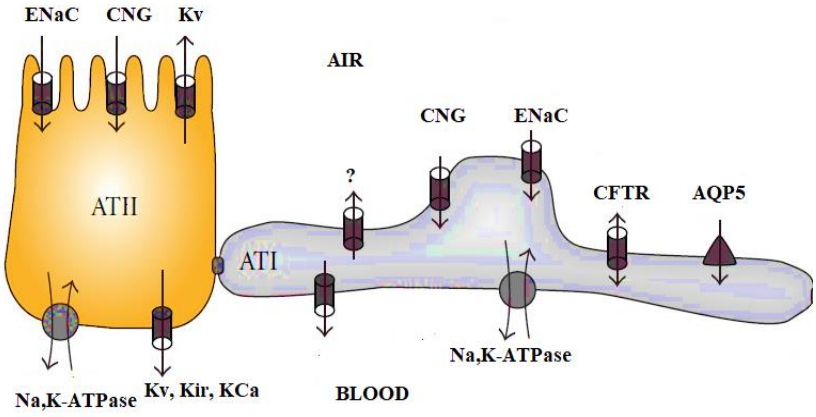


**Figure 1.1 Scheme of ion transport proteins expressed in alveolar epithelial type I and type II cells.** Epithelial sodium channel (ENaC), cyclic nucleotide-gated channel (CNG), sodium, potassium adenosine triphosphatase (Na,K-ATPase), voltage gated potassium channel (Kv), inward rectifying potassium channel (Kir), calcium-activated potassium channel (KCa), potassium channel with unknown molecular identity (?), cystic fibrosis transmembrane conductance regulator (CFTR), aquaporin 5 (AQP5). Figure was modified from Hollenhorst et al. 2011.

In mammalian lungs, alveolar type I (ATI) and type II (ATII) cells form the epithelial surface of the alveoli (Stone et al. 1992). Type II cells are cuboidal in shape and are characterized by the ability to produce and secrete surfactant. The majority of the alveolar region (95%) is covered by ATI cells which are larger and very thin therefore, reducing diffusion distance between the alveolar airspace and capillary blood. The main function of the alveoli is gas exchange during which oxygen from the airspace is transported into the blood and carbon dioxide out of the blood. However, efficient gas exchange requires precise regulation of the alveolar lining fluid (ALF) that covers the luminal surface of the alveolar epithelium (Scarpelli 2003).

The volume of the ALF depends on the equilibrium between passive fluid secretion from the vascular space and active fluid reabsorption from the alveoli (Matthay et al. 2002; Fronius et al. 2012). Accumulation of excess fluid in the alveolar space can be a consequence of impaired alveolar fluid clearance (AFC) and/or epithelial hyperpermeability initiated by a disruption of the epithelial barrier. The failure of the lungs to remove edema fluid (complication hallmark of ARDS) correlates with higher mortality (Ware and Matthay 2001). Resolution of the alveolar edema depends on the active transport of salt and water across the distal lung epithelium (Matthay and Zemans 2011).

There are numerous studies showing that fluid reabsorption in the lungs is a direct consequence of a two-step process of transepithelial $Na^+$ transport across the alveolar epithelium (Berthiaume et al. 1987; Jain et al. 1999; Matalon and Brodovich 1991). $Na^+$ ions enter the cells via amiloride-senstive, epithelial sodium channel (ENaC) expressed in the apical membrane of epithelial cells, next $Na^+$ is actively transported into the lung interstitium by the basolaterally located Na,K-ATPase. The process of $Na^+$ reabsorption produces a transepithelial osmotic gradient that drives passive movement of water to the interstitium. The removal of water takes place primarily paracellularly (Figure 1.2). Originally, it has been hypothesized that only ATII cells participate in active $Na^+$ transport across the alveolar epithelium. Recent studies using isolated ATI cells show that type I pneumocytes also express ion transporters including ENaC and Na,K-ATPase and are capable of active $Na^+$ transport (Flodby et al. 2016).

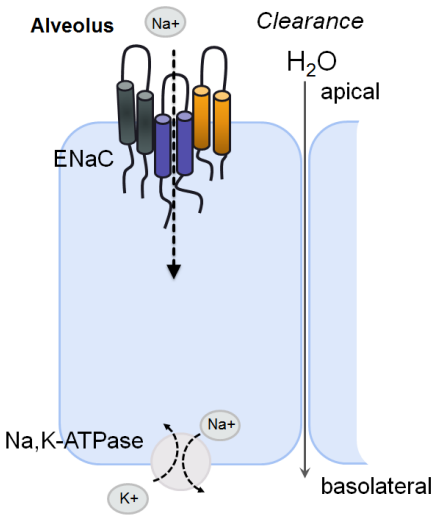


**Figure 1.2 Scheme of vectorial $Na^+$ transport mediated by ENaC and Na,K-ATPase across alveolar epithelial cells.** $Na^+$ enters alveolar epithelial cells through apically located and sodium permeable epithelial sodium channels, ENaCs and it is transported across the basolateral side of membrane via Na,K-ATPases. The active transport of $Na^+$ generates a transepithelial osmotic gradient and drives the movement of water out of the alveolar airspace.

### 1.4 Structural characteristics of ENaC

The epithelial sodium channel (ENaC) is also known as sodium channel non-neuronal 1 (SCNN1) and belongs to the ENaC/degenerin superfamily (Rossier et al. 2002). The highly selective ENaCs are composed of three non-identical (approximately 30% of sequence identity), but structurally related subunits named α, β, and γ that are most probably arranged in a heterotrimeric structure to form a fully functional protein (Bhalla and Hallows 2008). Studies in *Xenopus* oocytes showed that expression of all three ENaC subunits is necessary to mimic the channel features similar to those observed in native tissue, whereas co-expressing of either α-ENaC alone or combination of α/β-or α/γ-ENaC in oocytes produced smaller amiloride-sensitive current (Canessa et al. 1994; McNicholas and Canessa 1997; Bonny et al. 1999). These results clearly demonstrated that α-ENaC is the pore-forming subunit necessary for transepithelial $Na^+$ transport, while the β- and γ-subunits play a regulatory role in channel function, probably by controlling trafficking of the ENaC complex to the apical surface of the cells.

Additionally, two other ENaC subunits termed δ and ε have been described recently (Babini et al. 2003; Schwagerus et al. 2015). The latter one has been found in *Xenopus* renal cells (Babini et al. 2003) in contrary, the δ-subunit has been detected in respiratory epithelial cells of various species including human primary alveolar type II cells however, δ-ENaC is absent in rats and mice (Schwagerus et al. 2015). Some studies suggest that the δ-subunit, which is rather similar to α-ENaC can form a functional channel together with the β- and γ-subunits (Waldmann et al. 1995). Interestingly, δβγ-ENaC presents different sensitivity to amiloride than the αβγ-complex and has a higher single-channel $Na^+$ conductance (~12 pS) (Haerteis et al. 2009). Of note, Ly and coworkers have shown that the amiloride-sensitive current generated by δβγ-ENaC is reduced by Nedd4-2 however, the inhibition is probably mediated by the β- or γ-subunits ubiquitination due to the lack of a Nedd4-2 binding site in δ-ENaC (Ly et al. 2013).

Each ENaC subunit has a strictly defined topology, including two transmembrane segments (M1 and M2), a large extracellular loop, as well as a short $NH_2$- and COOH-terminal tail located intracellularly (Canessa et al. 1994) (Figure 1.3).

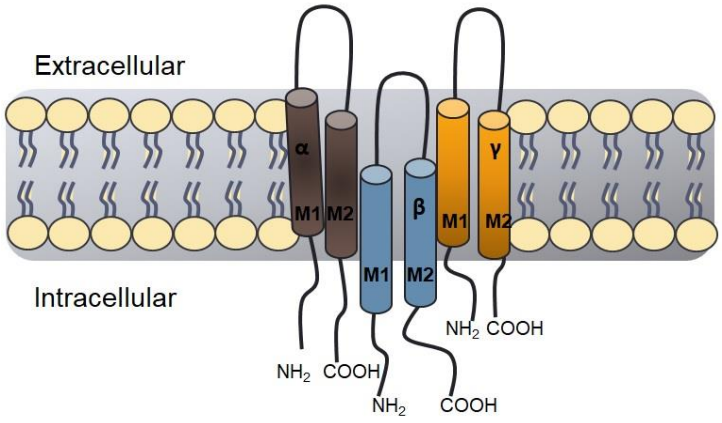


**Figure 1.3 Scheme of ENaC topology.** α-, β- and γ-subunit of ENaC are assembled into a heterotrimeric complex to create $Na^+$ selective channels expressed at the apical side of the cellular membrane. Each subunit contains two membrane spanning domains (M1, M2), an extracellular loop and cytoplasmic $NH_2$- and COOH-termini.

The membrane spanning domains of ENaC are important for regulation of channel conductance and cation selectivity (Ji et al. 2001). Prior to insertion into the cell surface (functional channel expression), ENaC undergoes maturation processes that are associated with N-linked glycosylation

and proteolytic cleavage of the α- and γ-subunits by intracellular proteases (Bhalla and Hallows 2008). Interestingly, a point mutation of cysteines that are localized in the extracellular loop of the channel prevented glycosylation and decreased channel delivery to the cell surface without effecting ENaC degradation, suggesting a role for the extracellular loop in channel trafficking (Green and Wanamaker 1997). Moreover, ENaC is inhibited by potassium-sparing diuretic amiloride (Renard et al. 1994) that is commonly used to estimate the contribution of the channel to transepithelial $Na^+$ transport. Several studies have addressed the question concerning the mechanism by which amiloride binds and inhibits ENaC and revealed that the M2 domain as well as the extracellular loop of α-ENaC are important for amiloride binding (Schild et al. 1997; Ji et al. 2001).

Notably, the intracellular tails of ENaC play a central role in the regulation of ENaC endocytosis and thus channel function. The cytoplasmic COOH-terminus contains a unique proline-rich domain (PY or PPxY motif) that is critically important for protein-protein interactions including the interaction with neural precursor cell expressed developmentally down-regulated protein (Nedd4-2) that mediates ubiquitin-dependent ENaC endocytosis (Abriel et al. 1999; Rotin and Staub 2011) and extracellular signal–regulated kinases (ERK)1/2 which directly phosphorylate β- and γ-ENaC (Shi et al. 2002). The intracellular N-terminus of ENaC participates in channel subunit assembly and gating (Adams et al. 1997; Prince and Welsh 1998). Interestingly, lysine residues located at this part of ENaC play an important role in endocytic retrieval of ENaC driven by Nedd4-2 mediated ubiquitination (Rotin and Staub 2012).

### 1.5 Tissue distribution and physiological roles of ENaC

ENaC is localized at the apical membrane of several epithelial tissues including lung, kidney, gastrointestinal tract, sweat glands and it is the rate-limiting step of $Na^+$ absorption. The proper function of ENaC is crucial for regulating total body salt and water homeostasis and normal blood pressure (Stockand et al. 2008; Butterworth 2010). In addition, ENaC is found in taste cells of the tongue, where most likely is a receptor for salt taste (Boughter et al. 1999) and in non-epithelial cells such as in specialized cutaneous sensory neurons where it plays a role in mechanosensation (Drummond et al. 2000).

In the lungs, ENaC is expressed in airway epithelial cells including Clara cells located in the distal airways and in both types of alveolar epithelial cells, in which it is responsible for maintaining alveolar fluid balance and consequently for optimal gas exchange (Matalon et al. 2002; Matalon et al. 2015). In this regards, abnormalities in ENaC function are associated with several diseases such as an inherited, autosomal-dominant salt-sensitive form of hypertension (Liddle's syndrome), a disorder that is directly linked to changes in ENaC cell surface expression due to the presence of characteristic mutations within the PY motif of the β- and γ-subunits that affect channel endocytosis (Abriel et al. 1999). Interestingly, a commonly used mouse model to study CF is characterized by β-ENaC overexpression. Mall and colleagues presented that overexpression of β-ENaC in mice leads to hyperabsorption of $Na^+$ and lung dehydration most probably due to abnormally high ENaC trafficking to the cellular surface (Mall et al. 2004). In contrary, reduction in ENaC function leads to an excess of lung fluid resulting from impaired $Na^+$ and water reabsorption. This type of ENaC dysfunction is observed in patients with type I pseudohypoaldosteronism (PHA1) (Kerem and Bistritzer 1999) and pulmonary edema (Matalon et al. 2002; Matalon et al. 2015).

### 1.5.1 Role of ENaC in lung fluid homeostasis

Fluid reabsorption across the distal lung epithelium is primarily driven by vectorial $Na^+$ transport that allows water clearance. This process is crucial for maintaining the alveolar space "dry" in order to allow normal oxygen and carbon dioxide exchange (Canessa et al. 1994; Matthay et al. 2002; Matalon et al. 2015). Up to date, several $Na^+$ channels have been found in alveolar epithelial cells, including the ones that are sensitive and those that are insensitive to amiloride. Two types of amiloride-sensitive channels are expressed in the alveolar epithelium, the highly selective $Na^+$ channels (HSC) such as ENaC and the non-selective cation channels (NSC) (Matthay et al. 2002; Althaus et al. 2011).

Since it has been demonstrated in studies in isolated lung models and *in vivo* using animals that addition of amiloride inhibits transepithelial $Na^+$ transport and AFC, it is believed that amiloride-sensitive sodium channels (ENaC-like channels) represent a key element of $Na^+$ uptake in alveolar epithelial cells and that they have a major contribution to alveolar fluid reabsorption (Basset et al. 1987; Matalon et al. 2002; Eaton et al. 2004).

The significance of ENaC in alveolar fluid balance has been shown in the studies described by Hummler et al., in which α-ENaC knock-out mice died early after birth (within 40 h) due to defective lung fluid clearance (Hummler et al. 1996).

An additional example underlining the role of ENaC in alveolar fluid clearance was demonstrated by lung-specific α-ENaC knock-down studies in rats *in vivo*, in which silencing of α-ENaC decreased AFC after β-adrenoceptor stimulation, whereas application of amiloride did not cause further AFC inhibition. These findings also suggested that β-adrenoceptor stimulation of AFC is dependent on ENaC expression (Li and Folkesson 2006).

These studies established amiloride-sensitive channels as crucial regulators of AFC. However, it is still not fully understood how $Na^+$ transporters are regulated during pathological conditions such as acute lung injury. Recent studies have shown that lung infections induce inflammatory cytokines and chemokines such as TNF-α, transforming growth factor beta 1 (TGF-β1) or interleukin 1 beta (IL-1β) that alter ENaC-mediated $Na^+$ transport (Wynne et al. 2017). Given the importance of ENaC in lung fluid balance, upregulation of these inflammatory cytokines and chemokines may significantly contribute to the persistence of pulmonary edema in patients with ARDS secondary to pneumonia (Figure 1.4). Since ENaC activity controls lung fluid homeostasis, one of the potential mechanisms to increase AFC under pathological conditions is to enhance the abundance of the channel at the apical surface of alveolar epithelial cells, which may lead to the improvement of patient outcomes (Ware and Matthay 2001; Geiser 2003; Bhattacharya and Matthay 2013).

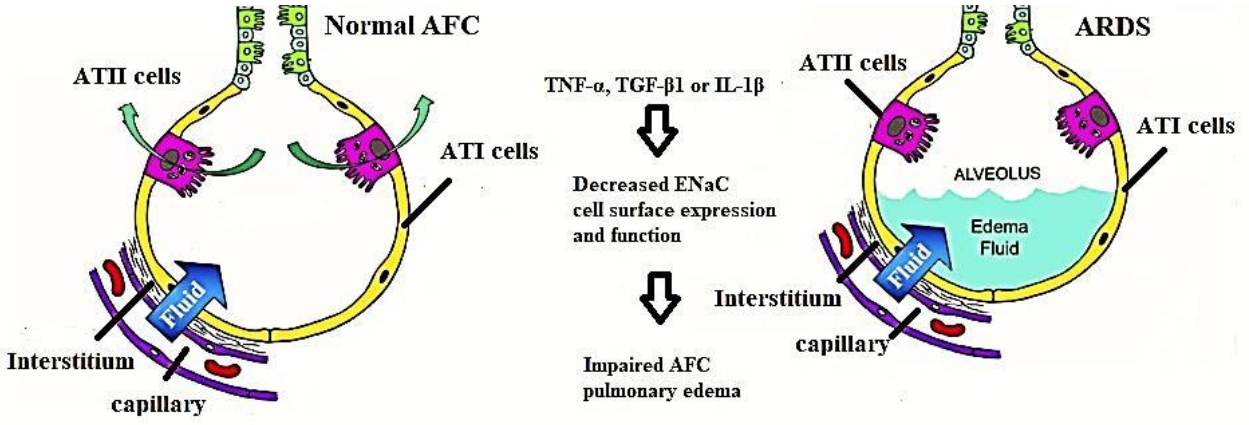


**Figure 1.4 The role of cytokines in mediating ARDS**. During lung infections, inflammatory cytokines are produced and lead to ENaC downregulation. The reduction in ENaC activity inhibits

reabsorption of excess alveolar fluid, thus impairing gas exchange. The figure was modified from Wynne et al. 2017.

### 1.6 Aspects of ENaC regulation

Because decreased ENaC function impairs resolution of pulmonary edema, studying the exact molecular mechanisms of ENaC regulation is important for understanding lung fluid homeostasis. ENaC function can be modified by a variety of extra- and intracellular factors. The $NH_2$- and COOH- termini of ENaC provide sites of protein binding and chemical modification in response to cellular signals that regulate channel activity by either modifying the open probability ($P_o$) or by varying the number of the channels located at the apical membrane of cells (Anantharam et al. 2006; Kashlan and Kleyman 2012).

#### 1.6.1 Regulation of ENaC via open probability ($P_o$)

Our knowledge is limited regarding the factors that alter open probability of ENaC. However, mutations of specific residues within the intracellular N-terminal tail of α-ENaC result in low $P_o$, suggesting that this segment of the channel structure is important for gating control (Grunder et al. 1999). For example, regulation of ENaC activity by phosphatidylinositol 4,5-bisphosphate ($PIP_2$) has been shown in studies in renal A6 collecting duct cells in which $PIP_2$ binding to the N-terminal domain of β and γ-ENaC increased single channel open probability (Yue et al. 2002). Furthermore, an increase in extracellular $Na^+$ concentration decreases ENaC activity by altering channel gating. This process is called $Na^+$ self-inhibition, occurs over seconds and can be blunted by treatment with external trypsin (Chraïbi and Horisberger 2002). In contrast, an increase in intracellular $Na^+$ levels (feedback inhibition) results in slower changes in ENaC activity. Interestingly, Kellenberger et al. demonstrated that channels with Liddle's syndrome mutation expressed in oocytes did not respond to $Na^+$-dependent inhibition, suggesting that the enhancement of ENaC activity in patients with Liddle's syndrome may be driven by a mechanism that decreases feedback inhibition (Kellenberger et al. 1998).

Regulation of channel open probability may also occur as a result of proteolytic cleavage of ENaC subunits (Eaton et al. 2010). It is well known fact that the α- and γ-subunits of ENaC contain a furin cleavage site. Furin is a serine protease that is localized in the trans-Golgi compartment and

mediates the cleavage of the above mentioned ENaC subunits that leads to release of an inhibitory tract thereby increasing channel open probability. In line with this notion, mutations of the furin cleavage site within α-ENaC inhibit channel activity and a significant reduction in $Na^+$ current is observed in furin-deficient Chinese hamster ovary cells (Hughey et al. 2004). Notably, after trafficking to the cell surface ENaC may be further cleaved by several extracellular channel-activating proteases (CAPs) (Vallet et al. 1997).

Interestingly, both cleaved and non-cleaved ENaC subunits are found at the surface of cells expressing ENaC (Eaton et al. 2010). Probably, immature ENaCs (non-cleaved) work as a channel pool that can be activated by proteases on demand.

Although there are many reports showing ENaC regulation via $P_o$, it is believed that long-term modification of channel activity occurs by changes of ENaC cell surface abundance (Rossier 2002).

### 1.6.2 Regulation of ENaC by apical membrane abundance

Regulation of ENaC may also occur via altering cell surface expression of the channel by either influencing channel transport to the cell surface or by affecting endocytosis (Ismailov et al. 1995; Waldmann et al. 1995). Most of the synthetized subunits of ENaC remain as immature proteins in the endoplasmic reticulum (ER) or in pre-Golgi compartments and only a small portion of ENaC molecules reaches the plasma membrane where it participates in $Na^+$ and water reabsorption. Mechanisms that regulate ENaC function at the cellular surface include control by hormones that either increase the number of new channel insertion or decrease ENaC retrieval and/or degradation (Eaton et al. 2010).

<u>Hormonal regulation</u>

Hormones such as aldosterone, vasopressin or insulin are known to regulate epithelial $Na^+$ transport via affecting ENaC transcription or by post-transcriptional pathways. For example, increased ENaC trafficking to the cell surface mediated by aldosterone is mediated by translocation of the hormone to the nucleus where it induces ENaC transcription (May et al. 1997; Chen et al. 1999). Additionally, aldosterone may enhance transcription of serum and glucocorticoid-induced kinase 1 (SGK1) that phosphorylates Nedd4-2 thereby affecting ENaC activity post-translationally (Bhalla et al. 2005; Snyder 2009).

Vasopressin modulates ENaC activity via Nedd4-2 phosphorylation driven by protein kinase A (PKA) that is activated in response to increased cAMP levels (Snyder 2009).

In addition, ENaC open probability and cell surface abundance can be positively regulated by insulin (Baquero and Gilbertson 2011). The insulin-mediated signaling pathway includes the activation of phosphoinositol 3-kinase (PI3-kinase) leading to synthesis of PIP3 that affects ENaC via activation of SGK1. Thus, hormonally-regulated increase of ENaC expression results in higher channel cell surface abundance and greater activity.

Ubiquitin-dependent endocytosis

The activity of numerous small molecule, transporters and ion channels including ENaC can be reduced by endocytosis into intracellular compartments. Removal of ENaC from the plasma membrane requires addition of ubiquitin molecules to the $NH_2$-terminus of the channel that act as a specific signal for channel internalization. The ubiquitin ligase, Nedd4-2 targets the ENaC complex for endocytosis and degradation by binding to the PY motif within the C-terminus of all ENaC subunits (Butterworth et al. 2007; Wiemuth et al. 2007; Kabra et al. 2008).

The process of ubiquitination requires covalent attachment of ubiquitin (8.5 kDa protein) to lysine residues of ENaC and is mediated by the E3 ubiquitin ligase, Nedd4-2 that functions in conjugation with the ubiquitin-activating and -conjugating enzymes, E1 and E2, respectively. The first step of ubiquitination is the creation of a high-energy thioester bond between the glycine 76 residue of ubiquitin and a cysteine of the E1 enzyme. The ubiquitin from E1 is further relocated to the E2 enzyme prior to the final step of ubiquitination in which, it is transferred by the E3 enzyme to the ε-amino group of a lysine located at the $NH_2$-terminus of the targeted protein. The process in which a protein is bound by a single ubiquitin molecule is called monoubiquitination. Additionally, more ubiquitin molecules can be added to the first one resulting in a ubiquitin chain, a process termed polyubiquitination. A single ubiquitin can be also added to several lysine residues, this type of modification is known as multimonoubiquitination (Eaton et al. 2010; Vadász et al. 2012).

ENaC can be ubiquitinated in various ways depending on the cell type or culture conditions. Although most studies indicate that ENaC subunits undergo mono or multimonoubiquitination (Wiemuth et al. 2007), some reports have shown polyubiquitination of the channel as well (Malik

et al. 2005; Butterworth 2010). It has been proposed that those ENaC subunits that are not transported to the cell surface are polyubiquitinated, while plasma membrane ENaCs undergo monoubiquitination (Rotin and Staub 2011). Despite of the differences in ENaC ubiquitination patterns, it is clear that mutation of key lysine molecules in the $NH_2$-terminus prolongs channel half-life due to its retention at the apical surface (Hendron et al. 2002).

Nedd4-2-driven ubiquitination of ENaC most likely occurs at the cell surface and results in internalization via clathrin-mediated pathways (Wang et al. 2006; Lu et al. 2007). The PY motif of COOH-terminus of ENaC overlaps with the tyrosine-based endocytosis domain Yxxϕ. This internalization motif mediates binding of the channel to the $\mu_2$ of adaptor protein-2 (AP-2), a clathrin adaptor that facilities entry of ENaC to clathrin-coated pits. Mutation of Yxxϕ of β-ENaC results in increased ENaC activity (Shimkets et al. 1997). A second possible pathway of ENaC endocytosis is an indirect interaction between ubiquitin and a ubiquitin-binding protein, such as epsin. It has been reported that co-expression of epsin together with Nedd4-2 decreases ENaC activity (Wiemuth et al. 2007). Following internalization, ENaC is designated for lysosomal or proteasomal degradation or recycled back to the plasma membrane (Butterworth et al. 2007). The pattern of ENaC ubiquitination determines the fate of the channel. For instance, it is supposed that proteosomal degradation occurs after ENaC polyubiquitination, while monoubiquitinated channels are degraded via lysosomes. Interestingly, some ubiquitinated ENaC molecules are held back from a degradation by deubiquitination, mediated by deubiquitinating enzymes (DUBs) such as ubiquitin carboxyl-terminal hydrolase isozyme L3 (UCH-L3) (Butterworth 2010).

Although it has been confirmed by many studies that ubiquitination generally initiates ENaC endocytosis and/or downregulation, there are some reports suggesting that ubiquitination may also activate the channel by promoting conformational changes in the extracellular loop leading to enhanced proteolytic cleavage (Rotin and Staub 2011).

### 1.7 Characterization of ENaC/Nedd4-2 interaction

The initial description of ENaC/Nedd4-2 interaction was presented in a two-hybrid screen study in which a truncated version of β-ENaC, which contained the PY motif was used as a bait (Staub et al. 1996). These studies revealed that the COOH-terminus of ENaC is critically important for

interactions with the WW domain of Nedd4-2 and shed light on the mechanism of channel trafficking from the plasma membrane.

Additionally, studies in oocytes have shown that Nedd4-2-mediated decrease of ENaC cell surface abundance requires the presence of lysine residues localized at the N-terminus of the channel that are the target for ubiquitin modification (Hendron et al. 2002).

Moreover, overexpression of Nedd4-2 significantly reduces ENaC-mediated $Na^+$ transport, whereas Nedd4-2 knock-down increases ENaC expression (Snyder et al. 2004; Knight et al. 2006; Rotin and Staub 2012).

The PY motif of ENaC

Each ENaC subunit contains a conserved PY (PPPXY, P-proline, X-any amino acid and Y-tyrosine) domain located at the COOH-terminus that serves as a Nedd4-2 binding site and allows possible ubiquitination. The first evidence showing that the ENaC/Nedd4-2 interaction is phisiologically significant was demonstrated in Madin-Darby canine kidney (MDCK) cells. In this study co-expression of PY-mutants of ENaC (Liddle's syndrome) resulted in increased channel activity compared to the wild type channels that was secondary to enhanced apical abundance of ENaC due to impaired channel ubiquitination (Staub et al. 1997).

Structural features of Nedd4-2

Nedd4 (neuronal precursor cell expressed developmentally down-regulated gene 4) proteins belong to the HECT family of E3 ligases (Rotin and Kumar 2009). There are eight members of the Nedd4 ubiquitin ligase family in mammals. Among them, two structurally related proteins, Nedd4-1 and Nedd4-2 have been studied in detail. Nedd4-2, the isoform that is important for modulating ENaC trafficking, endocytosis and degradation contains a calcium phospholipid binding domain (C2) at the $NH_2$-terminus, multiple WW segments (four in human, three in rodents) and a carboxyl HECT (homologous to E6-associated protein C-terminus) domain (Snyder 2005; Rotin and Staub 2012).

The significance of the C2 domain in ENaC regulation has been shown in a study in MDCK cells in which increased cytosolic $Ca^{2+}$ levels led to relocation of Nedd4-2 to the proximity of the cellular surface (where the E3 ligase interacts with ENaC), while deletion of the C2 domain blocked E3

ubiquitin ligase translocation (Plant et al. 1997). These findings showed a possible mechanism of ENaC regulation by $Ca^{2+}$ however, so far no further studies have confirmed this hypothesis.

The HECT domain is the catalytic domain of Nedd4-2 and thus, mutations of the cysteine residues within this region prevent inhibition of ENaC by Nedd4-2 (Abriel et al. 1999). It has been shown that the second and the third WW domains of Nedd4-2 interact with all ENaC subunits. However, binding of ENaC to the WW3 segment results in the greatest reduction in ENaC activity (Kamynina et al. 2001). A surface plasmon resonance study revealed that the binding of Nedd4-2 WW domains to β- and γ-ENaC has very slow dissociation, suggesting that the association between these proteins is almost irreversible (Asher et al. 2003).

Phosphorylation as a key mechanism regulating interaction of ENaC and Nedd4-2

Recent studies convincingly demonstrated that phosphorylation is a critical mechanism that regulates interaction of ENaC and Nedd4-2 and thus, ENaC-dependent $Na^+$ transport (Debonneville et al. 2002; Carattino et al. 2005). The association between these two proteins can be regulated by kinases that mediate phosphorylation of either Nedd4-2 or ENaC at specific phospho-sites. For instance, PKA and SGK-1 have been shown to phosphorylate the same residue of Nedd4-2 preventing ENaC ubiquitination and endocytosis (Bhalla et al. 2005). Recently, glucocorticoid-induced leucine zipper protein-1 (GILZ-1) has been suggested as an important regulator of ENaC function (Soundararajan et al. 2010). This aldosterone-induced protein activates ENaC by recruiting SGK-1 and preventing ERK activation. Moreover, several other kinases are known to activate ENaC including IκB kinase-β that phosphorylates Nedd4-2 or casein kinase 2 that mediates phosphorylation of β- and γ-ENaC (Lebowitz et al. 2004).

In contrast, some kinases are known to improve Nedd4-2-dependent ENaC ubiquitination and thus decrease channel activity. For example, ERK facilitates ENaC/Nedd4-2 interaction by direct phosphorylation of ENaC, thereby inhibiting the channel (Shi et al. 2002; Lazrak et al. 2012). Moreover, cellular stress leads to activation of AMPK that acts as cellular energy sensor. It has been reported that AMPK-driven down-regulation of ENaC is mediated by an increase in Nedd4-2 activity probably through indirect phosphorylation of the E3 ligase (Bhalla et al. 2006; Almaça et al. 2009). Recently also JNK1 has been shown to be involved in phosphorylation of Nedd4-2. This phosphorylation leads to an increased Nedd4-2 activity promoting ubiquitination of ENaC-α

(Hallows et al. 2010). Eaton and co-workers demonstrated activation of PKC-δ in PKC-α knock-out (KO) mice that leads to activation of ERK1/2 and increases endocytosis of ENaC via ubiquitination mediated by Nedd4–2 (Eaton et al. 2014).

## 2. Thesis objectives

The major aim of the current work was to investigate whether hypercapnia modulates expression and function of ENaC in alveolar epithelial cells.

Vectorial $Na^+$ transport across the alveolar epithelium is driven by an interplay of ENaC and Na,K-ATPase. Previous work from our group demonstrated that elevated $CO_2$ levels impair alveolar epithelial function by inhibition of the Na,K-ATPase (Briva et al. 2007; Vadász et al. 2008; Vadász et al. 2012). The hypercapnic effects on the Na,K-ATPase have been shown to be dependent on intracellular calcium levels and activity of AMPK and PKC-ζ that by phosphorylation of the Na,K-ATPase α-subunit promotes endocytosis of the sodium pump, thereby decreasing AFC (Vadász et al. 2008). Further studies have shown that downregulation of the Na,K-ATPase requires activation of JNK, a downstream target of AMPK (Vadász et al. 2012; Dada et al. 2015). Based on these findings, we hypothesized that hypercapnia may impair function of alveolar epithelial cells by regulating ENaC cell surface abundance.

To study the effects of hypercapnia on ENaC functional expression, specific questions were formulated:

I. Does hypercapnia alter cell surface expression of ENaC in alveolar epithelial cells?
II. Does ubiquitination drive ENaC endocytosis initiated by elevated $CO_2$ levels? And if so, which ENaC subunit(s) is (are) prone to be ubiquitinated?
III. Does hypercapnia modify transepithelial $Na^+$ transport by inducing ENaC cell surface retrieval?
IV. Does the process of ENaC ubiquitination depend on the E3 ubiquitin ligase, Nedd4-2?
V. Which key players are involved in ENaC regulation upon hypercapnic exposure and particularly which signaling events promote ENaC/Nedd4-2 interaction upon hypercapnia?

The possible signaling pathways involved in hypercapnia-induced ENaC downregulation are illustrated in Figure 2.1, which presents our working hypothesis.

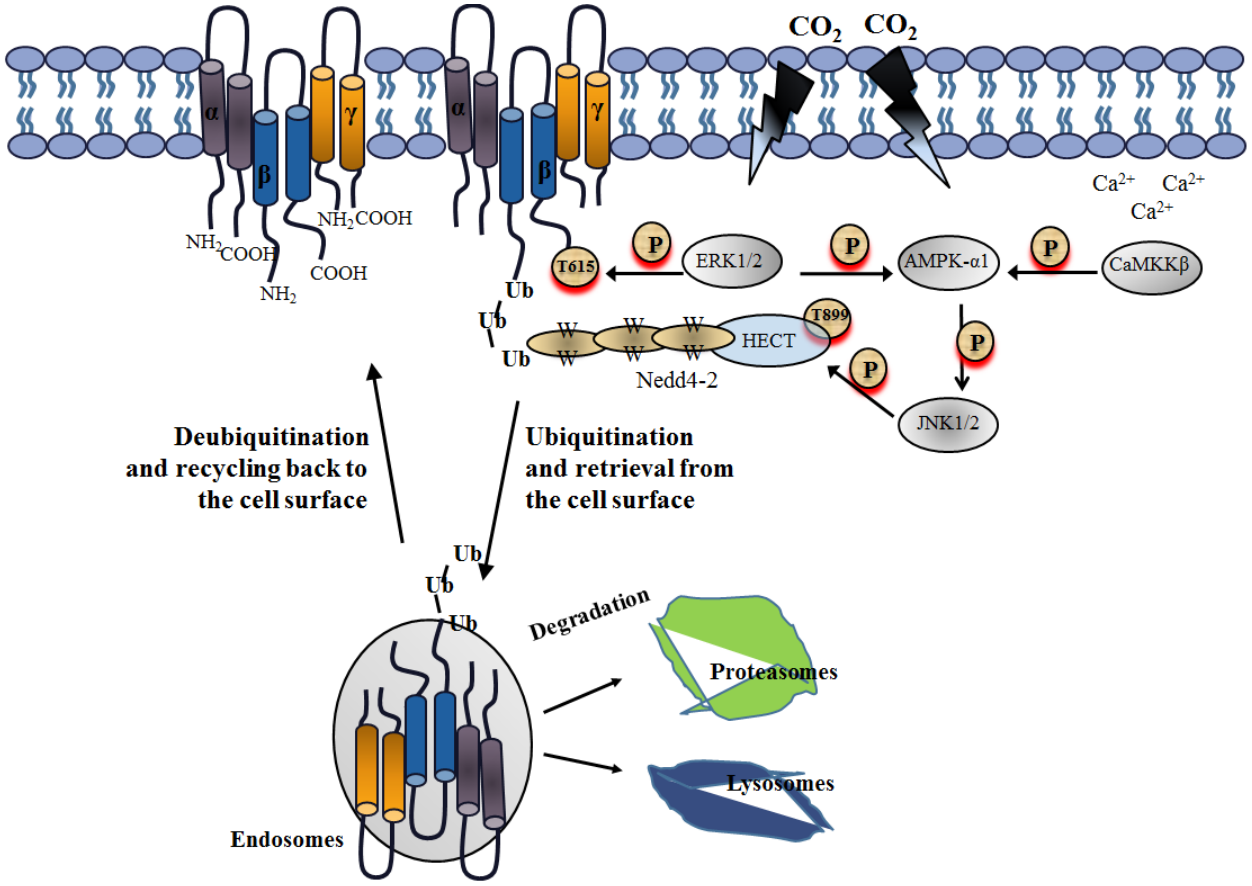


**Figure 2.1 Proposed signaling pathway of $CO_2$-regulated ENaC ubiquitination and endocytosis.** $CO_2$-induced polyubiquitination of β-ENaC and endocytosis of the α/β-ENaC complex are dependent on ERK1/2- and CaMKK-β-mediated activation of AMPK-α1. Active AMPK induces JNK1/2-dependent phosphorylation of Nedd4-2 at T899 residue, promoting E3 ubiquitin ligase translocation to the cell membrane where it mediates ubiquitination of ENaC β-subunit. Additionally, ERK1/2 via direct phosphorylation of β-ENaC at T615 residue facilitates ENaC/Nedd4-2 interaction. Ubiquitinated channels are internalized and either recycled back to the cellular surface or degraded in proteasomes or lysosomes.

# 3. Materials and Methods

## 3.1 Instruments

Table 3.1 List of electronic devices used in experiments.

| **Device** | **Supplier** |
|---|---|
| 4D-Nucleofector System | Lonza, Cologne, Germany |
| BioPhotometer - Spectrophotometer | BioRad, Munich, Germany |
| Developer Curix 60 Processing Machine | Agfa, Morstel, Belgium |
| Electrophoresis and Blotting System | BioRad, Munich, Germany |
| HeraCell 150 - Cell Incubator | Thermo Scientific, Dreieich, Germany |
| Heraeus Fresco Micro Centrifuge | Thermo Scientific, Dreieich, Germany |
| Humidified Chamber | BioSpherix Ltd. New York, USA |
| Gel imaging system | BioRad, Munich, Germany |
| KNF Laboport vacuum pump flyer | KNF, Freiburg, Germany |
| LabChart software | ADInstruments, Colorado Springs, USA |
| Mettler H20T Precision Lab Scale Balance | Mettler Toledo, Giessen, Germany |
| Microcentrifuge, Ministar, Silverline | VWR, Bruchsal, Germany |
| Milli-Q Water Purification System | Millipore, Schwalbach, Germany |
| Mini-PROTEAN Tetra Cell | BioRad, Munich, Germany |
| Msc-Advantage- Smart flow | Thermo Scientific, Dreieich, Germany |
| NanoDrop 1000 | Thermo Scientific, Dreieich, Germany |
| Neubauer Improved Cell Counting Chamber | Labor Optik, Friedrichsdorf, Germany |
| pH-Meter 766 | Knick, Berlin, Germany |
| Pipetes | Gilson, Limburg-Offheim, Germany |
| Plymax 1040-Waving Platform Shaker | Heidolph, Schwabach, Germany |
| PowerPac Basic Power Supply | BioRad, Munich, Germany |
| PowerLab 8/35 | ADInstruments, Colorado Springs, USA |
| RapidLab Blood Gas Analyzer | Siemens, Erlangen, Germany |
| Thermocycler | Biometra GmbH, Göttingen, Germany |
| Thermomixer | Eppendorf, Hamburg, Germany |
| Transblot SD Semi-Dry Transfer Cell | BioRad, Munich, Germany |
| Ussing chamber equipment:<br>(Heat Block, Snapwell Chambers, Ag/AgCl Electrodes, Electrode Lead Sets, voltage/current Clamp) | Physiologic Instruments, San Diego, USA |

### 3.2 Plasmids

All plasmids used in the studies are listed in Table 3.2. Vectors expressing ENaC subunits were generated as described previously (Buchbinder 2013; Gwoździńska et al. 2017). pRK5-HA-ubiquitin plasmid was obtained from Ted Dawson [Addgene #17608], (Lim 2005). pCI-HANEDD4L plasmid was a gift from Joan Massague [Addgene #27000], (Gao et al. 2009). pCI-HANEDD4L_T899A contained mutation in T899 residue was created using Quick Change Mutagenesis Kit (described in section 3.21). The mutated β-ENaC lacking T615 ($\beta_{\Delta T615}$ENaC) was created by Gibson assembly technique (described in Section 3.22).

Table 3.2 List of plasmids employed in cell transfection experiments.

| **Vector backbone** | **Gene insert** | **Resistance** |
|---|---|---|
| pcDNA3.1V5/His (β-ENaC-V5) | β-subunit of human epithelial sodium channel NM_000336.2. | Ampicillin |
| pcDNA3.1V5/His_ ΔT615 ($\beta_{\Delta T615}$-ENaC-V5) | β-subunit of human epithelial sodium channel with T615 deletion. | Ampicillin |
| pCI-HANEDD4L | Human Nedd4L (Nedd4-2), E3 ubiquitin protein ligase | Ampicillin |
| pCI-HANEDD4L_T899A | Human Nedd4L (Nedd4-2), E3 ubiquitin protein ligase with point mutation T899A | Ampicillin |
| pCMV-HA-C (HA-γ-ENaC-myc) | γ-subunit of human epithelial sodium channel NM_001039 | Kanamycin |
| pEYFP-C1 (eYFP-α-ENaC-Flag) | α-subunit of human epithelial sodium channel NM_001038 | Kanamycin |
| pRK5-HA-Ubiquitin | Human ubiquitin | Ampicillin |

### 3.3 siRNAs

Table 3.3 List of siRNAs employed in knock-down studies.

| **siRNA** | **Concentration [nM]** | **Supplier** |
|---|---|---|
| AMPK-α1 (sc-29673) | 50 | Santa Cruz Biotechnology |
| Nedd4-L (sc-75894) | 100 | Santa Cruz Biotechnology |
| Negative control (SR-CL000-005) | 50-100 | Eurogentec |

### 3.4 Inhibitors

Table 3.4 List of inhibitors employed in the studies.

| Compound | Vehicle | Concentration |
|---|---|---|
| Amiloride, ENaC inhibitor | DMSO | 10 μM |
| Compound C, AMPK inhibitor | DMSO | 20 μM |
| Complete, proteases inhibitor | $H_2O$ | 1 tablet/1ml |
| SP600125, JNK inhibitor | DMSO | 25 μM |
| STO609, CaMKK-β inhibitor | DMSO | 20 μg/ml |
| U0126, MEK-1 and MEK-2 inhibitor | DMSO | 10 μM |

### 3.5 Antibodies

Table 3.5 Antibodies used in the studies.

| Antibody name (cat. number) | Species | Dilution | Supplier |
|---|---|---|---|
| Anti-GFP (11814460001) | mouse | 1:1000 | Roche |
| Anti-V5 (V8137-2mg) | rabbit | 1:50 (IP) | Sigma-Aldrich |
| Anti-V5 (R960-25) | mouse | 1:1000 | Invitrogen |
| Anti-Transferrin Receptor (13-6800) | mouse | 1:1000 | Invitrogen |
| Anti-HA.11 (MMS-101P) | mouse | 1:750 | Covance |
| Anti- β-actin (A20066-2ml) | rabbit | 1:1000 | Sigma-Aldrich |
| Anti-Nedd4-L (sc85081) | rabbit | 1:1000 | Santa Cruz |
| Phospho-AMPK-α1 (Thr172) (#4188) | rabbit | 1:1000 | Cell Signaling |
| Anti-AMPK-α1 (sc2793) | mouse | 1:1000 | Cell Signaling |
| Phospho-p44/42 MAPK (ERK1/2) (Thr202/Tyr204) (#9106) | mouse | 1:1000 | Cell Signaling |
| p44/42 MAPK (ERK1/2) (#9102) | rabbit | 1:1000 | Cell Signaling |
| Phospho-c-Jun (Ser63) (#9261) | rabbit | 1:750 | Cell Signaling |
| Anti-JNK (ab179461) | rabbit | 1:1000 | Abcam |
| Alexa Fluor 488 (A-11008) | rabbit | 1.500 | Thermo Scientific |
| Phospho-anti SCNN1B(T615) (ab79172) | rabbit | 1:750 | Abcam |
| IgG, HRP linked (31450) | mouse | 1:5000 | Thermo Scientific |
| IgG, HRP linked (7074S) | rabbit | 1:5000 | Cell Signaling |

### 3.6 Cell lines and bacterial strains

Cell lines:

Isolation of primary rat alveolar epithelial type II (ATII) cells were performed according to the legal regulations of the German Animal Welfare Act and were approved by the regional authorities of the State of Hessen.

- Primary rat ATII cells were isolated as described previously (Vadász et al. 2008; Buchäckert et al. 2012).
- Human adenocarcinoma alveolar epithelial cell line (A549) were purchased from the American Type Culture Collection, (ATCC-CCL-185)
- Human airways epithelial cells (H441) were purchased from the American Type Culture Collection, (ATCC-HTB-174) in the $55^{th}$ passage.

Bacterial strains:

- *E. coli* DH5α (New England Biolabs, Ipswich, USA) was used for DNA transformation and plasmid isolation.
- *XL1-Blue* super competent cells were provided with Quick Change Mutagenesis Kit (Stratagene, La Jolla, USA) and were used for site directed mutagenesis experiments.

### 3.7 Culture media and growth conditions of eukaryotic cells

All cell types were maintained in a humidified atmosphere of 5% $CO_2$ and 95% air at 37 °C (unless stated otherwise). The cells were subcultured when 80% of confluency was achieved. After removing media, cells were washed with sterile phosphate buffered saline (PBS; Life Technology, Darmstadt, Germany), incubated in 1 ml of trypsin solution (Life Technology) for 5 min and re-suspended in culture media. The culture medium was replaced every 48 h.

ATII cells were grown on 60 mm culture dishes (Sarstedt, Nümbrecht, Germany) in 4 ml of culture media containing high glucose (4,5 g/L) Dulbecco's Modified Eagle's media (DMEM; Life Technology) supplemented with 10% fetal bovine serum (FBS; PAA Laboratories, Egelsbach, Germany), 100 $Uml^{-1}$ penicillin and 100 $\mu gml^{-1}$ streptomycin (both from PAN-Biotech, Aidenbach, Germany). 24 h after isolation cells were used in experiments. After nucleofection, ATII cells were seeded on permeable membrane supports (BD Falcon, Heidelberg, Germany) under liquid/liquid conditions in full DMEM media for 18 h and then were used for analysis.

A549 cells were grown in the same culture conditions as described for ATII cells. Cells were used only between passage 4 and 13. Transfected cells were seeded on 6-well tissue culture plates (~2x $10^6$ cells/well) (BD Falcon).

H441 cells were cultured in Roswell Park Memorial Institute Media (RPMI 1640; Life Technology) supplemented with 10% FBS, 1% insulin-transferrin-sodium selenite (ITS) and 1 mM sodium pyruvate (Sigma Aldrich), 100 $Uml^{-1}$ penicillin and 100 $\mu gml^{-1}$ streptomycin.

For Ussing chamber recordings, H441 cells were re-suspended in culture media and seeded on the transwell clear inserts [12 mm diameter, 0.4 μm pore size] (Corning, Sigma Aldrich) at a density of 500,000 cells/$cm^2$. In the first 24 h cells were cultured under liquid/liquid conditions after which the fluid from the apical compartment was aspirated and 100 nM dexamethasone (Sigma Aldrich) was added to the basolateral side. Cells were kept under air/liquid conditions for the next 6 days and were then used for transepithelial ion transport studies.

### 3.8 Transfection of eukaryotic cells

The amount of total ENaC protein expressed in epithelial cells is relatively large compared to the number of the channels located at the cell membrane (functional expression). It has been estimated that approximately 10–30% of the channel is located outside of the endoplasmatic reticulum (ER) in native cells, whereas in transfected cells only 1-2% of total ENaC can be found at the cell surface (Hughey et al. 2004; Eaton et al. 2010). To improve the expression of ENaC in the alveolar epithelial cells and to increase the recognition signal for the antibodies, plasmids encoding ENaC subunits were delivered to the cells by applying nucleofection (Lonza, Cologne, Germany). Nucleofection creates pores in cellular and nuclear membranes by using electrical pulses thus representing an alternative to viral and phospholipid-based methods of DNA delivery. As we have previously reported, this method allows transport of oligonucleotides to slow- or non-proliferating cells like ATII cells with high viability and efficiency (Grzesik et al. 2013).

#### 3.8.1 Nucleofection of ATII cells

ATII cells were washed 3 times with PBS, trypsinized and counted one day after isolation. The required number of cells (4 x $10^6$ cells per reaction) was centrifuged (90 g, 10 min 20 °C). The pellets were suspended in 100 µl of P3 nucleofection solution (specific for primary cell lines and provided with the kit) mixed with DNA, placed in a cuvette and pulsed with the cell-type-specific nucleofection program. Transfected cells were cultured on transwell supports in DMEM with 4.5 g/L glucose supplemented with 10% FBS (v/v) and 1% penicillin-streptomycin mix (v/v).

#### 3.8.2 Nucleofection of A549 cells

A549 cells were plated on culture dishes and reached approximately 60% confluency on the day of transfection. After washing with PBS and trypsinization, cells were counted and re-suspended in 100 µl SF solution (provided with the kit). Next, A549 cells were mixed with 4-6 µg of the desired DNA(s) and transfected in nucleofection cuvettes. After 10 min of incubation the transfected cells were diluted 1:1 in cultured media and plated (~2 x $10^6$ cells per 35 mm dish).

### 3.8.3 Transfection with siRNA

In some studies, A549 cells were transfected with siRNA using Lipofectamine RNAiMAX (Invitrogen, Waltham, USA) 24 h before nucleofection with ENaC plasmids.

A549 cells were transfected with siRNA (concentrations are specified in Table 3.3) and Lipofectamine RNAiMax (7 µl per reaction), both diluted in Opti-MEM (Life Technology). The diluted siRNA was added to the diluted Lipofectamine RNAiMax after 5 min of preincubation at the room temperature. The siRNA-lipid mix was incubated for additional 20 min at the same temperature and then added to the cells. After 24 h, cells were collected and transfected with ENaC plasmids by nucleofection.

## 3.9 Hypercapnia treatment

To investigate effects of hypercapnia on ENaC expression and function, cells were treated with 40 mmHg (normocapnia, Ctrl) or 120 mmHg $CO_2$ (hypercapnia, $CO_2$) for various times (specified along the thesis). The normocapnic and hypercapnic media were prepared in 4.5 g/L glucose DMEM and F12 supplement (Thermo Scientific, Dreieich, Germany). To keep the pH constant (7.4) at 40 mmHg or 120 mmHg $CO_2$ the buffering capacity of the media was altered by changing its initial pH with Tris base. The desired $CO_2$ levels were achieved by equilibrating the solutions overnight in a humidified chamber. In the chamber, cells were treated with a $pCO_2$ of 120 mmHg while maintaining 21% $O_2$ balanced with $N_2$. Before and after treatment with $CO_2$, the level of $CO_2$ and pH were controlled by using a Rapidlab blood gas analyzer.

Table 3.6 Composition of normocapnic and hypercapnic media.

| **Supplement** | **Normocapnic media [ml]** | **Hypercapnic media [ml]** |
|---|---|---|
| DMEM media with FBS and penicillin-streptomycin mix | 3 | 3 |
| Ham´s F-12 medium | 1 | 1 |
| Tris base solution 0.5 M (pH 7.4) | 0.5 | - |
| Tris base solution 0.5 M (pH 11) | - | 0.5 |

### 3.10 Biotinylation of cell surface proteins

To analyze the effects of hypercapnia on ENaC expression at the plasma membrane, cells were washed with PBS containing $Mg^{2+}$ and $Ca^{2+}$ and incubated with membrane impermeable biotin (Pierce Biotechnology, Waltham, USA) dissolved in PBS (1 mg/ml) for 20 min. After biotinylation, excess biotin was removed through three 10 min washes with 100 mM glycine (Sigma Aldrich). Next, cells were rinsed two further times with ice-cold PBS and lysed with lysis buffer (50 mM HEPES, 150 mM NaCl, 1 mM EGTA, 10% Glycerol, 1% TritonX100) containing a protease inhibitor (Complete; Sigma Aldrich) for 20 min. Later, cells were scraped and the collected lysates were centrifuged for 10 min at 10000 rpm at 4 °C. Protein concentrations were quantified using Quick-Start Bradford-Assay (BioRad), according to the instructions of the manufacturer. Protein absorbance was measured using a Biophotometer. 120 µg protein was incubated with streptavidin-agarose beads (Pierce Biotechnology) overnight at 16 rpm, 4 °C. On the next day beads were washed with buffer A, B, C and 10 mM Tris (Table 3.7)

Table 3.7 Buffers employed for washing of agarose beads.

| **Buffer A** | **Buffer B** | **Buffer C:** |
|---|---|---|
| 150 mM NaCl | 500 mM NaCl | 500 mM NaCl |
| 50 mM Tris pH 7.4 | 20 mM Tris pH 7.4 | 20 mM Tris pH 7.4 |
| 5 mM EDTA | 5 mM EDTA | 0.2% BSA |

To elute biotin-labeled proteins, resins were boiled in 2X Laemmli sample buffer containing 10% β-mercaptoethanol and 20 mM DTT at 98 °C for 10 min. Proteins were analyzed by SDS-PAGE and western blotting.

### 3.11 SDS-PAGE and western blotting

Western blot experiments were performed to analyze the effects of hypercapnia on ENaC expression and to determine the phosphorylation status of proteins involved in the hypercapnic signaling pathway.

50-120 µg protein was combined with 2X Laemmli sample buffer and heated to 98 °C for 10 min prior to loading into the gel. Blots were run in 8% polyacrylamide gels (Roth, Karslruhe, Germany) (Table 3.8). Electrophoresis was carried out in running buffer (Table 3.9) at 100-120 V for 1.5 h.

Table 3.8. SDS-PAGE gel composition.

| 8% separating gel (20 ml) | Volume [ml] | 5% stacking gel (10 ml) | Volume [ml] |
|---|---|---|---|
| $H_2O$ | 9.3 | $H_2O$ | 6.8 |
| 1.5 M Tris pH 8.8 | 5.3 | 1.5 M Tris pH 6.8 | 1.3 |
| 30% Acrylamide/Bis | 5.0 | 30% Acrylamide/Bis | 1.7 |
| 10% SDS | 0.2 | 10% SDS | 0.1 |
| 10% APS | 0.2 | 10% APS | 0.01 |
| TEMED | 0.012 | TEMED | 0.001 |

Protein transfer to a nitrocellulose membrane (BioRad) was performed using the semi-dry method at 400 mA for 60 min in transfer buffer (Table 3.9). The membranes were blocked with 5% (m/v) fat-free dried milk (Sigma Aldrich) for 1 h and incubated with primary antibody overnight at 4 $^{o}$C.

Table 3.9 Running and transfer buffers.

| Running Buffer (1L) | Amount [g] | Transfer Buffer (1L) | Amount |
|---|---|---|---|
| Tris | 30 | Tris | 2.45 g |
| Glycine | 144 | Glycine | 12.2 g |
| SDS | 100 | Methanol | 20% [v/v] |

On the next day, membranes were washed 3 times with washing buffer (T-TBS) (Table 3.10) and the secondary antibody conjugated to horseradish peroxidase (HRP) was added for 1 h. Unspecific antibody binding was reduced by 3 times washing with T-TBS after removing the secondary antibody. Next, membranes were incubated with a SuperSignal West Pico or a Femto Chemiluminescent Substrate detection kit (Thermo Scientific), films were developed, and the density of proteins was quantified using the ImageJ software (National Institutes of Health, Bethesda, Maryland, USA). To reprobe the blots, membranes were treated with stripping buffer (Table 3.10) for 50 min at the room temperature, blocked again in 5% milk and another antibody was added.

Table 3.10 Washing and stripping buffers.

| Washing Buffer (TBS-T) (1L) | Amount | Striping Buffer (25 ml) | Volume [ml] |
|---|---|---|---|
| Tris | 2.45 g | 1M Glycine | 2.5 |
| NaCl | 8.0 g | $H_20$ | 22.5 |
| Tween 20 | 1 ml | 37% HCl | 0.25 |

### 3.12 Ubiquitination experiments

To assess the level of ENaC ubiquitination, A549 cells were transfected with ENaC plasmids (2 μg of each) and HA-ubiquitin (3 μg). In some studies, cells were co-transfected with a plasmid encoding HA-Nedd4-2 (wild type or T899A mutant, 2 μg) or a siRNA against AMPK-α1 or Nedd4-2 (or scrambled siRNA). After transfection cells were exposed to normocapnic (Ctrl; 40 mmHg of $CO_2$) or hypercapnic ($CO_2$; 120 mmHg of $CO_2$) media for 15-30 min and lysed on ice in lysis buffer. Proteins were resolved on a 8% polyacrylamide gel. The immunoblots were performed with anti-GFP, anti-V5 or anti-HA antibodies to detect α-, β- or γ-ENaC, respectively. X-ray films were overexposed to detect ENaC ubiquitin conjugates, which represent only a minor fraction of the total ENaC proteins. An increase in ENaC ubiquitination due to elevation in $CO_2$ levels was further confirmed by co-immunoprecipitation described in paragraph 3.14.

### 3.13 Phosphorylation studies

For studying phosphorylation of specific kinases implicated in the hypercapnia-induced ENaC downregulation, cells were exposed to normal (Ctrl; 40 mmHg of $CO_2$) or elevated ($CO_2$; 120 mmHg of $CO_2$) $CO_2$ levels for different time intervals. After treatment, cells were washed with PBS twice and were lysed on ice in lysis buffer. Next, samples having equal amount of protein were resuspended in 2X Laemmli sample buffer and heated to 98 $^{o}$C for 10 min prior to loading into the gel. The proteins were subjected to western blot analysis with first phospho-specific antibodies and then blots were reprobed with an antibody against the protein of interest to detect total protein levels. Phospho and total protein levels were measured and quantified using the ImageJ software.

### 3.14 Co-Immunoprecipitation

To investigate protein-protein interaction co-immunoprecipitation (co-IP) was carried out. The first set of co-IP experiments was performed to detect ubiquitinated ENaC isoforms. To this end, A549 cells were nucleofected with β-ENaC and HA-ubiquitin and exposed to normocapnic (Ctrl; 40 mmHg of $CO_2$) or hypercapnic ($CO_2$; 120 mmHg of $CO_2$) media for 30 min. Next, cells were washed three times with PBS and lysed in lysis buffer for 20 min. 750 μg protein was precleared with A/G agarose beads (Santa Cruz, Heidelberg, Germany). Precleared lysates were rotated with

anti-V5 antibodies overnight at 4 °C. Then, antigen-antibody complexes were immunoprecipitated by adding 80 μl of A/G agarose beads, rotated overnight at 4 °C and washed 4 times with lysis buffer containing protease inhibitor, Complete. Agarose beads were combined with 2X Laemmli sample buffer and heated to 98 °C for 10 min prior to loading on the gel. β-ENaC ubiquitinated isoforms were detected with anti-HA antibody.

To elucidate the role of Nedd4-2 in β-ENaC ubiquitination, immunoprecipitation of β-ENaC was performed. A549 cells were transfected with plasmids coding human β-ENaC-V5 and human HA-Nedd4-2 and were exposed to normocapnic or hypercapnic media for 30 min. To confirm the β-ENaC–Nedd4-2 interaction, precleared lysates were incubated with rabbit anti-V5 antibody overnight, next the antibody-antigen complexes were combined with A/G agarose beads. Western blot was first probed with mouse anti-HA antibody to detect Nedd4-2 and then reprobed with anti-V5 antibody to confirm the presence of β-ENaC in the precipitated complex. Anti-rabbit IgG was used as negative control (Sigma Aldrich).

### 3.15 Immunofluorescence microscopy

Immunofluorescent staining was performed to study membrane expression of α-ENaC. A549 cells were treated with normocapnia ("Ctrl" 40 mmHg of $CO_2$) or hypercapnia ("$CO_2$" 120 mmHg of $CO_2$) for 30 min and then were fixed by incubation with 4% paraformaldehyde for 10 min (Thermo Scientific). A549 cells were washed three times with PBS and permeabilized with 0.1% saponin (Sigma Aldrich) for 5 min. Unspecific binding was blocked by incubation with 5% BSA (PAA Laboratories) diluted in PBS for 1 h at room temperature. After overnight incubation with a 1:50 dilution of the anti-α-ENaC antibody, cells were washed three times with PBS and incubated for 1 hour at room temperature with 1:500 dilution of Alexa Fluor-488 secondary antibody. Stained cells were washed with PBS three times and 3 μl of ProLong Gold with DAPI (Thermo Scientific) were applied. Images were obtained using a fluorescent microscope (Leica DMIL), a digital camera (Leica DFC 420C) and the software Leica application suite 330.

### 3.16 Real time PCR

Total RNA was extracted form A549 cells after 30 min exposure to normocapnic ("Ctrl" 40 mmHg of $CO_2$) or hypercapnic ("$CO_2$" 120 mmHg of $CO_2$) solutions, using the standard protocol of

RNeasy-Kit (Qiagen, Hilden, Netherlands). The RNA was diluted in RNA-free water and the concentration was determined by NanoDrop 1000. RNA samples were kept at -70 °C. 1 µg of total RNA was used to generate cDNA using an iScript cDNA synthesis kit (BioRad). The reaction mix is showed in Table 3.11.

Table 3.11Mix for cDNA synthesis.

| **Component** | **Volume [µl]** |
|---|---|
| 5x Reaction buffer | 4 |
| RNA 1µg | x |
| Reverse transcriptase | 1 |
| $H_2O$ | to 20 |

Finally, the cDNA was diluted 1:5 or 1:10 and qRT-PCR was performed with Syber Green Master Mix (BioRad) using cycle conditions showed below:

| | | | |
|---|---|---|---|
| Initial Denaturation | 60 s | 95°C | |
| Denaturation | 60 s | 95°C | } x40 |
| Primer annealing and elongation | 30 s | 55°C | |
| Cool down | - | 4°C | |

α-ENaC and β-ENaC mRNA expression levels were normalized to human glyceraldehyde 3-phosphate dehydrogenase (GAPDH) as an endogenous control. The primer sequences used for real-time analysis were synthesized by Eurofins Genomic (Ebersberg, Germany) and are shown in Table 3.12.

Table 3.12 Primer sequences for real-time PCR.

| **Targets** | **Sequence (5'->3')** |
|---|---|
| αENaC | Fwd ACTTCAGCTACCCCGTCAGC<br>Rev GAGCGTCTGCTCTGTGATGC |
| βENaC | Fwd GCACCGTGAATGGTTCTGAG<br>Rev CGGATCATGTGGTCTTGGAA |
| GAPDH | Fwd AGCACCAGGTGGTCTCCTCT<br>Rev CTCTTGTGCTCTTGCTGGGG |

### 3.17 Electrophysiology

To investigate the effects of elevated $CO_2$ levels on transepithelial $Na^+$ transport, Ussing chamber experiments were performed on H441 cells. For these measurements, cells were grown on clear inserts [12 mm diameter with 0.4 μm pore size] (Corning) in the presence of 100 nM dexamethasone until a tight epithelium was formed. Next, the monolayers were treated with normocapnic ("Ctrl" 40 mmHg of $CO_2$) or hypercapnic ("$CO_2$" 120 mmHg of $CO_2$) media for 30 min and mounted into a Ussing chamber filled with Kreb's solution (117 mM NaCl, 2.7 mM KCl, 1.2 mM $MgSO_4$, 1.2 mM $KH_2PO_4$, 25 mM $NaHCO_3$, 1.8 mM $CaCl_2$, 11mM Glucose) at 37 °C. The chambers were attached to a voltage clamp amplifier through Ag/AgCl electrodes filled with 3M KCl-agar (Sigma Aldrich). Short circuit currents ($I_{sc}$) were measured and recorded using LabChart version 8.

To calculate the amount of amiloride-sensitive ($I_{amil\text{-}sens}$) current in H441 monolayers, $I_{sc}$ was measured before and after incubation with 10 μM amiloride (Sigma Aldrich). At least three filters, with different cell passages, were used for the experiments.

### 3.18 Bacterial culture media and growth conditions

Bacteria were grown in Luria–Bertani (LB) media (Sigma Aldrich) overnight at 180 rpm, at 37 °C in the presence of proper antibiotics (Table 3.5). The antibiotic concentrations were as follows: ampicillin (100 μg/mL) and kanamycin (30 μg/mL) (both, Sigma Aldrich). For longer storage glycerol stocks were prepared from the overnight culture mixed with 50% of glycerol (Sigma Aldrich). Strains were stored at 80 °C in cryovials.

### 3.19 Transformation of competent cells

Preparation of competent cells:

To prepare competent cells, fresh, overnight bacterial culture (*E. coli*-DH5α) was grown till $OD_{600}$ of 0.4. Bacteria were kept on ice for 20 min prior to centrifugation at 3000 g at 4 °C for 10 min. Pellets were gently re-suspended in 17 ml cold CCMB80 buffer: 80 mM $CaCl_2$, 20 mM $MnCl_2$, 10 mM $MgCl_2$, and 10 mM KOAc, 10% Glycerol and incubated additional 20 min on ice. Bacteria

were centrifuged as described previously and pellets were re-suspended in 4.2 ml CCMB80 buffer. Chemically competent cells were aliquoted, frozen and stored at -80 °C.

Transformation:

The chemically competent bacteria were transformed with plasmids by heat shock method (Sambrook and Russell 2001). Briefly, competent cells were mixed with 100 ng of DNA and incubated on ice for 30 min. Then mixture of cells and DNA were placed into water bath at 42 °C for 45 s and placed again on ice for 2 additional minutes. After this time 450 µl of SOC medium (Invitrogen, Darmstadt, Germany) was added and cells were shook at 250 rpm, at 37 °C for 1.5 h. Transformed bacteria were cultured on LB agar plates containing a proper antibiotic and incubated overnight at 37 °C.

### 3.20 DNA isolation and purification

Plasmids were isolated using plasmid Maxi kit (Qiagen) according to the standard protocol. All buffers were provided with the kit. Briefly, 200 ml of overnight cultured bacteria containing the desired DNA were centrifuged at 6000 rpm for 15 min at 4°C. The medium was removed, and the pellets were re-suspended in 10 ml of resuspension buffer containing RNase A (P1). Lysis was performed by addition of 10 ml SDS-alkaline buffer (P2). After 5 min of incubation at room temperature, 10 ml of neutralization buffer (P3) was added. The cell lysates were incubated for 20 min on ice prior to centrifugation at 20000 rpm at 4 °C for 30 min. QIA filter columns were washed with 10 ml equilibration buffer (QBT) and the supernatant from the previous step was loaded onto the column. After washing with 60 ml of wash buffer (QC), DNA was eluted with 15 ml of elution buffer (QF) and precipitated with 10.5 ml cold isopropanol. After centrifugation at 15000 rpm for 30 min, DNA pellets were washed with 70% ethanol (Otto-Fischer GmbH, Saarbrücken, Germany) centrifuged again (15000 rpm at 4 °C for 5 min) and dried on air. Finally, DNA was dissolved in 100 µl TE buffer and plasmid concentration was measured by NanoDrop 1000.

### 3.21 Site-directed mutagenesis

Site-directed mutagenesis was performed to generate human Nedd4-2 mutant (T899A) encoded in pCI-HANEDD4L plasmid. The specific substitution was performed using Quick-Change Site-

Directed Mutagenesis kit (Stratagene, La Jolla, USA) in accordance with the manufacturer's instructions. The reaction is based on amplification of a plasmid coding the protein of interest with high-fidelity DNA polymerase (*PfuUltra*) and primers containing the desired mutation in the sequence (Table 3.13). The cycle parameters used in experiment are shown below:

| | | | |
|---|---|---|---|
| Initial Denaturation | 60 s | 95 °C | |
| Denaturation | 50 s | 95 °C | x18 |
| Primer annealing | 50 s | 60 °C | |
| Elongation | 7 min | 68 °C | |
| Cool down | - | 4 °C | |

Table 3.13 Primer sequences for SDM

| **Primers** | **Sequence (5'->3')** |
|---|---|
| NeddT899A_fwd | ACTGCAGTTTGTCGCAGGGACATCG CGAG |
| NeddT899A_rev | CTCGCGATGTCCCTGCGACAAACTGCAGT |

After PCR amplification, the product of the reaction was treated with 0.5 µl DpnI (provided with the kit) at 37 °C for 1 h to remove methylated, parental DNA. DpnI-treated DNA and control plasmid were transformed to ultra-competent cells (XL10-Gold) by the heat shock method as described in Section 3.19 and plated on LB-agar plates containing ampicillin (100 µg/mL). The positive colonies were subcultured into LB media and grown overnight at 37 °C. DNA was isolated and sequenced to confirm the presence of the desired mutation as described in Section 3.24.

### 3.22 Gibson assembly

The extracellular signal-regulated kinase (ERK) has been reported as a potential regulator of ENaC/Nedd4-2 interaction (Shi et al. 2002). To study the role of ERK1/2-dependent phosphorylation of β-ENaC, the codon encoding the T615 residue was deleted from β-ENaC-positive pcDNA 3.1V5/His plasmid by using the Gibson assembly method. This technique allows assembly of multiple DNA fragments in a single reaction. Briefly, plasmid amplification was carried out in a way that resulted in PCR products that did not include the T615 residue (β-ΔT615) using two sets of primers shown in Table 3.14. The two amplified fragments were assembled together using Gibson master mix according to the manufacturer's protocol (New England Biolabs, Frankfurt, Germany). Following the transformation of the assembled plasmid to highly competent

*E. coli* DH5α, cells were plated on 100 mg/L ampicillin LB-agar plates and incubated overnight at 37 °C. The grown colonies were collected and screened by sequencing to confirm the presence of the desired mutation.

Table 3.14 Primer sequences for Gibson assembly experiments.

| **Primers:** | **Sequence (5'->3')** |
|---|---|
| βENaCΔT615_Frg1_fwd | GCCCTGCCCATCCCAGGCCCGCCCCCCAACTATGAC |
| βENaCΔT615_Frg1_rev | ATCGTAGTTATCTACACGACGGGGAGTCAGGCAACTATG |
| βENaC ΔT615_Frg2_fwd | AGTTGCCTGACTCCCCGTCGTGTAGATAACTACGATACGGGAGGGC |
| βENaC ΔT615_Frg2_rev | GTCATAGTTGGGGGGCGGGCCTGGGATGGGCAGGGC |

### 3.23 Agarose gel

1% agarose gels was prepared according to the standard procedure (Sambrook and Russell 2001) to assess the size of PCR products. The DNA was mixed with 5X loading buffer prior to loading into the gel and electrophoresis was performed in 1x TAE buffer (4.8 g Tris, 100 ml EDTA (pH 8), 57 ml acetic acid, supplemented with 5 mg/L of ethidium bromide) at 150 V, 250 mA for 1 h.

### 3.24 DNA sequencing

DNA sequencing was performed by SeqLab Company (Göttingen, Germany). To confirm the mutation in Nedd4-2, the reaction was performed with EBV-rev primers using Sanger Cycle Sequencing/Capillary Electrophoresis. Deletion of T615 of β-ENaC was proven by DNA sequencing using BGH-rev primer. The sequences were compared using the bioinformatics tool BLAST.

### 3.25 Data analysis and statistic

All experiments were performed at least in triplicates using cells from different passages. Data were statistically analyzed using one-way analysis of variance (ANOVA) followed by a multiple comparison with Dunnet test and are presented as mean ± standard error of the means (SEM). *P* values of less than 0.05 were considered statistically significant. For the analysis and data presentation Graph Pad prism 6 (GraphPad software, San Diego, CA) was used.

# 4. Results

Primary ATII cell cultures play an essential role in studies focusing on alveolar epithelial barrier function and transepithelial ion transport. Thus, our key studies were performed in this cell type. However, due to the high complexity of some assays and the need of co-transfection with up to four constructs, which is extremely challenging in this cell type, most of the studies were performed in human A549 cells that are regularly used as a substitute for pneumocytes *in vitro* (Sporty et al. 2008) and have been shown to express all elements of the $Na^+$ transport machinery similarly to primary pneumocytes (Matalon et al. 2015).

While A549 cells express ENaC and the Na,K-ATPase, this cell line does not form tight polarized monolayers that leads to relatively low transepithelial electrical resistance (TEER) (Elbert et al. 1999). In contrast, several studies reported that the human H441 cell line is capable of forming physiologically relevant TEER when grown on the permeable supports (Hermanns et al. 2004; Neuhaus et al. 2012). Moreover, these cells express markers characteristic for human ATII and are a well-established model for pulmonary sodium transport (Salomon et al. 2014), thus the impact of high $CO_2$ levels on transepithelial $Na^+$ transport was studied using H441 cells.

To study the effects of hypercapnia on ENaC expression and function, cells were treated with 120 mmHg of $CO_2$. Such high $CO_2$ concentrations in blood and tissues may occur in patients with pulmonary diseases, including patients with ARDS who require lung-protective mechanical ventilation (Vadász et al. 2012; Bellani et al. 2016). However, the increase in $CO_2$ concentrations in turn, decreases pH. In order to differentiate between the effects of elevated $CO_2$ levels and the associated acidosis, the level of extracellular pH ($pH_e$) was maintained at 7.4 in all experiments. Importantly, it has been previously reported that treatment of cells with elevated $CO_2$ concentrations at a $pH_e$ of 7.4 causes only a minor and temporary decrease in intracellular pH ($pH_i$) that rapidly returns to baseline (Briva et al. 2007).

### 4.1 Hypercapnia alters ENaC expression at the cell surface of alveolar epithelial cells

ENaC-mediated $Na^+$ transport across the alveolar epithelium controls alveolar fluid homeostasis and provides a thin diffusion barrier for efficient gas exchange (Matthay et al. 2002). Since AFC depends on optimal function of ENaC (Canessa et al. 1994; Voilley et al. 1994; Matthay and Zemans 2011; Fronius et al. 2012), the elevated $CO_2$-induced changes in channel activity (which in part depends on the abundance of these channels at the cell surface) may lead to impaired resolution of pulmonary edema in patients with ARDS.

Although hypercapnia-mediated downregulation of the Na,K-ATPase has been demonstrated previously (Briva et al. 2007; Vadász et al. 2008; Welch et al. 2010; Vadász, et al. 2012), the influence of elevated $CO_2$ levels on ENaC regulation remained to be elucidated.

The DNA constructs expressing human α-, β- and γ-ENaC were generated in our laboratory as described previously (Buchbinder 2013; Gwoździńska et al. 2017). Anti-GFP antibodies recognized YFP- and FLAG-tagged α-ENaC construct and revealed a band at 118kDa [α-ENaC (90 kDa) plus YFP (27 kDa) and FLAG (1 kDa)]. V5-tagged β-ENaC construct was detected with anti-V5 antibody, at 96kDa [β-ENaC (95 kDa) plus V5 (1 kDa). Anti-HA antibodies identified myc- and HA-tagged γ-ENaC at 97 kDa (γ-ENaC (95 kDa) plus myc (1kD) and HA (1kDa)) (Figure 4.1).

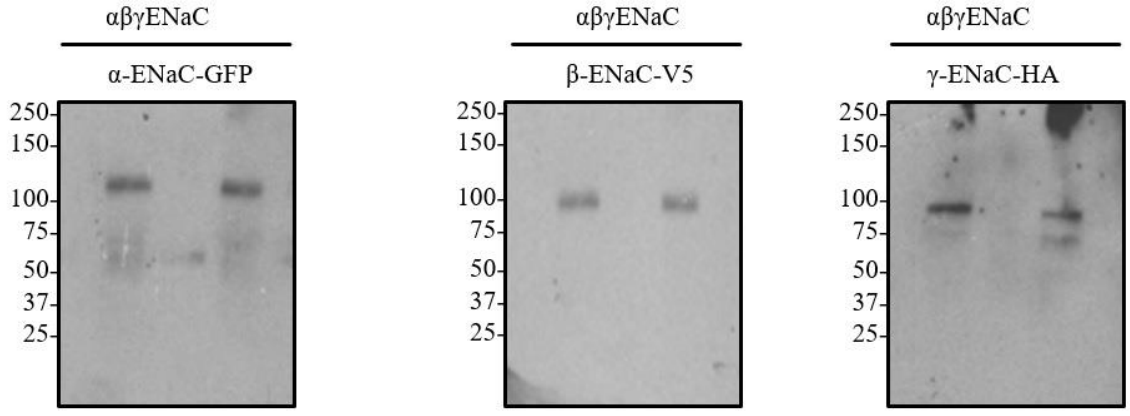


**Figure 4.1 Representative western blots of epitope-tagged epithelial sodium channel (ENaC) subunits at the cell surface of A549 cells.** A549 cells were co-transfected with α-, β- and γ-ENaC and biotin-streptavidin pull down assays followed by western blot analysis were performed with

anti-GFP, anti-V5 and anti-HA antibodies to recognize α-ENaC (118 kDa), β-ENaC (96 kDa) and γ-ENaC (97 kDa), respectively.

Since simultaneous co-expression of three ENaC subunits had negative effects on cell viability, we decided to investigate the impact of hypercapnia on the α/β-ENaC complex. Although ENaC is a multimeric channel that may contain different combinations of three structurally related subunits, at least one α- or δ-subunit of ENaC is required to produce amiloride-sensitive current (Canessa et al. 1994; McNicholas and Canessa 1997; Hanukoglu and Hanukoglu 2016). β- and γ-ENaC are crucial for channel trafficking and interestingly, they have high amino-acids homology, thus probably exhibit similar function (Bhalla and Hallows 2008).

Biotin-streptavidin pull down assays were performed to study the cell surface abundance of α- and β-ENaC in A549 and ATII cells upon exposure to 40 mmHg or 120 mmHg of $CO_2$ (normocapnia; Ctrl and hypercapnia; $CO_2$, respectively) at a $pH_e$ of 7.4 for 30 min. Expression of the α/β-ENaC complex at the plasma membrane was significantly higher in cells exposed to normocapnia compared to those exposed to hypercapnia. Treatment of cells with high $CO_2$ levels decreased number of α- and β-ENaC molecules at the cell surface of A549 cells by approximately 60% (Figure 4.2).

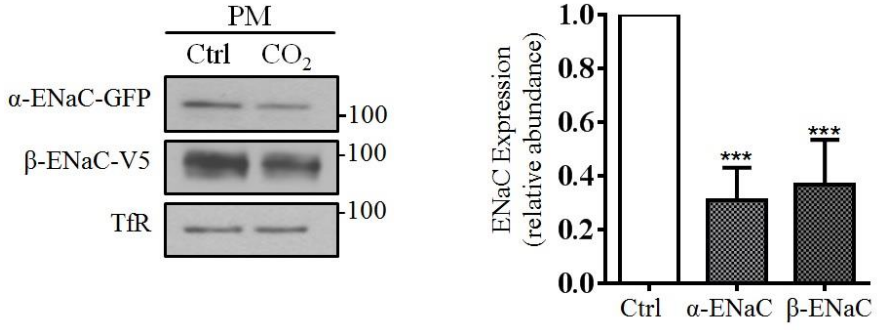


**Figure 4.2 Representative western blots and quantification of α- and β-ENaC expression at the surface of A549 cells upon normocapnia and hypercapnia.** A549 cells were transfected with α- and β-ENaC and were treated with 40 mmHg $CO_2$ (Ctrl) or 120 mmHg $CO_2$ ($CO_2$) for 30 min at a $pH_e$ of 7.4. The plasma membrane (PM) expression of the proteins was determined by cell surface biotinylation and subsequent immunoblotting with anti-GFP (α-ENaC), anti-V5 (β-ENaC) and

anti-transferrin receptor (TfR) antibody. TfR was used as a loading control. Bars represent mean ± SEM. n=3, ***p<0.001.

Having shown that hypercapnia affected cell surface stability of ENaC proteins in A549 cells, we next asked whether elevated $CO_2$ levels cause similar effects in primary ATII cells. The transfection of these cells remains difficult however, we recently reported that nucleofection leads to highly efficient DNA delivery without affecting integrity of ATII cells, even when high amount of plasmidic DNA is delivered (Grzesik et al. 2013). Rat primary ATII cells were nucleofected with plasmids encoding α- and β-ENaC and were treated with normocapnia (Ctrl) or hypercapnia ($CO_2$) for 30 min at a $pH_e$ of 7.4. 18 h after transfection the density of ENaC subunits at the plasma membrane was determined by cell surface biotinylation. Analysis of α- and β-ENaC membrane expression revealed that elevated $CO_2$ levels increased ENaC endocytosis in ATII cells (Figure 4.3). The hypercapnia-treated cells exhibited a reduction of α-ENaC cell surface expression by approximately 70%, compared to α-ENaC levels measured upon normocapnic exposure. The concentration of β-ENaC at the plasma membrane was decreased by ~50% upon exposure to elevated $CO_2$. These data are similar to the results obtained using immortalized human A549 cells, suggesting that ENaC regulation by hypercapnia is comparable in both cell lines.

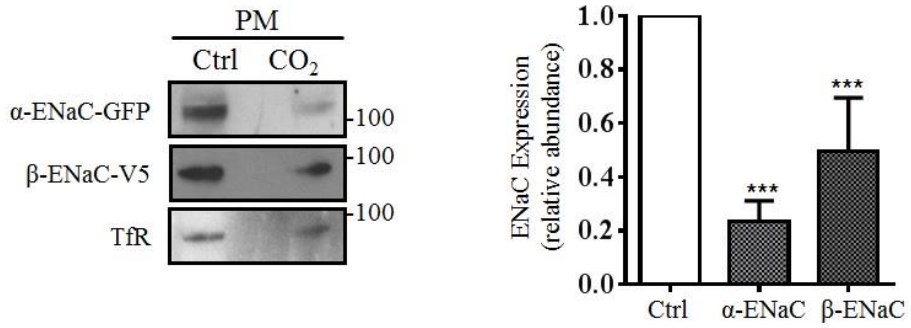


**Figure 4.3 Representative western blots and quantification of α- and β-ENaC expression at the surface of ATII cells upon normocapnia and hypercapnia treatment.** ATII cells were co-transfected with α- and β-ENaC and exposed to 40 mmHg $CO_2$ (Ctrl) or 120 mmHg $CO_2$ ($CO_2$) for 30 min at a $pH_e$ of 7.4. By streptavidin pull downs and western blot analysis the plasma membrane (PM) expression of the ENaC proteins and transferrin receptor (TfR) was determined. Bars represent mean ± SEM. n=3, ***p<0.001.

The importance of α-ENaC in AFC has been reported previously (Hummler et al. 1996). Our results from the biotinylation assays indicated a significant reduction of α-ENaC cell surface abundance upon acute hypercapnia exposure. To further confirm these effects of hypercapnia, immunofluorescence studies were conducted in which localization of α-ENaC was observed after exposure of A549 cells to normocapnic (Ctrl) or hypercapnic ($CO_2$) solutions at a $pH_e$ of 7.4 for 30 min. In cells treated with hypercapnia, immunofluorescence images showed a predominantly intracellular localization of α-ENaC and a marked decrease of channel abundance at the cell surface when compared to normocapnic controls, suggesting that hypercapnia induces translocation of ENaC form the cell surface to intracellular compartments (Figure 4.4).

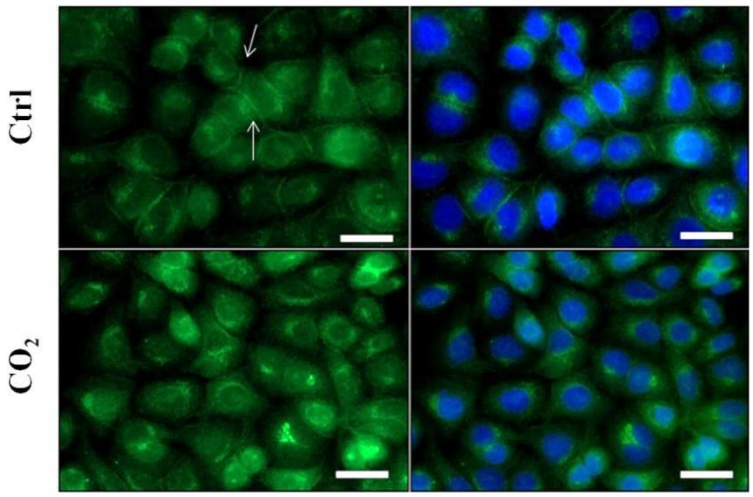


**Figure 4.4 Fluorescent images of subcellular localization of α-ENaC in A549 cells upon normocapnic and hypercapnic exposure.** A549 cells were treated with 40 mmHg $CO_2$ (Ctrl) or 120 mmHg $CO_2$ ($CO_2$) for 30 min at a $pH_e$ of 7.4 and cellular distribution of α-ENaC was assessed by using an anti α-ENaC antibody followed by Alexa Fluor 488-conjugated secondary antibody. Nuclei were labeled with DAPI. Scale bar =10 μm.

### 4.2 Short-term hypercapnia does not modify total intracellular level of ENaC in alveolar epithelial cells

Next, we evaluated the impact of elevated $CO_2$ concentrations on total intracellular levels of ENaC in A549 and ATII cells. Both cell types were transfected with α- and β-ENaC prior to exposure to normocapnia (Ctrl) or hypercapnia ($CO_2$) for 30 min at a $pH_e$ of 7.4 and total amounts of α- and β-

ENaC proteins were determined in whole cell lysates. Importantly, intracellular concentrations of the channel subunits remained unchanged in A549 (Figure 4.5A) and in ATII cells (Figure 4.5B) further confirming that elevated $CO_2$ levels probably induced trafficking of ENaC from the plasma membrane.

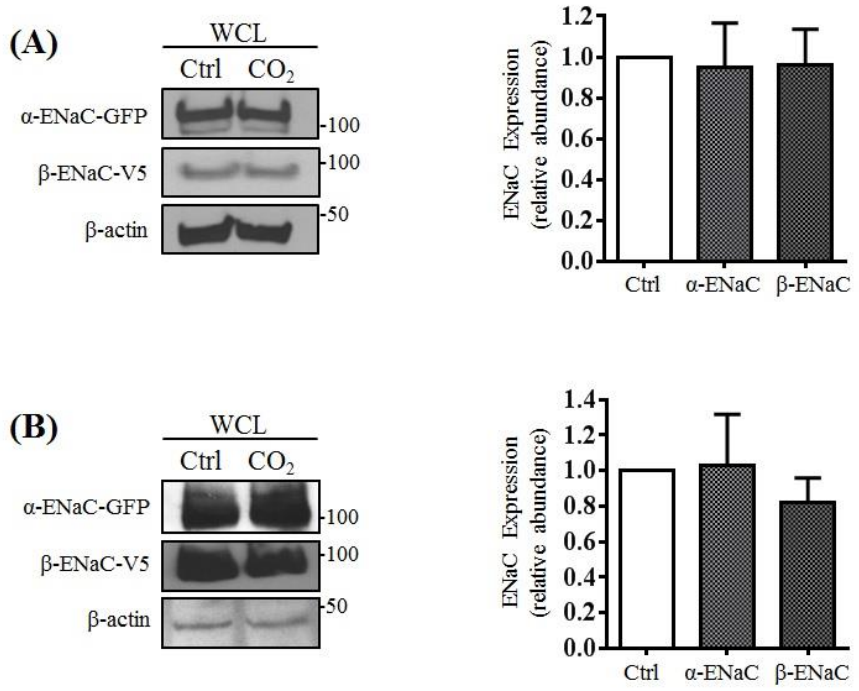


**Figure 4.5 Representative immunoblots and quantifications of intracellular expression levels of ENaC in human and rat alveolar epithelial cells upon normocapnia and hypercapnia treatment.** (A) A549 cells were co-transfected with α- and β-ENaC and were exposed to 40 mmHg $CO_2$ (Ctrl) or 120 mmHg $CO_2$ ($CO_2$) for 30 min at a $pH_e$ of 7.4. The whole cell levels (WCL) of ENaC proteins were determined by western blot analysis with anti-GFP (α-ENaC) and anti-V5 (β-ENaC) antibodies. (B) ATII cells were co-transfected and exposed to normo- or hypercapnia as described above and the total levels of ENaC proteins were assessed by western blot analysis with the above mentioned antibodies. β-actin was used as a loading control. Bars represent mean ± SEM. n=3-4.

### 4.3 Impact of acute hypercapnia on ENaC mRNA expression

In next phase of our studies, the potential effects of hypercapnia on mRNA expression of ENaC subunits were investigated. To this end, A549 cells were treated with either normocapnia (Ctrl) or

hypercapnia ($CO_2$) for 30 min at a $pH_e$ of 7.4. After treatment, isolated mRNA was converted to a complementary DNA (cDNA) and real-time PCR was performed. Of note, the levels of transcripts encoding α- and β-ENaC were not changed upon acute hypercapnia treatment (Figure 4.6). These results are in agreement with previous findings showing that short-term exposure of ENaC to various pathological stimuli (hypoxia or TGF-β) at least initially do not change the transcriptional expression of the channel (Gille et al. 2014; Peters et al. 2014).

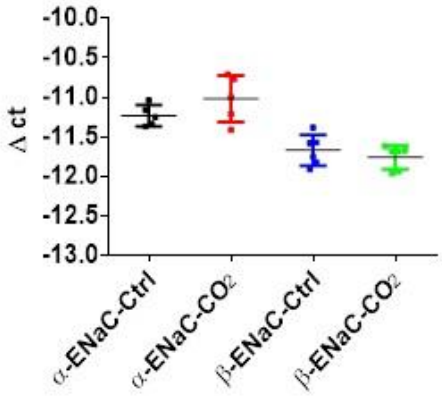


**Figure 4.6 Relative mRNA levels of α- and β-ENaC upon acute hypercapnia treatment**. A549 cells were exposed to 40 mmHg $CO_2$ (Ctrl) or 120 mmHg $CO_2$ ($CO_2$) for 30 min at a $pH_e$ of 7.4 prior to RNA isolation (n=3). The mRNA levels of ENaC subunits were analyzed by real-time PCR and normalized to GAPDH.

### 4.4 Hypercapnia increases ENaC endocytosis by promoting β-ENaC polyubiquitination

Cell surface expression of ENaC is regulated by ubiquitin-dependent endocytosis (Knight et al. 2006; Eaton et al. 2010; Rotin and Staub 2012), thus the aim of the next studies was to assess the role of ubiquitination in the hypercapnia-mediated increase in ENaC retrieval from the cell surface. To this end, each ENaC subunit was overexpressed with human epitope-tagged ubiquitin: either HA-tagged (HA-Ub) (in case of α- and β-ENaC overexpression) or His-tagged (His-Ub) (when cells were transfected with γ-ENaC). After transfection A549 cells were treated with normocapnia (Ctrl) or hypercapnia ($CO_2$) for 15 min and immunoblotting was performed. Hypercapnia significantly increased ubiquitination of β-ENaC (but not α or γ) in total cell lysate of A549 cells as was detected by overexposing films after treating the membranes with the various antibodies

against the tags of the ENaC constructs, which allows identification of ubiquitinated proteins. The results showed that a very short exposure to hypercapnia (15 min) promotes β-ENaC polyubiquitination detected as a "characteristic smear" above the predicted size of β-ENaC (96kDa) (Figure 4.7B). In contrast, short-term hypercapnia did not promote ubiquitination of α- or γ-ENaC (Figure 4.7A and C, respectively).

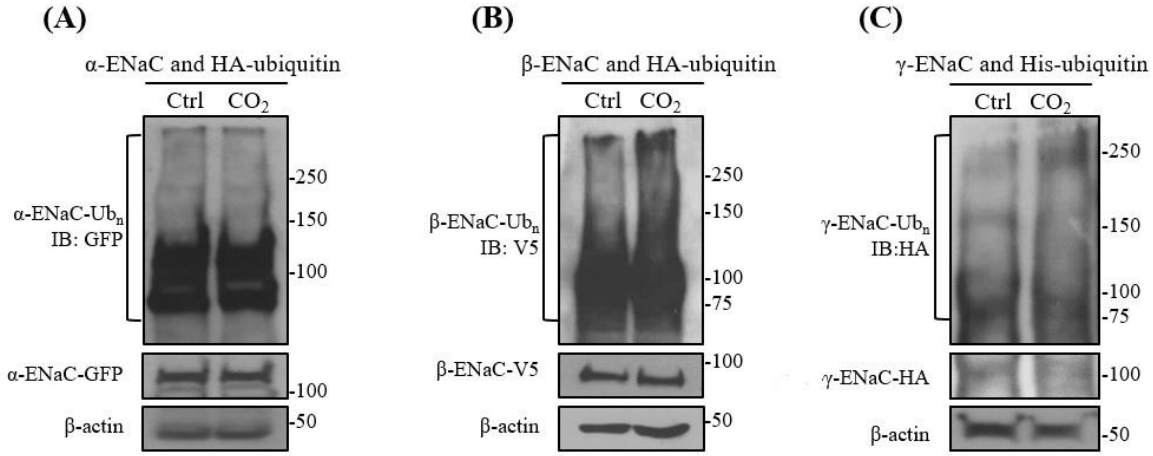


**Figure 4.7 Representative immunoblots of α-, β-and γ-ENaC ubiquitination in A549 cells upon normocapnic and hypercapnic exposure.** A549 cells were transfected with (A) α-ENaC and HA-ubiquitin, (B) β-ENaC and HA-ubiquitin or (C) γ-ENaC and His-ubiquitin prior to exposure to 40 mmHg $CO_2$ (Ctrl) or 120 mmHg $CO_2$ ($CO_2$) for 15 min at a $pH_e$ of 7.4. Total ubiquitinated α-, β- and γ-ENaC were detected by immunoblotting with anti-GFP, anti-V5 and anti-HA antibodies, respectively. β-actin was used as loading control.

An increase in β-ENaC polyubiquitination upon elevated $CO_2$ concentrations was confirmed by the next set of experiments, in which ubiquitinated ENaC isoforms were detected by co-immunoprecipitation. In these studies, A549 cells were co-transfected with β-ENaC and HA-ubiquitin prior to treatment with normocapnia (Ctrl) or hypercapnia ($CO_2$) for 30 min. β-ENaC was immunoprecipitated with rabbit anti-V5 antibody and its ubiquitinated conjugates were identified using a mouse anti-HA antibody. The exposure of cells to hypercapnia resulted in a typical polyubiquitination smear, similar to that observed when using overexposure of films (Figure 4.8).

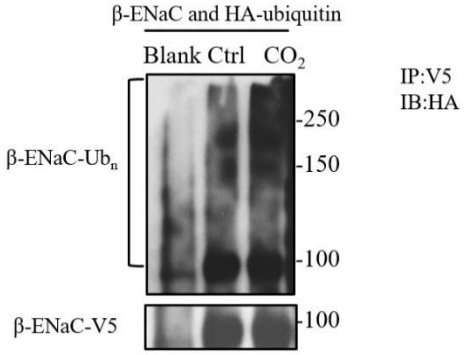


**Figure 4.8 A representative immunoprecipitation experiment presenting β-ENaC polyubiquitination in A549 cells upon normal and elevated $CO_2$ exposure.** A549 cells were co-transfected with β-ENaC-V5 and human HA-tagged ubiquitin prior to exposure to 40 mmHg $CO_2$ (Ctrl) or 120 mmHg $CO_2$ ($CO_2$) for 30 min at a $pH_e$ of 7.4. β-ENaC was immunoprecipitated with anti-V5 antibody and its ubiquitinated conjugates were visualized by using a mouse anti-HA-antibody.

### 4.5 Hypercapnia inhibits epithelial $Na^+$ transport

Several $Na^+$ channels and $Na^+$-coupled transporters have been found to be expressed in alveolar epithelial cells so far, of which ENaC has been associated with the most important role in AFC (Canessa et al. 1994; Voilley et al. 1994; Matalon and Brodovich 1999; Fronius et al. 2012). Thus, we hypothesized that the hypercapnia-induced reduction in ENaC cell surface expression may contribute to reduced alveolar fluid transport capacity and persistence of pulmonary edema.

To this end, the effects of acute hypercapnia on $Na^+$ transport across polarized monolayers of H441 cells were evaluated by electrophysiological studies. The confluent cell monolayers were treated with normocapnia (Ctrl) or hypercapnia ($CO_2$) for 30 min. at a $pH_e$ of 7.4 prior to mounting to an Ussing chamber. The transepithelial potential ($V_t$) was continuously recorded and short circuit current ($I_{sc}$) was calculated. The bioelectrical properties of H441 cells under normocapnic and hypercapnic conditions were compared and revealed impairments of total ($I_{sc}$) as well as amiloride-sensitive ($I_{amil\text{-}sens}$) currents, suggesting downregulation of ENaC activity secondary to the reduction of ENaC cell surface expression in response to elevated $CO_2$ levels. In normocapnia-treated cells, a mean $I_{sc}$ of 9.5 $\mu A/cm^2$ was detected across H441 monolayers. This current was inhibited by approximately 50% after addition of 10 μM amiloride. Treatment of cells with high

$CO_2$ levels decreased $I_{sc}$ to 7.0 µA/cm$^2$, which corresponds to a 25% decrease compared to $I_{sc}$ of normocapnia-treated cells (Figure 4.9A). Elevated $CO_2$ levels primarily affected the amiloride-sensitive fraction of the current, which decreased from 6.2 µA/cm$^2$ in control cells to 3.8 µA/cm$^2$ after hypercapnia treatment, representing a 40% decrease in $I_{amil\text{-}sens}$ (Figure 4.9B). In contrast, the amiloride-insensitive current ($I_{amil\text{-}insens}$) remained unchanged (Figure 4.9C). Similarly, there was no significant difference in $R_t$ between the short-term normocapnic and hypercapnic conditions (Figure 4.9D).

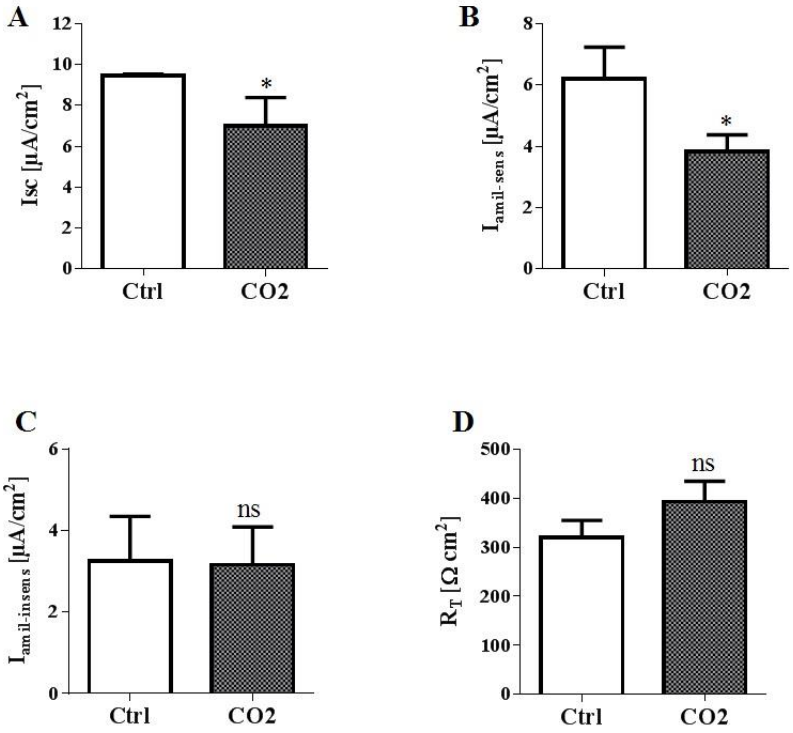


**Figure 4.9 Hypercapnia decreases basal and amiloride-sensitive current of H441 cells.** (A-D) Data from three independent experiments showing comparision between (A) total current; $I_{sc}$, (B) amiloride-sensitive current; $I_{amil\text{-}sens}$ (C) amiloride-insensitive current; $I_{amil\text{-}insens}$ and (D) transepithelial resistance; $R_T$ of H441 monolayers treated with 40 mmHg $CO_2$ (Ctrl) or 120 mmHg $CO_2$ ($CO_2$) for 30 min at a $pH_e$ of 7.4. Amiloride (10µM) was added at the end of the experiments to the apical compartment. Bars shows mean ± SEM (n = 3; * $p < 0.05$).

### 4.6 Nedd4-2 drives elevated $CO_2$-induced ENaC polyubiquitination and retrieval from the cell surface

Various studies have identified Nedd4-2 as a key regulator of ENaC stability in the cytoplasm and cellular membrane (Abriel et al. 1999; Snyder et al. 2001; Knight et al. 2006; Boase et al. 2011; Rotin and Staub 2011). To determine the possible contribution of Nedd4-2 to β-ENaC polyubiquitination in the hypercapnic signaling pathway we first, co-transfected A549 cells with β-ENaC-V5 and HA-Nedd4-2 and exposed to normocapnia (Ctrl) or hypercapnia ($CO_2$) for 30 min. β-ENaC was immunoprecipitated with anti-V5 antibody and the presence of Nedd4-2 in immunoprecipitated complex was confirmed by immunoblotting with anti-HA antibody. We found that Nedd4-2 was associated with β-ENaC in A549 cells when exposed to either regular or elevated $CO_2$ levels, suggesting that Nedd4-2 binds to β-ENaC during normal protein turnover, but also in stress conditions such as upon hypercapnia (Figure 4.10).

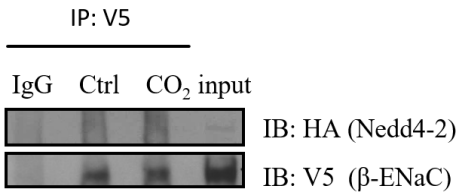


**Figure 4.10 A representative co-immunoprecipitation experiment presenting binding of β-ENaC to Nedd4-2 upon normocapnic and hypercapnic exposure.** A549 cells were co-transfected with β-ENaC-V5 and HA-Nedd4-2 prior to treatment with 40 mmHg $CO_2$ (Ctrl) or 120 mmHg $CO_2$ ($CO_2$) for 30 min at a $pH_e$ of 7.4. β-ENaC was immunoprecipitated from the total lysate with an anti-V5 antibody and Nedd4-2 was detected with an anti-HA antibody. IgG and input were used as negative and possitive controls, respectively.

Next, endogenous levels of Nedd4-2 were silenced by a specific siRNA. A549 cells were treated with siRNA against Nedd4-2 or scrambled (si-Scr) siRNA 24 h prior to nucleofection with β-ENaC and HA-ubiquitin. Next, cells were exposed to normocapnia (Ctrl) or hypercapnia ($CO_2$) for 30 min at a $pH_e$ of 7.4 and the levels of β-ENaC ubiquitination were detected with overexposure of films after treating the membranes with an anti-V5 antibody. Indeed, our data demonstrated that knock-down of Nedd4-2 significantly prevented the $CO_2$-induced polyubiquitination of β-ENaC (Figure 4.11).

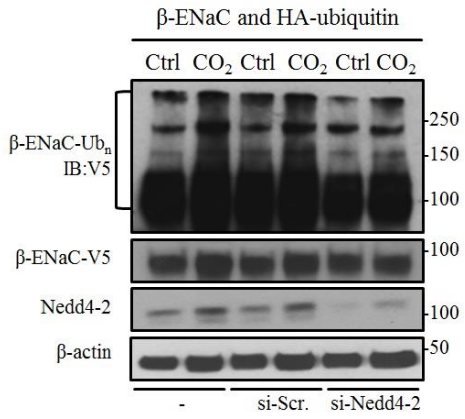


**Figure 4.11 Nedd4-2 mediates hypercapnic polyubiquitination of β-ENaC.** A549 cells were co-transfected with β-ENaC, HA-ubiquitin, and siRNA targeting Nedd4-2 or a scrambled (si-Scr.) siRNA prior to exposure to 40 mmHg $CO_2$ (Ctrl) or 120 mmHg $CO_2$ ($CO_2$) for 30 min at a $pH_e$ of 7.4. β-ENaC polyubiquitinated isoforms were determined by western blot with anti-V5 antibody.

To next test whether Nedd4-2 silencing changed ENaC plasma membrane expression upon hypercapnia treatment, biotin-streptavidin pull down assays were performed. A549 cells were treated with siRNA targeting Nedd4-2 or a scrambled siRNA 24 h before transfection with ENaC plasmids. Then cells were exposed to normocapnia (Ctrl) or hypercapnia ($CO_2$) for 30 min. In line with our previous findings, suggesting the involvement of Nedd4-2 in the hypercapnia-induced ubiquitination of β-ENaC, A549 cells transfected with siRNA against Nedd4-2 showed a significant increase of α- and β-ENaC concentrations at the cell surface compared to cells transfected with a scrambled siRNA and treated with elevated $CO_2$ levels (Figure 4.12).

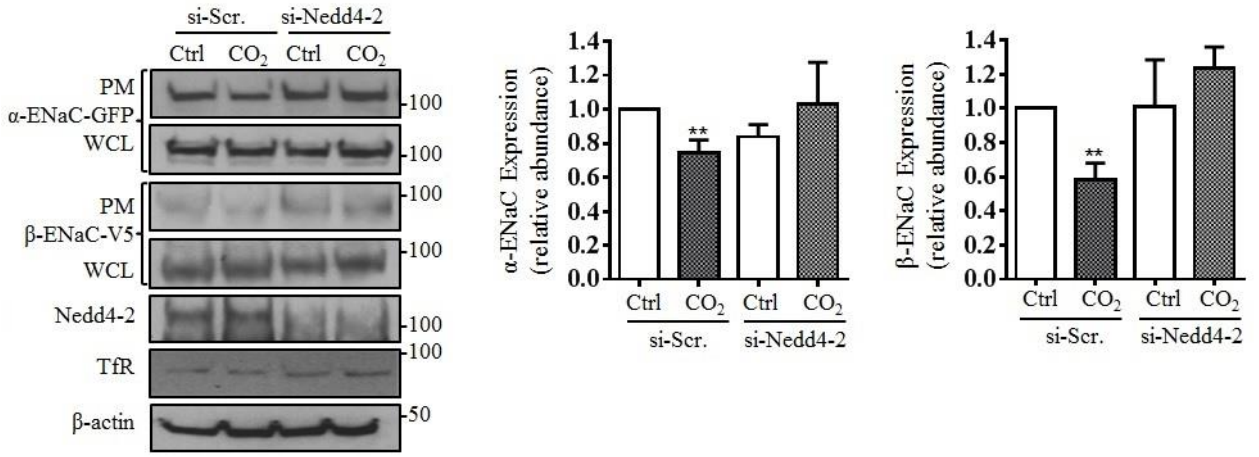


**Figure 4.12 Silencing of Nedd4-2 prevents hypercapnia-induced endocytosis of the α/β-ENaC complex.** A549 cells were co-transfected with α-, β-ENaC and a siRNA against Nedd4-2 or a scrambled (si-Scr.) siRNA prior to exposure to 40 mmHg $CO_2$ (Ctrl) or 120 mmHg $CO_2$ ($CO_2$) for 30 min at a $pH_e$ of 7.4. The plasma membrane (PM) expression of ENaC subunits and transferrin receptor (TfR) was determined by streptavidin pull-down followed by western blot analysis. Representative western blots of ENaC proteins and Nedd4-2 are presented. Bars show mean ± SEM (n = 3; ** $p < 0.01$)

## 4.7 Hyperapnia-induced internalization of α/β-ENaC complex is mediated by ERK1/2-dependent phosphorylation of β-ENaC

Since silencing of Nedd4-2 prevented the hypercapnia-induced β-ENaC polyubiquitination, we speculated that the interaction of these two proteins may be promoted by hypercapnia. Since hypercapnia significantly increased Nedd4-2-dependent polyubiquitination of β-ENaC, we hypothesized that a kinase or kinases activated by hypercapnia may directly or indirectly enhance interaction of β-ENaC and Nedd4-2, as it is well documented that several target proteins undergo phosphorylation prior to ubiquitination (Nguyen et al. 2013)

First, we tested activation of ERK1/2 in A549 cells upon hypercapnia exposure. For this, cells were exposed to normal (Ctrl) or elevated ($CO_2$) $CO_2$ levels for up to 45 min at a pH of 7.4. In line with a previous report (Welch et al. 2010), our results showed a rapid and time-dependent ERK1/2 phosphorylation (that correlates with the activity of the kinase) (Blenis 1993; Cobb and Goldsmith 1995) induced by $CO_2$ that returned to basal level after 45 min of hypercapnia treatment (Figure

4.13A). Since a marked increase of ERK1/2 activity during hypercapnia was detected, next the effect of ERK1/2 activation on β-ENaC phosphorylation status was assessed. A549 cells were transfected with β-ENaC and exposed to normal (Ctrl) or elevated ($CO_2$) $CO_2$ levels for 5 to 15 min. Immunoblots were performed with anti-phospho SCNN1B antibody (specifically recognizes β-ENaC when phosphorylated at the T615). In agreement with previous reports (Shi et al. 2002; Yang et al. 2006; Lazrak et al. 2012; Eaton et al. 2014), we detected a time-dependent increase of β-ENaC phosphorylation at the T615 residue in the presence of active ERK1/2 (Figure 4.13B).

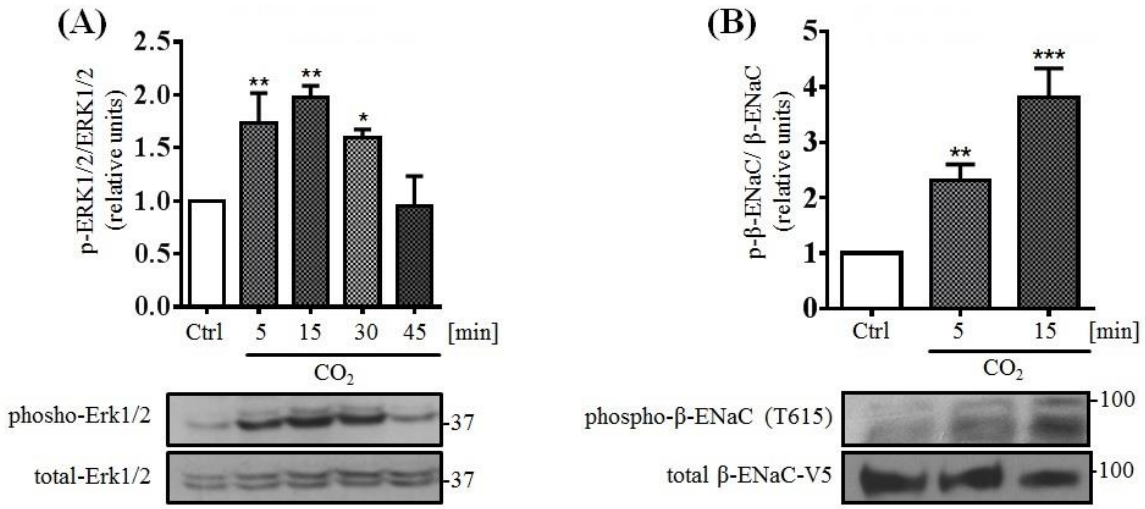


**Figure 4.13 Representative western blots and quantification of time-dependent activation of ERK1/2 and phosphorylation of β-ENaC at T615 residue upon normocapnia and hypercapnia treatment**. (A) A549 cells were treated with 40 mmHg $CO_2$ (Ctrl) for 15 min or 120 mmHg $CO_2$ ($CO_2$) for 5 to 45 min at a $pH_e$ of 7.4. Phosphorylated and total levels of ERK1/2 were measured by western blot analysis. The graph shows phospho/total ERK1/2 ratio. (B) A549 cells were transfected with β-ENaC prior to exposure to normocapnia (Ctrl) for 15 min or hypercapnia ($CO_2$) for 5-15 min. Phoporylation of β-ENaC at the T615 residue and total level of β-ENaC were determined by immunoblotting with anti-phospho SCNN1B antibody and with anti-V5 antibody, respectively. The graph presents phospho/total β-ENaC ratio. Representative western blots are shown. Bars show mean ± SEM (n = 3; * $p < 0.05$; ** $p < 0.01$; *** $p < 0.001$).

To further investigate whether activation of ERK1/2 was necessary for the hypercapnia-induced ubiquitination of ENaC, A549 cells were transfected with β-ENaC and HA-ubiquitin. 18 h later the

transfected cells were pretreated with 10 μM U0126 (MEK inhibitor, upstream of ERK1/2) for 30 min before exposure to normal (Ctrl) or elevated ($CO_2$) $CO_2$ levels for additional 30 min. The polyubiquitination of β-ENaC was determined by immunoblotting with an anti-V5 antibody. Importantly, ERK1/2 inhibition prevented the hypercapnia-induced phosphorylation and polyubiquitination of the β-subunit of ENaC (Figure 4.14).

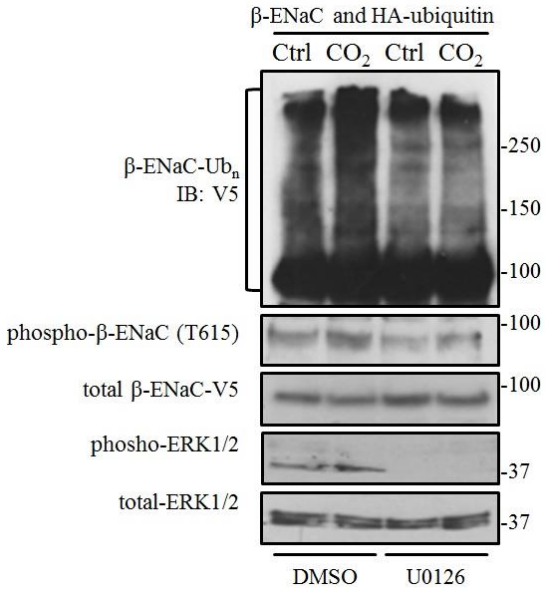


**Figure 4.14 Inhibition of ERK1/2 prevents hypercapnia-induced polyubiquitination of β-ENaC in A549 cells.** A549 cells were co-tranfected with β-ENaC and HA-ubiquitin before treatment with 40 mmHg $CO_2$ (Ctrl) or 120 mmHg $CO_2$ ($CO_2$) for 30 min at a $pH_e$ of 7.4 in the presence or absence of 10 μM U0126 (30 min pretreatment). Ubiquitinated β-ENaC was detected with anti-V5 antibody. Representative western blots are shown.

The above described studies confirmed that ERK1/2 via β-ENaC phophorylation affects ENaC ubiquitnation upon hypercapnia exposure. To futher study if the hypercapnia-induced ENaC endocytosis is also dependent on ERK1/2, we measured cell surface abundance of ENaC subunits by biotinylation assays after A549 cells were exposed to normocapnia or hypercapnia for 30 min at a $pH_e$ of 7.4 in the presence or absence of 10 μM U0126 (30 min pretreatment). Indeed, pretreatment of A549 cells with U0126 prevented the hypercapnia-induced decrease in cell surface ENaC abundance (Figure 4.15). Thus, hypercapnia-induced activation of ERK1/2 leads to direct

phosphorylation of β-ENaC, which drives polyubiquitination and subsequent endocytosis of ENaC from the alveolar epithelial cell surface.

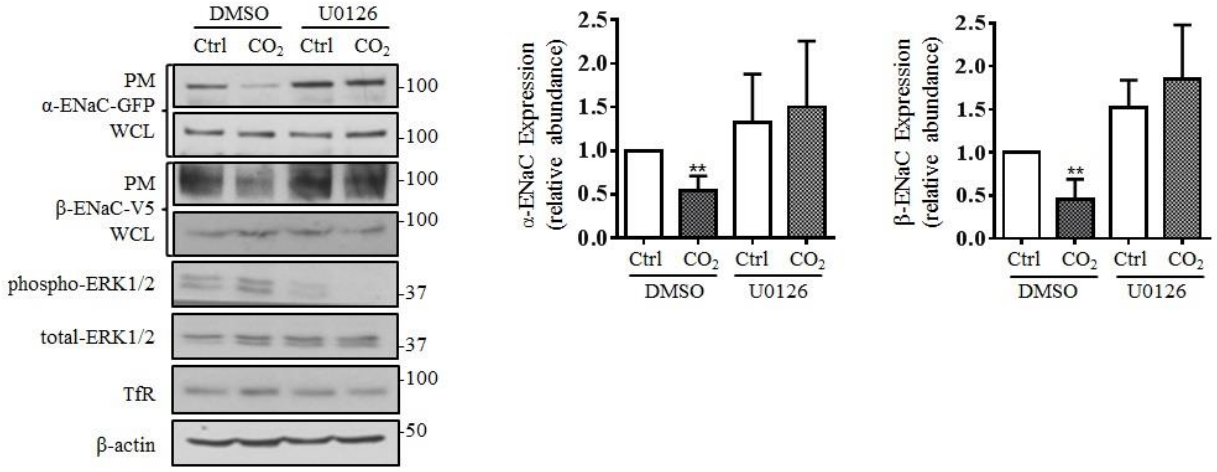


**Figure 4.15 Inhibition of ERK1/2-mediated β-ENaC phosphorylation prevents retrieval of the α/β-ENaC complex from the cell surface.** A549 cells were co-transfected with α- and β-ENaC and were exposed to 40 mmHg $CO_2$ (Ctrl) or 120 mmHg $CO_2$ ($CO_2$) for 30 min at a $pH_e$ of 7.4 in the presence or absence of U0126 (10 μM, 30 min pretreatment). The plasma membrane (PM) abundance of ENaC proteins and transferrin receptor (TfR) was measured by biotinylation assay followed by western blot analysis. Representative western blots of ENaC proteins located at the cell surface and total cellular protein levels, as well as phophorylation levels of ERK1/2 are shown. Bars show mean ± SEM (n = 3; ** $p < 0.01$).

As we demonstrated a central role for β-ENaC phosphorylation at T615 in the trafficking of the channel during hypercapnia, in subsequent experiments we removed T615 from the amino-acids sequence of β-ENaC by the Gibson assembly technique to investigate whether prevention of β-ENaC phosphorylation at this residue may attenuate the hypercapnia-induced decrease of ENaC cell surface abundance. Therefore, A549 cells were transfected with α-ENaC and either wild type (β-WT) or mutant (β-ΔT615) β-ENaC and were then exposed to normocapnia (Ctrl) or hypercapnia ($CO_2$) for 30 min. Cell surface expression of the ENaC subunits was assessed by biotin-streptavidin pull down. In line with our previous studies, preventing the ERK-dependent β-ENaC phosphorylation at the T615 residue rescued the cell surface abundance of the α/β-ENaC complex

upon hypercapnia (Figure 4.16). Thus, our results demonstrate that hypercapnia negatively controls the trafficking of α/β-ENaC by initiation of a specific $CO_2$-induced signaling pathway that includes activation of ERK1/2 and phophorylation of β-ENaC.

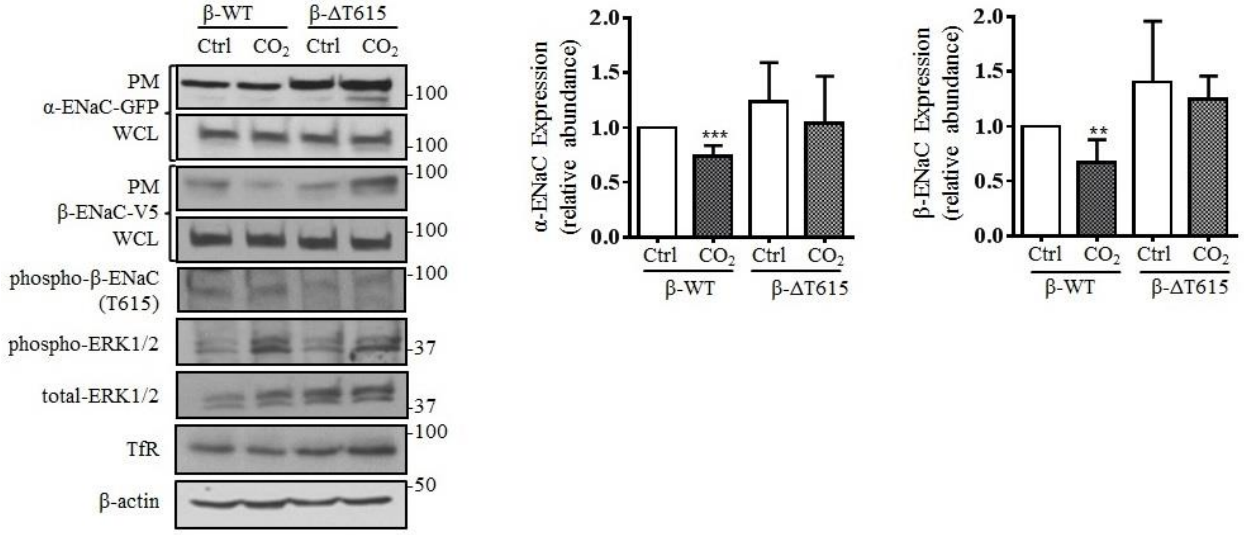


**Figure 4.16 Deletion of the T615 residue of β-ENaC prevents the hypercapnia-induced ENaC endocytosis.** A549 cells were co-transfected with α-ENaC and either wild type (WT) or mutated (ΔT615) β-ENaC prior to exposure to 40 mmHg $CO_2$ (Ctrl) or 120 mmHg $CO_2$ ($CO_2$) for 30 min at a $pH_e$ of 7.4. The plasma membrane (PM) density of ENaC proteins was measured by biotin-streptavidin pull down assay. Representative western blots are shown. Bars show mean ± SEM (n = 4; *** $p < 0.001$; ** $p < 0.01$).

## 4.8 Hypercapnia affects ubiquitination and cell surface expression of ENaC by JNK-dependent Nedd4-2 phosphorylation

Since JNK1/2 is also implicated in the $CO_2$–induced signaling cascade in alveolar epithelial cells leading to inhibition of the Na,K-ATPase, as reported previously by our laboratory (Vadász et al. 2012), we next investigated the role of JNK in ENaC trafficking during $CO_2$ exposure. First, we studied the activation of JNK1/2 in A549 cells treated with hypercapnia by measuring the phosphorylation levels of c-Jun (a downstream target of JNK and thus indicator of JNK activity (Cargnello and Roux 2011). Consistent with our previous observations, JNK1/2 activation by hypercapnia was rapid and transient (Figure 4.17).

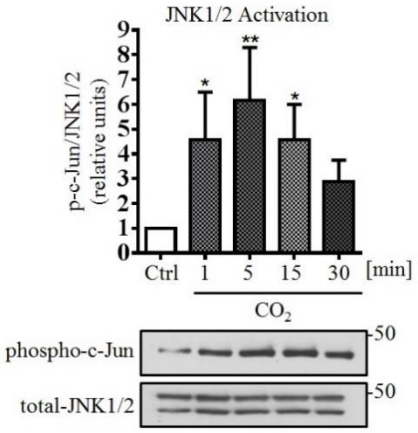


**Figure 4.17 Representative western blots and quantification of time dependent activation of JNK 1/2 by hypercapnia.** A549 cells were treated with 40 mmHg $CO_2$ (Ctrl) for 5 min or 120 mmHg $CO_2$ ($CO_2$) for 1 to 30 min at a $pH_e$ of 7.4. Activation of JNK was determined by measuring phosphorylation of c-Jun, a downstream target of JNK1/2. The graph shows phospho-c-Jun/total JNK1/2 ratio. Western blots of phopho-c-Jun and the total level of JNK1/2 are shown. Bars show mean ± SEM (n = 3; * $p < 0.05$; ** $p < 0.01$)

It has been previously demonstrated that JNK1 phosphorylates Nedd4-2 at the T899 residue thereby increasing activity of the E3 ligase. In polarized kidney epithelial cells (HEK 293), overexpression of a Nedd4-2 mutant lacking T899 was sufficient to attenuate α-ENaC ubiquitination compared to overexpression of wild type Nedd4-2 (Hallows et al. 2010). Moreover, overexpression of a constitutively active variant of JNK1 decreased ENaC-mediated sodium current in these cells. To evaluate the potential role of activated JNK in ENaC endocytosis during hypercapnia, we performed a site directed mutagenesis assay, in which the T899 residue of Nedd4-2 was replaced by alanine (T899A). First, we tested the impact of the mutated Nedd4-2 on β-ENaC polyubiquitination. To this end, A549 cells were transfected with β-ENaC, HA-ubiquitin and either wild type (WT) or mutant (T899A) Nedd4-2 prior to exposure to normocapnia (Ctrl) or hypercapnia ($CO_2$) for 30 min. Indeed, the level of hypercapnia-induced β-ENaC polyubiquitination in A549 cells expressing mutated Nedd4-2 in which the threonine residue cannot be phosphorylated by JNK was significantly reduced (Figure 4.18), suggesting that phosphorylation of Nedd4-2 at the T899 residue may impact ENaC trafficking during hypercapnia.

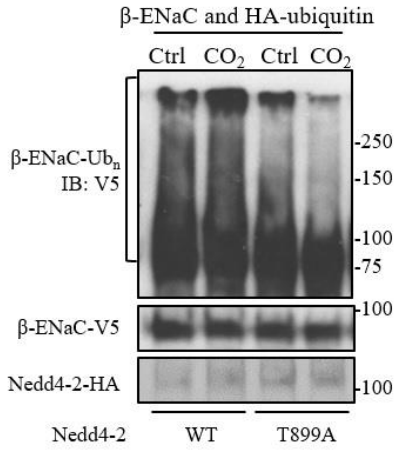


**Figure 4.18 JNK-dependent Nedd4-2 phosphorylation drives hypercapnia-induced β-ENaC polyubiquitination.** A549 cells were co-tranfected with β-ENaC, HA-ubiquitin and either wild type (WT) or mutant (T899A) Nedd4-2 prior to treatment with 40 mmHg $CO_2$ (Ctrl) or 120 mmHg $CO_2$ ($CO_2$) for 30 min at $pH_e$ of 7.4. Ubiquitinated β-ENaC was detected with anti-V5 antibody.

Next, we tested if a decrease in β-ENaC polyubiquitination due to the lack of phophorylation at T899 residue of Nedd4-2 prevents the hypercapnia-induced ENaC endocytosis. A549 cells were co-transfected with α/β-ENaC and either WT or T899A mutant Nedd4-2. Next, cells were treated with normocapnia (Ctrl) or hypercapnia ($CO_2$) for 30 min and ENaC cell surface density was estimated by streptavidin pull down and immunoblotting. Notably, overexpression of the Nedd4-2 mutant fully prevented the high $CO_2$-induced endocytosis of ENaC (Figure 4.19).

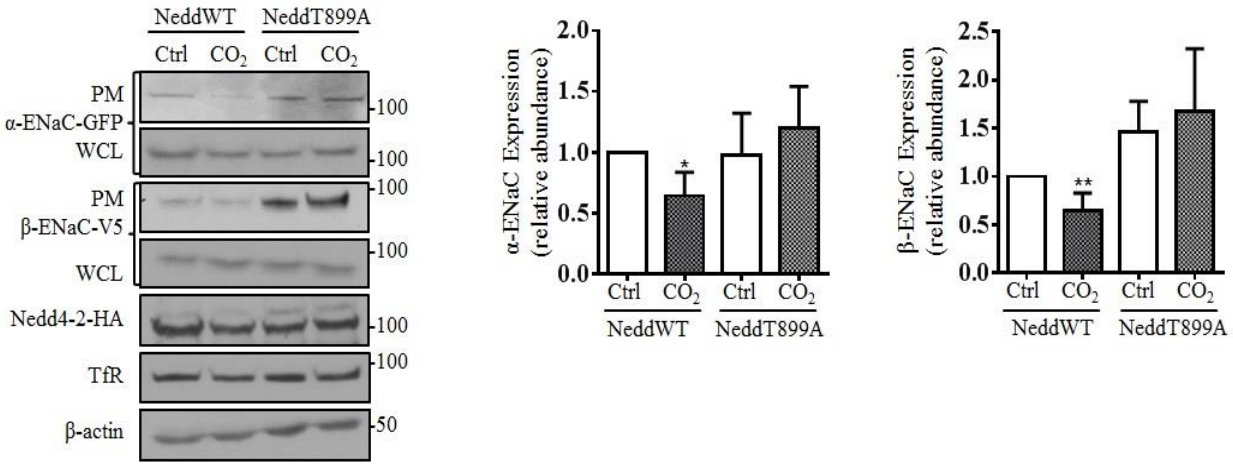


**Figure 4.19 Overexpression of the Nedd4-2 mutant (T899A) prevents endocytosis of the α/β-ENaC complex upon hypercapnia exposure.** A549 cells were co-transfected with α-, β-ENaC and either wild type (NeddWT) or mutant (NeddT889A) Nedd4-2 before treatment with 40 mmHg $CO_2$ (Ctrl) or 120 mmHg $CO_2$ ($CO_2$) for 30 min at a $pH_e$ of 7.4. Plasma membrane (PM) expression of ENaC proteins was measured by biotin-streptavidin pull down assay. Western blots of α-, β-ENaC and transferrin receptor (TfR) at the cell surface and total protein abundance of ENaCs, β-actin, and Nedd4-2 are shown. Bars show mean ± SEM (n = 4; * $p < 0.05$; ** $p < 0.01$).

Finally, the role of JNK in the hypercapnia-induced endocytosis of ENaC was determined. A549 cells were pretreated with the specific JNK inhibitor, SP600125 and were then exposed to normal (Ctrl) or elevated ($CO_2$) $CO_2$ levels for 30 min. In line with the above described findings, pretreatment of cells with SP600125 prevented the hypercapnia-induced internalization of ENaC (Figure 4.20). These results suggest that two distinct members of the MAPK superfamily, ERK1/2 and JNK1/2, are implicated in downregulation of ENaC upon exposure of alveolar epithelial cells to elevated $CO_2$ levels, targeting different proteins, namely β-ENaC and Nedd4-2, respectively.

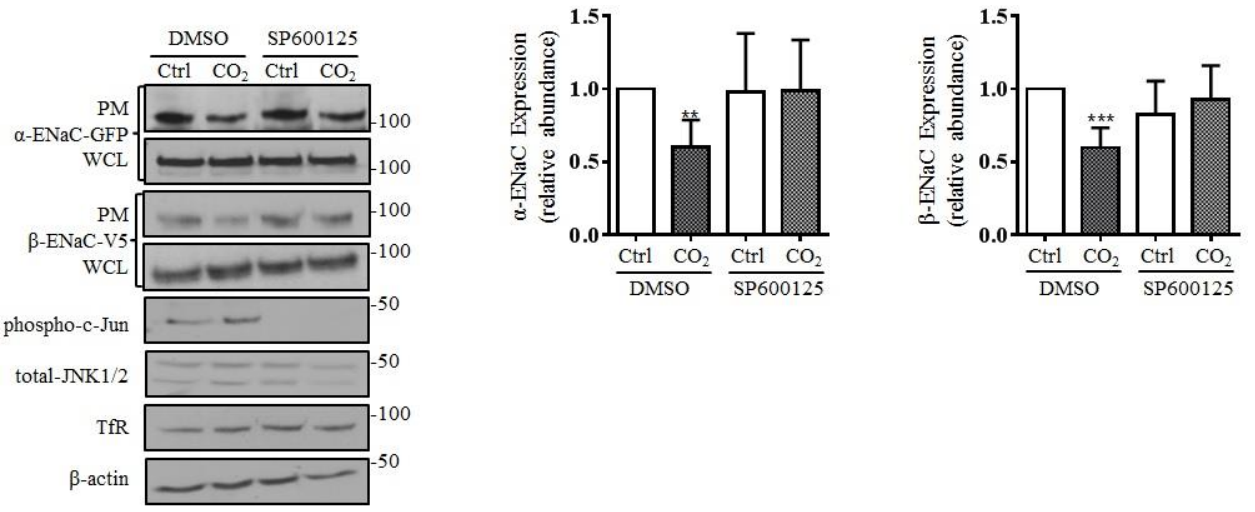


**Figure 4.20 JNK1/2 inhibition prevents elevated $CO_2$-induced endocytosis of the α/β-ENaC complex.** A549 cells were co-transfected with α- and β-ENaC and exposed to 40 mmHg $CO_2$ (Ctrl) or 120 mmHg $CO_2$ ($CO_2$) in the presence or absence of SP600125 (25 μM, 30 min pretreatment) for 30 min at a $pH_e$ of 7.4. The plasma membrane (PM) density of ENaC subunits was assessed by biotinylation and immunoblotting. Representative western blots are shown. Bars show mean ± SEM (n = 4; ** $p < 0.01$; *** $p < 0.001$).

### 4.9 Elevated $CO_2$ levels promote endocytosis of the α/β-ENaC complex by AMPK-α1 activation

Recently, the regulatory role of AMPK in ENaC/Nedd4-2 interaction has been reported (Woollhead et al. 2005; Bhalla et al. 2006; Almaça et al. 2009). Moreover, our group has previously identified AMPK-α1 as another important signaling molecule involved in the dysregulation of Na,K-ATPase during hypercapnia exposure (Vadász et al. 2008). Based on these findings, we hypothesized that the AMPK/Nedd4-2 axis may also regulate functional expression of ENaC in the alveolar epithelium during hypercapnia. To test this hypothesis, first we measured the levels of phospho-AMPK-α1 in A549 cells exposed to elevated $CO_2$ concentrations. Confirming our previous observations, hypercapnia induced the phosphorylation of AMPK-α1 in a time-dependent manner. AMPK-α1 activation was fast, transient and returned to baseline within 45 min of exposure to hypercapnia (Figure 4.21A). Moreover, the activity of AMPK-α1 was measured in A549 cells treated with normocapnia (Ctrl) or hypercapnia ($CO_2$) in the presence of the ERK inhibitor, U0126 (10 μM, 30 min pretreatment) for 30 min. The results demonstrated that phosphorylation of AMPK

was strongly dependent on the activity of ERK1/2 (Figure 4.21B), confirming that AMPK is a downstream target of ERK1/2 in the hypercapnic signaling pathway (Welch et al. 2010).

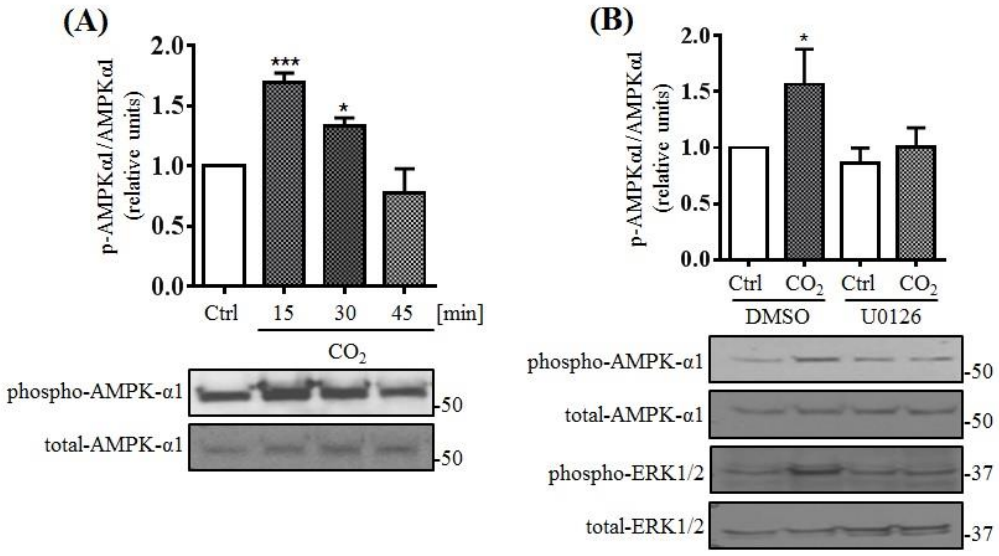


**Figure 4.21 Hypercapnia induces ERK1/2-dependent activation of AMPK-α1.** (A) A549 cells were treated with 40 mmHg $CO_2$ (Ctrl) for 15 min or 120 mmHg $CO_2$ ($CO_2$) for 15 to 45 min at a $pH_e$ of 7.4. The levels of phosphorylated and total AMPK-α1 were measured by immunoblotting. Graph shows phospho/total AMPK-α1 ratio. (B) A549 cells were exposed to normo- vs hypercapnia for 15 min at a pH of 7.4 in the presence of DMSO (vehicle) or U0126 (10 μM, 30 min pretreatment) and phosphorylation levels of AMPK-α1 and ERK1/2 were determined by immunoblotting. Graph shows phospho/total AMPK-α1 ratio. Representative blots are shown. Bars show mean ± SEM (n = 3; *p < 0.05; *** p < 0.001).

Next, we aimed to determine whether activation of AMPK-α1 is required for downregulation of ENaC upon hypercapnia. To this end, we first tested the levels of β-ENaC polyubiquitination in A549 cells exposed to normocapnia (Ctrl) or hypercapnia ($CO_2$) for 30 min after pharmacological inhibition or silencing of AMPK-α1, using a specific AMPK inhibitor, compound C or a siRNA respectively. In A549 cells pretreated with compound C prior to hypercapnia treatment, polyubiquitination of β-ENaC was significantly reduced (Figure 4.22A). The effects of elevated $CO_2$ levels on β-ENaC polyubiquitination were also abolished after AMPK-α1 silencing (Figure 4.22B). These results suggest that the hypercapnia-induced AMPK-α1 activation is required to promote polyubiquitination of β-ENaC.

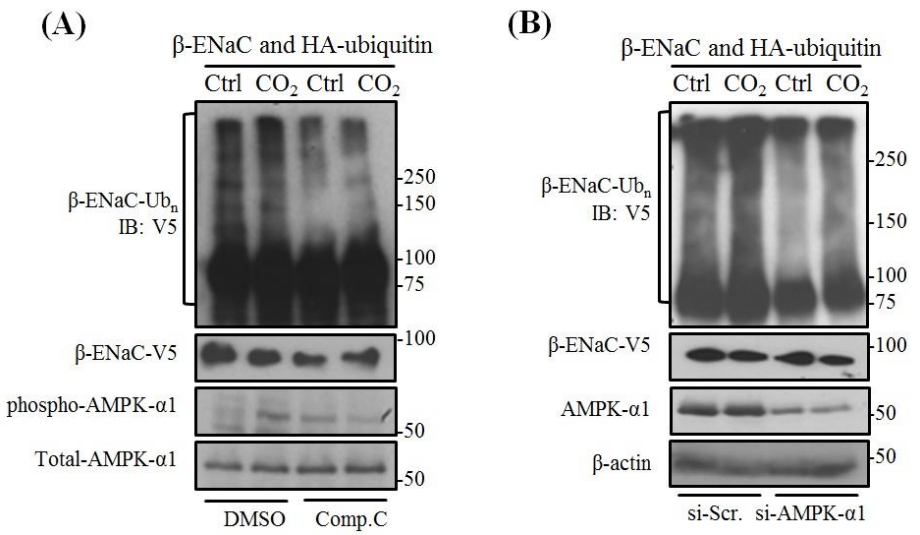


**Figure 4.22 Active AMPK-α1 mediates β-ENaC polyubiquitination upon hypercapnia.** (A) A549 cells were co-tranfected with β-ENaC and HA-ubiquitin and were treated with 40 mmHg $CO_2$ (Ctrl) or 120 mmHg $CO_2$ ($CO_2$) for 30 min at a $pH_e$ of 7.4 in the presence or absence of compound C (Comp. C; 20 μM, 30 min pretreatment). Ubiquitinated β-ENaC was detected with anti-V5 antibody. (B) A549 cells were transfected with either a siRNA against AMPK-α1 (si-AMPK-α1) or a scrambled siRNA (si-Scr.) and with β-ENaC and HA-ubiquitin prior to treatment with normocapnia or hypercapnia and ubiquitinated isoforms of β-ENaC were detected as described above. Representative western blots of β-ENaC, phopho-AMPK-α1 and total AMPK-α1 are shown.

We next tested whether activation of AMPK was also necessary for the hypercapnia-induced retrieval of the α/β-ENaC complex from the cell surface. To assess that, A549 cells were transfected with α- and β-ENaC and treated with DMSO or compound C prior to normocapnia or hypercapnia exposure for 30 min and expression of the ENaC subunits at the plasma membrane was determined. Our results showed that AMPK-α1 inhibition stabilized the ENaC complex at the cell surface during hypercapnia (Figure 4.23).

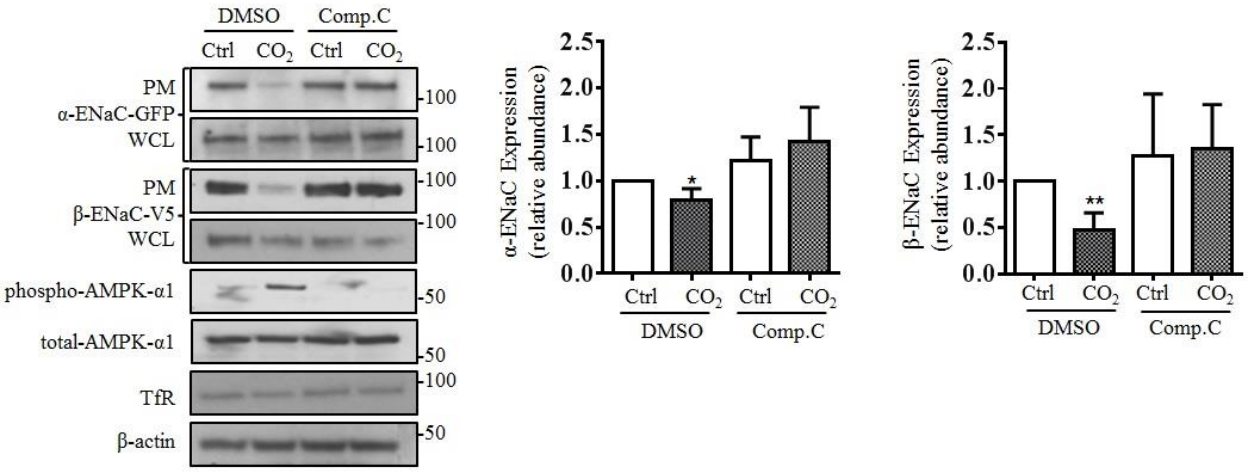


**Figure 4.23 Inhibition of AMPK-α1 prevents elevated $CO_2$-induced α/β-ENaC complex endocytosis.** A549 cells were co-transfected with α- and β-ENaC and exposed to 40 mmHg $CO_2$ (Ctrl) or 120 mmHg $CO_2$ ($CO_2$) for 30 min at a $pH_e$ of 7.4 in the presence or absence of compound C (20 µM, 30 min pretreatment). The plasma membrane (PM) expression of the α/β-ENaC complex was evaluated by streptavidin pull down followed by western blot analysis. Bars show mean ± SEM (n = 4; * $p < 0.05$; ** $p < 0.01$).

Paralleling the results obtained with pharmacological inhibition of AMPK, a specific siRNA targeting AMPK-α1 also prevented the hypercapnia-induced ENaC endocytosis (Figure 4.24).

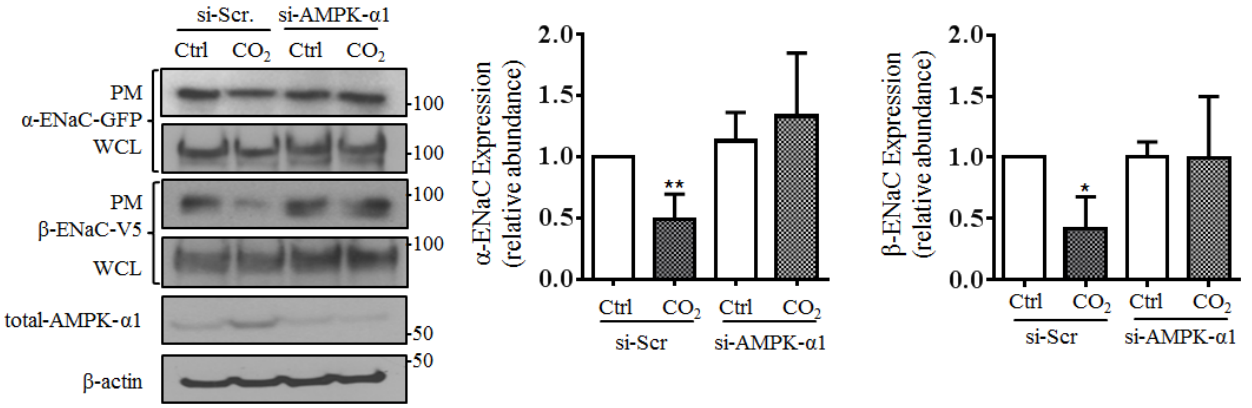


**Figure 4.24 Silencing of AMPK increases cell surface stability of ENaC upon hypercapnia exposure.** A549 cells were co-transfected with α-, β-ENaC and siRNA targeting either AMPK-α or scrambled (si-Scr). Next cells were treated with 40 mmHg $CO_2$ (Ctrl) or 120 mmHg $CO_2$ ($CO_2$) for 30 min at a $pH_e$ of 7.4. The plasma membrane (PM) expression of ENaC proteins was measured by biotinylation and western blots. Representative immunoblots of ENaC proteins and AMPK-α silencing are shown. Bars shows mean ± SEM (n = 4; * $p < 0.05$; ** $p < 0.01$).

These studies established that AMPK-α1 is strongly activated during hypercapnia and is downstream of ERK1/2. Several reports have shown that phosphorylation status of AMPK is regulated by other kinases including CaMKK-β (Woods et al. 2005; Gusarova et al. 2011). To further explore the role of CaMKK-β in the hypercapnia-induced and AMPK-mediated ENaC downregulation, A549 cells were exposed to normal or elevated $CO_2$ levels in the presence or absence of the CaMKK-β inhibitor, STO609 (20 µg/ml, 30 min preincubation) and activation of AMPK-α1 was assessed. Our results showed that during hypercapnia the phosphorylation of AMPK-α1 was driven by CaMKK-β (Figure 4.25A). Next, the biotinylation assay was applied to measure the level of ENaC proteins at the cell surface of A549 cells exposed to normocapnia or hypercapnia in the presence of STO609. Similar to the results obtained with U0126 (MEK inhibitor), the plasma membrane abundance of the α/β-ENaC complex was restored to normal levels when phosphorylation of AMPK-α1 was prevented upon exposure to elevated $CO_2$ concentrations (Figure 4.25B).

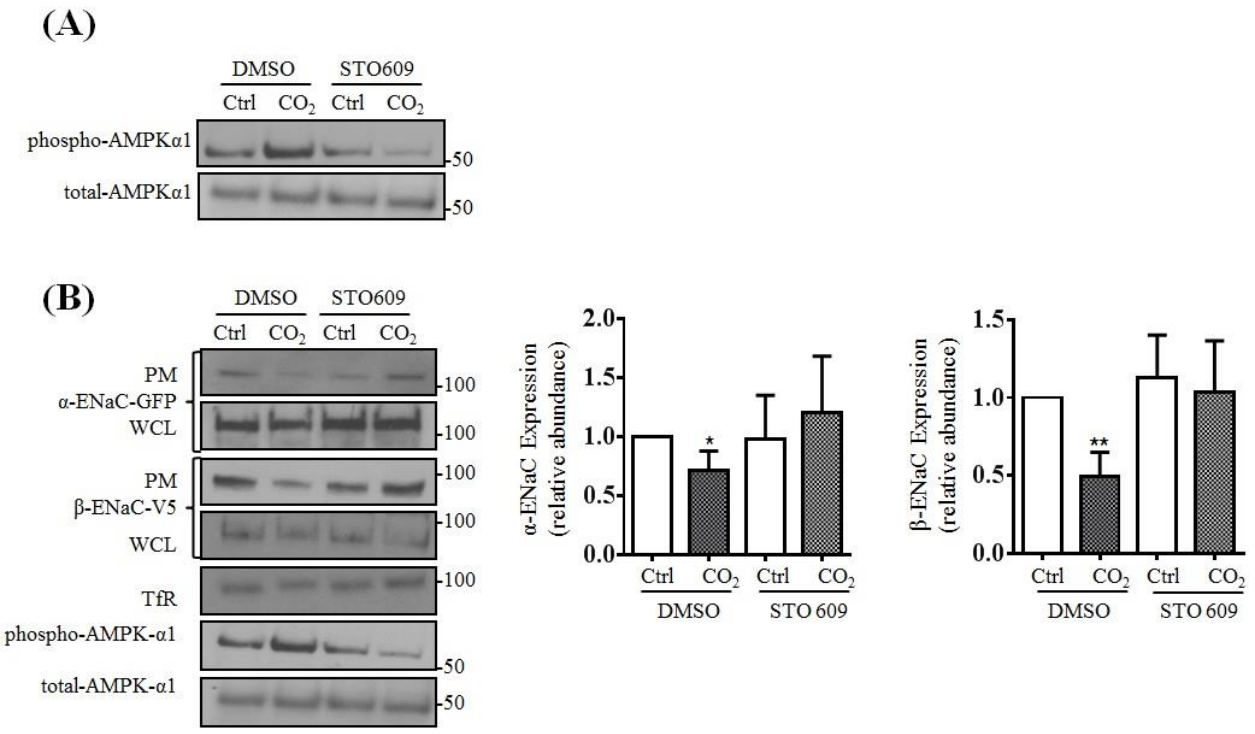


**Figure 4.25 Inhibition of CaMKK-β prevents elevated $CO_2$-induced endocytosis of the α/β-ENaC complex.** (A) A549 cells were treated with 40 mmHg $CO_2$ (Ctrl) or 120 mmHg $CO_2$ ($CO_2$) for 15 min at a $pH_e$ of 7.4 in the presnece or absence of STO609 (20 µg/ml, 30 min preincubation). Phosphorylated and total levels of AMPK-α1 were determined by western blot analysis. (B) A549 cells were co-transfected with α- and β-ENaC and exposed to normocapnia or hypercapnia for 30 min in the presence or absence of STO609. The plasma membrane (PM) expression of ENaC proteins was assessed by biotin-streptavidin pull down followed by immunoblotting. Representative western blots are shown. Bars show mean ± SEM (n = 4; * $p < 0.05$; ** $p < 0.01$).

Additionally, we observed that pharmacological inhibition of AMPK-α1, via compound C, strongly prevented the phosphorylation of c-Jun (Figure 4.26). This observation are in line with the previous finding describing that $CO_2$-induced activation of JNK requires activation of AMPK (Vadász et al. 2012). Collectively, these latter results suggest that AMPK-dependent JNK activation mediates Nedd4-2 phosphorylation at T899, thereby promoting polyubiquitination of ENaC-β and internalization of the α/β-ENaC complex.

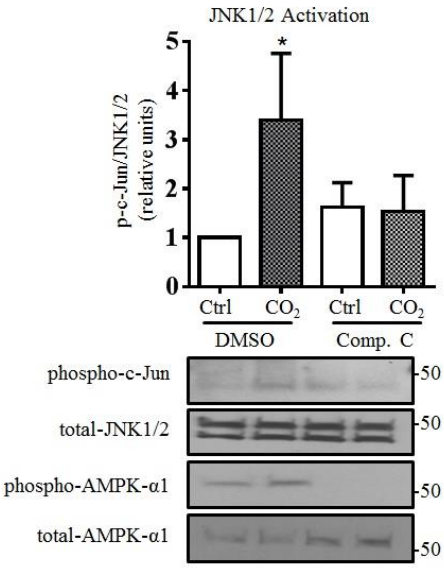


**Figure 4.26 Activation of AMPK-α1 is required to promote JNK phosphorylation during exposure to elevated $CO_2$ levels.** A549 cells were treated with 40 mmHg $CO_2$ (Ctrl) or 120 mmHg $CO_2$ ($CO_2$) for 5 min at a $pH_e$ of 7.4 in the presence or absence of compound C (20 µM, 30 minutes). Phosphorylation levels of c-Jun, AMPK-α1 and total amounts of JNK1/2 and AMPK-α1 were measured by western blot analysis. The graph shows phospho c-Jun/total JNK1/2 ratio. Representative western blots of phophorylated c-Jun and are shown. Bars show mean ± SEM (n = 3; * $p < 0.05$).

## 5. Discussion

Optimal alveolar fluid balance is maintained through the activity of ENaC and CFTR expressed at the apical surface of epithelial cell and via the basolateral Na,K-ATPase (Matthay et al. 2002). Dysregulation of these transporters may result in lung flooding, as observed in ARDS, which disturbs gas exchange leading to hypoxia and hypercapnia (Ware and Matthay 2001; Vadász and Sznajder 2017) or in lung dehydration, as in cystic fibrosis (Bangel et al. 2008). While in majority of patients with ARDS hypoxia can be corrected by mechanical ventilation with $O_2$ supplementation, the lung protective ventilation strategies with low tidal volumes that are required to prevent further ventilator-induced lung damage often leads to further $CO_2$ retention (Vadász et al. 2012; Bellani et al. 2016).

Although the $CO_2$ sensor remains unidentified, recent studies have shown that hypercapnia is sensed by lung cells and impairs alveolar epithelial function by Na,K-ATPase downregulation (Briva et al. 2007; Chen et al. 2008; Vadász et al. 2008; Dada et al. 2015). Most recently, the effects of high $CO_2$ levels on CFTR and the hemichannel, connexin 26 have been described (Turner 2014; de Wolf et al. 2017) however, the potential impact of hypercapnia on ENaC has not been previously investigated.

In this study, we investigated the molecular mechanism by which acute hypercapnia (dys)regulates functional expression of ENaC. We performed a series of experiments, which demonstrate that short-term hypercapnia reduces ENaC cell surface expression thus inhibiting ENaC-driven transepithelial $Na^+$ transport. We established that elevated $CO_2$ levels initiate activation of ERK1/2 that directly phosphorylates β-ENaC at the T615 residue. Furthermore, ERK1/2- and CaMKK-β-driven activation of AMPK-α1 stimulates JNK1/2-mediated Nedd4-2 phosphorylation at the T899 residue. These phosphorylation events promote interaction of β-ENaC and the E3 ligase, Nedd4-2 leading to enhanced polyubiquitination of β-ENaC and thus increased endocytosis of the α/β-ENaC complex from the cell surface of alveolar epithelial cells.

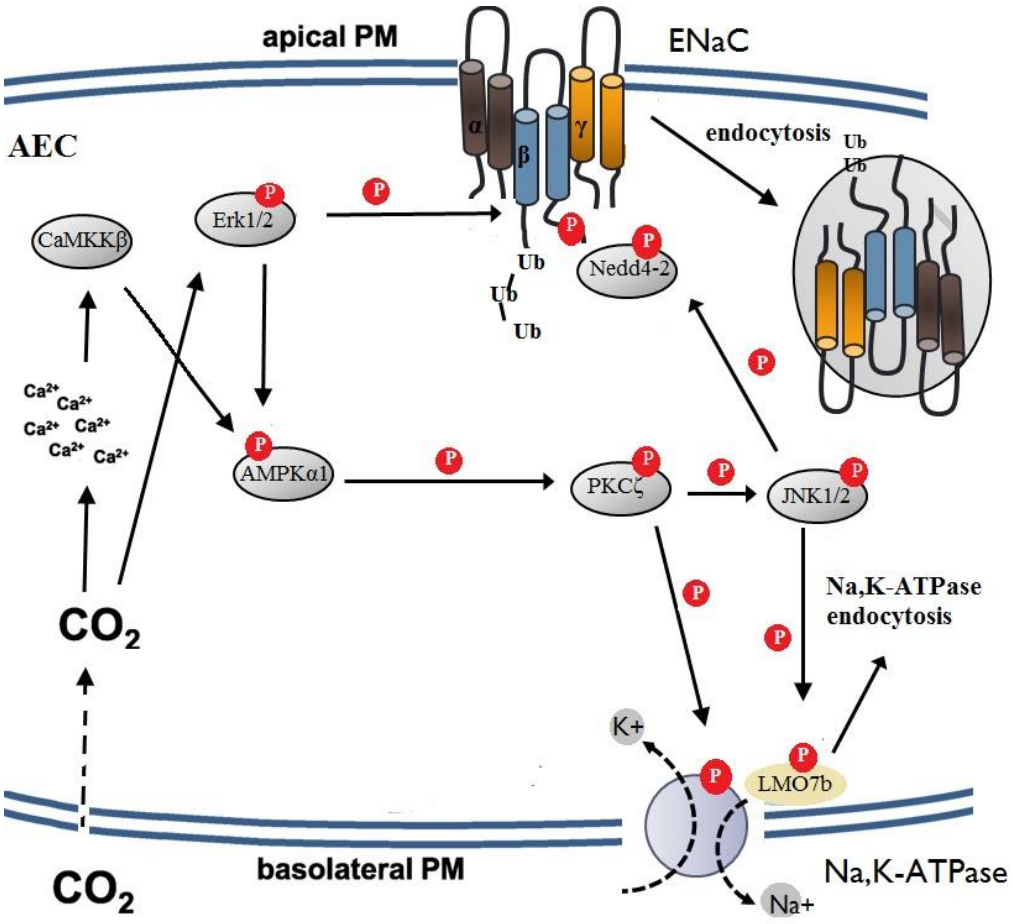


**Figure 5.1 Schematic representations of the signaling pathways impairing cell surface expression of the epithelial $Na^+$ channel (ENaC) upon acute hypercapnia.** In alveolar epithelial cells (AEC), hypercapnia increases intracellular $Ca^{2+}$ concentrations leading to activation of $Ca^{2+}$/calmodulin-dependent kinase kinase (CaMKK-β), which phosphorylates and activates AMP-activated protein kinase (AMPK). Activated AMPK promotes c-Jun N-terminal kinase (JNK)-mediated phosphorylation of the E3 ligase Nedd4-2, which promotes ENaC β-subunit polyubiquitination, leading to endocytosis of the α/β-ENaC complex. In parallel, hypercapnia stimulates activation of ERK1/2 (upstream of AMPK), which directly phosphorylates β-ENaC thus facilitating the interaction with Nedd4-2 and further promotes ENaC complex endocytosis. Subsequently, activated AMPK stimulates protein kinase C (PKC)-ζ -mediated phosphorylation of the Na,K-ATPase α-subunit, leading to endocytosis of the transporter. Moreover, PKC-ζ activates JNK1/2, which phosphorylates LMO7b (the scaffolding protein) additionally promoting endocytosis of the Na,K-ATPase. Collectively, these signaling pathway downregulates both ENaC and Na,K-ATPase cell surface expression leading to inhibition of alveolar fluid clearance.

## 5.1 Hypercapnia inhibits transepithelial $Na^+$ transport by promoting polyubiquitination of β-ENaC and endocytosis of the α/β-ENaC complex in alveolar epithelial cells

Maintenance of low ALF volume by reabsorbing excess lung fluid is one of the primary functions of the alveolar epithelium and is a result of vectorial $Na^+$ transport driven by ENaC and Na,K-ATPase (Matthay et al. 2002; Mutlu and Sznajder 2005). It is well documented that patients with ARDS who cannot remove pulmonary edema efficiently have worse outcomes (Ware and Matthay 2001). Importantly, $CO_2$ retention is often detected in those patients and has been shown to impair alveolar fluid balance (Vadász et al. 2012; Vadász and Sznajder 2017). Of note, hypercapnia is an independent risk factor in critically ill patients and particularly in those with ARDS and is associated with higher mortality (Nin et al. 2017; Tiruvoipati et al. 2017).

Here, we report that hypercapnia impairs plasma membrane stability of ENaC thereby reducing transepithelial $Na^+$ transport. Functional ENaC is located at the apical surface of epithelial cells and endocytosis of the channel is one of the major mechanisms controlling ENaC activity and thus alveolar fluid clearance (Butterworth 2010; Eaton et al. 2010). Based on the previously observed impact of hypercapnia on Na,K-ATPase function (Vadász et al. 2008), we hypothesized that elevated $CO_2$ levels may also affect functional expression of ENaC. Consistent with this hypothesis, our studies showed that elevated $CO_2$ concentrations lead to a decrease in plasma membrane expression of the α/β-ENaC complex in primary rat ATII cells and in a human cell line. Importantly, the alterations in ENaC cell surface stability upon hypercapnia occurred without any obvious change in the intracellular levels of ENaC. The apparent lack of impact of short-term hypercapnia on total ENaC expression, suggests that an acute exposure to elevated $CO_2$ concentrations regulate the trafficking rather than the degradation of the channel. Similarly, intracellular levels of ENaC were not changed by short-term hypoxic exposure, as has been reported by Gille and co-workers (Gille et al. 2014). Moreover, no changes in ENaC mRNA levels upon hypercapnic exposure were detected when compared to normocapnic controls. Indeed, several pathogenic factors that are associated with ARDS, such as hypoxia (Wodopia et al. 2000), IL-4 (Galietta et al. 2002), TGF-β (Frank et al. 2003) or TNF-α (Dagenais et al. 2004) have been reported to modulate mRNA expression of ENaC. However, the effects of hypercapnia on ENaC transcription might depend on the duration of exposure to elevated $CO_2$ concentrations. As has been reported in context of ENaC regulation by hypoxia and TGF-β, long-term exposure to low $O_2$

concentrations or TGF-β impairs ENaC transcription and translation in AEC (Frank et al. 2003; Clerici and Plane 2009). In contrast, acute treatment with 1% $O_2$ or TGF-β alters ENaC activity without changing mRNA expression (Gille et al. 2014; Peters et al. 2014). These observations correlate with our results, showing that hypercapnia causes only posttranslational modifications of ENaC over the short time frame (30 min) of treatment.

It is well established that ENaC ubiquitination (a post translational modification) is one of the key pathways contributing to retrieval of the channel from the plasma membrane (Knight et al. 2006; Eaton et al. 2010; Rotin and Staub 2012). As we observed that hypercapnia increased ENaC retrieval from the plasma membrane of AECs, we next hypothesized that the alterations in the cell surface expression of the channel may be a consequence of elevated $CO_2$-induced ubiquitination of ENaC. To test this hypothesis, we studied ubiquitination of ENaC α-, β-and γ-subunits upon a short (15 min) hypercapnic exposure. Results from these experiments showed an increased polyubiquitination of ENaC-β in response to elevated $CO_2$ levels, whereas ubiquitination status of α- and γ-ENaC remained unaffected, thus suggesting differential sensitivity of the various channel subunits to hypercapnia. These data also indicate that the β-subunit of ENaC serves as a substrate of hypercapnia-induced ubiquitination. Of note, a numbers of studies show different ENaC ubiquitination patterns in response to different stimuli, reporting that α-, β- and γ-ENaC may be either multimono- or polyubiquitinated (Wiemuth et al. 2007; Zhou et al. 2007). These ubiquitination patterns of the various ENaC subunits subsequently promote endocytosis and/or degradation of the channel (Eaton et al. 2010). Whether one or more ENaC subunits undergo ubiquitination is dependent on the stimulus (Staub et al. 1997; Zhou et al. 2007; Rotin and Staub 2012). While some stimuli target α-ENaC for ubiquitination (Staub et al. 1997; Hallows et al. 2010; Gille et al. 2014), others lead to ubiquitination of β-ENaC in which mutations of the PY recognition motif of *SCNN1B* gene prevent ubiquitination thus resulting in $Na^+$ hyperabsorption (Abriel et al. 1999; Malik et al. 2005). We observed that hypercapnia led to polyubiquitination of β-ENaC and subsequent endocytosis of the α/β-ENaC complex. This is in line with the well-known role of β-ENaC regulating trafficking of the ENaC channel complex (Firsov et al. 1996).

Acute lung injury is associated with impaired alveolar fluid clearance that contributes to persistence of pulmonary edema. Decreased fluid removal may be a consequence of reduced ENaC activity. Many pathogenic factors that are upregulated in the setting of ARDS contribute to a decreased

ENaC-driven $Na^+$ transport and thus reabsorption of alveolar fluid. For example, TNF-α diminishes amiloride-sensitive current in ATII cells (Dagenais et al. 2004). Moreover, TNF-α also decreases expression of tight junction proteins, such as zonula occludens protein 1 thus increasing alveolar epithelial permeability leading to further accumulation of alveolar fluid (Wittekindt 2017). Interestingly, TNF-α has also been shown to activate ENaC via direct binding of the lectin-like domain of TNF, which can be mimicked by a so-called TIP peptide to α-ENaC. This binding rescues impaired ENaC activity in the presence of pneumococcal pneumolysin (PLY) (Czikora et al. 2014).

Frank and colleagues reported reduced amiloride-sensitive $Na^+$ transport in lung epithelial cells in response to TGF-β (Frank et al. 2003). In line with these observations, Peters and co-workers reported that TGF-β induced internalization of the β-ENaC from the alveolar epithelial cell surface leading to decreased AFC (Peters et al. 2014). Additionally, a negative impact of IL-1β on ENaC cell surface expression and amiloride-sensitive current has been shown in alveolar epithelial cells (Roux et al. 2005). These studies revealed that the inhibition of ENaC apical expression and activity occurs via p38 MAPK-dependent pathways.

Hypercapnia is another factor frequently found in patients with ARDS (Vadász et al. 2012; Nin et al. 2017). The potentially negative and positive effects of elevated $CO_2$ levels on the lungs and particularly in the setting of lung injury remain highly debated (Vadász et al. 2012). While earlier studies reported predominantly beneficial effects of hypercapnia on the lung, it appears that the potentially positive effects were rather a consequence of the acidosis that resulted from hypercapnia as opposed to the elevated $CO_2$ levels *per se* (Higgins et al. 2009). More recently, it has been demonstrated in various species including rodents *in vivo* and human cells that elevated $CO_2$ levels negatively affect the function of alveolar epithelium independently of pH. Several elements of the hypercapnia-induced signaling pathway have been described revealing that elevated $CO_2$ concentrations lead to activation of the metabolic sensor AMPK-α1 thereby promoting Na,K-ATPase endocytosis via PKC-ζ-dependent phosphorylation of the Na,K-ATPase α-subunit (Briva et al. 2007; Vadász et al. 2008).

A previous work focusing on the hypoxia-induced signaling pattern leading to a decrease in ENaC activity in rat AECs revealed a correlation between increased ubiquitination and decreased

amiloride-sensitive $Na^+$ transport upon hypoxia (Gille et al. 2014). In contrast, Tan and co-workers demonstrated that an increased α-ENaC abundance at the apical membrane of H441 cells in response to apical fluid expansion is associated with augmented $Na^+$ transport (Tan et al. 2011). These observations are in line with our results, demonstrating that elevated $CO_2$ levels decrease total and amiloride-sensitive $Na^+$ current as a consequence of ENaC endocytosis. Our cell surface protein labeling studies showed that hypercapnia decreases membrane abundance of ENaC and increases polyubiquitination of the β-subunit of the channel, thus providing insights into the molecular mechanisms involved in the $CO_2$-induced $Na^+$ transport inhibition. Of note, the transepithelial resistance of cellular monolayers remained unaffected after hypercapnia, suggesting that the decrease in transepithelial $Na^+$ current was not due to impaired cell viability or barrier integrity. However, as transepithelial vectorial $Na^+$ transport is mediated by the concerted action of ENaC and Na,K-ATPase, the question remains, whether hypercapnia decreases amiloride-sensitive $Na^+$ transport solely due to direct inhibition of ENaC or indirectly as well, as a secondary effect of impaired Na,K-ATPase function. For example, Krause *et al*. demonstrated inhibited amiloride-sensitive $Na^+$ absorption due to decreased Na,K-ATPase activity in H441 cell exposed to acute hypoxia (30 min) and $H_2S$ (Krause et al. 2016). The Na,K-ATPase generates the driving force for $Na^+$ entry across the apical membrane, thus downregulation of ENaC may represent a cellular mechanism to prevent $Na^+$ overload during stress conditions. Thus, it is possible (and indeed probable) that the hypercapnia-induced Na,K-ATPase dysfunction in turn also inhibits ENaC function. Further studies involving measurement of ouabain-sensitive $Na^+$ current (mediated by Na,K-ATPase) are warranted to further tease out the relative contributions of direct and indirect effects of hypercapnia on ENaC function. The hypercapnia-induced downregulation of amiloride-sensitive $Na^+$-current may contribute to inhibition of AFC in hypercapnic patients with ARDS. While in most cases it is challenging to reduce hypercapnia without causing further lung injury or taking rather invasive measures such as extracorporeal membrane oxygenation, targeting the hypercapnia-induced signaling pathway which mediates ENaC downregulation may contribute to resolution of lung injury.

## 5.2 Elevated $CO_2$ levels promote ENaC endocytosis by Nedd4-2-mediated ubiquitination of β-ENaC

It is well established that binding of the E3 ligase, Nedd4-2 to the COOH-termini of the various ENaC subunits is prerequisite for ubiquitination of the channel and subsequent endocytosis and/or degradation (Abriel et al. 1999; Snyder et al. 2001; Lu et al. 2007; Kimura et al. 2011; Rotin and Staub 2012; Boase et al. 2011), although other E3 ligases may control ENaC trafficking in the lungs as well (Downs et al. 2013).

Since our results showed a strong increase in β-ENaC ubiquitination upon hypercapnia, we hypothesized that Nedd4-2 may be implicated in the process of ENaC internalization. In line with this hypothesis, our experiments showed that genetic ablation of Nedd4-2 with a specific siRNA fully prevents β-ENaC polyubiquitination upon hypercapnic treatment. Moreover, hypercapnia-induced redistribution of α/β-ENaC complex form the cell surface to intracellular stores was also reduced by Nedd4-2 knock-down. These findings are consistent with studies reported by Snyder and colleagues showing that Nedd4-2 silencing increased amiloride-sensitive $Na^+$ current in H441 cells (Snyder et al. 2004). Additionally, these authors also presented that a mutation in β-ENaC (R566X) associated with Liddle's syndrome blocks the effects of Nedd4-2 siRNA, further confirming the central role of Nedd4-2 in ENaC endocytosis. Moreover, our co-immunoprecipitation data showed that β-ENaC and Nedd4-2 are assembled into a complex upon hypercapnia. Similarly, Malik *et al*. reported that Nedd4-2 was co-immunoprecipitated with α- and β-ENaC in A6 cells (Malik et al. 2005). In our studies, the association between these two proteins was detected also during normocapnic exposure, suggesting that Nedd4-2 plays role in ENaC turnover in both normal and pathological conditions. ENaC inhibition by hypoxia has been described as a result of Nedd4-2-driven ubiquitination and endocytosis (Gille et al. 2014). These observations are similar to our findings and may explain reduction in ENaC-driven $Na^+$ transport upon acute hypercapnia treatment. Taken together, these data confirm contribution of Nedd4-2 in ENaC ubiquitination and internalization upon hypercapnic exposure.

### 5.3 Hypercapnia induces ENaC endocytosis by phosphorylation-dependent ubiquitination of ENaC β-subunit

So far, our results showed that Nedd4-2 is a possible regulator of ENaC cell surface expression in the hypercapnic signaling cascade. Next, we set out to identify the molecular mechanisms by which Nedd4-2 mediates β-ENaC polyubiquitination upon elevated $CO_2$. It has been previously shown that phosphorylation of target molecules may be required for initiation of ubiquitination probably by potentiating binding of the E3 ligase to the substrate (Butterworth et al. 2005; Hunter 2007).

In mammals, at least 14 different MAPK signaling elements have been identified so far, categorized into 7 groups (Cargnello and Roux 2011). Our data suggest that the MAPK family member ERK1/2 plays a central role in the hypercapnia-induced downregulation of ENaC. Several studies confirmed that ERK directly phosphorylates threonine residues located in the C-terminus of the β- and γ-subunit of ENaC leading to enhanced docking of Nedd4-2 and thus causing ENaC internalization (Shi et al. 2002; Yang et al. 2006; Alli et al. 2012; Eaton et al. 2014). For example, Eaton and coworkers have reported that ERK activation inhibits ENaC via decreasing its cell surface density and $P_o$ in PKC-α knock-out mice in which elevated levels of ROS drive PKC-δ activation leading to decreased dephosphorylation of ERK, which in turn increases Nedd4-2-mediated ubiquitination and endocytosis of ENaC (Eaton et al. 2014). Moreover, an inhibition of amiloride-sensitive $Na^+$ absorption driven by activation of ERK signaling has also been reported in murine collecting duct epithelial cells (mCT1) exposed to epithermal growth factor (EGF) (Shen and Cotton 2003). The relationship between increased activation of ERK and decreased levels of ENaC activity has also been documented in an *in vitro* study in rat ATII cells exposed to $Cl_2$ in which reduced transepithelial $Na^+$ transport was observed due to increased concentrations of reactive intermediates that mediated the phosphorylation of ERK. A similar inhibition of ENaC-driven $Na^+$ transport was shown in lung slices of mice exposed to $Cl_2$ (Lazrak et al. 2012).

Based on these findings, we hypothesized that increased β-subunit polyubiquitination upon hypercapnia may be a consequence of higher ERK activity that drives β-ENaC phosphorylation leading to increased binding of Nedd4-2 to β-ENaC at the cell surface. Our experiments show that elevated $CO_2$ concentrations promote rapid and time dependent ERK1/2 phosphorylation in A549 cells. This is in line with previous studies reporting a comparable rapid and transient activation of ERK1/2 by elevated $CO_2$ levels in rat ATII cells (Welch et al. 2010). Activation of ERK1/2 was

followed by phosphorylation of the T615 residue of β-ENaC similarly to what has been observed in a previous study (Shi et al. 2002). Moreover, treatment of cells with a specific inhibitor of ERK fully prevented polyubiquitination of β-ENaC and increased cell surface density of the α/β-ENaC complex upon hypercapnic exposure confirming a crucial role of active ERK in ENaC endocytosis. This is in line with the findings reported by Lazrak and co-workers, in which inhibition of amiloride-sensitive $Na^+$ current resulted from decreased total levels of α-ENaC that was prevented by blocking ERK activity (Lazrak et al. 2012).

A previous study has showed that mutations of T615 of β-ENaC and T623 of γ-ENaC to alanine prevents ERK-dependent phosphorylation and reduces channel endocytosis in *Xenopus* oocytes (Yang et al. 2006). These findings are in line with our results, in which the effect of hypercapnia-induced ENaC retrieval form the cell surface was significantly reduced by deletion of the T615 residue from the amino acid sequence of β-ENaC. Although we were unable to mutate T615 to A by site directed mutagenesis due to the high GC content present in the PY region of β-ENaC, deletion of this specific threonine confirmed that active ERK1/2 promotes ENaC retrieval from the plasma membrane via phosphorylation-dependent polyubiquitination of β-subunit. It is important to emphasize that deletion of this specific threonine from the β-ENaC sequence did not influence channel trafficking to the cell surface that was demonstrated by biotinylation experiments using cells overexpressing the β-ENaC mutant (ΔT615).

### 5.4 JNK1/2-dependent phosphorylation of Nedd4-2 decreases cell surface abundance of α/β-ENaC during hypercapnia

Phosphorylation of Nedd4-2 is considered as an important mechanism for modulation of E3 ligase activity, representing an alternative way controlling ubiquitination of ENaC and other targets of the ligase (Bhalla et al. 2005). For example, PKA, SGK1 and with no lysine 1 (WNK1) have been reported to upregulate ENaC via inhibition of Nedd4-2 signaling (Snyder et al. 2004; Edinger et al. 2009; Xu et al. 2005). In contrast, active JNK1/2 (member of the MAPK family and an important regulator of cellular adaptation processes) activates Nedd4-2 thereby leading to ENaC downregulation (Hallows et al. 2010). Interestingly, JNK is crucial for elevated $CO_2$-induced downregulation of the Na,K-ATPase (Vadász et al. 2012; Dada et al. 2015) and it has been recently reported that active JNK leads to phosphorylation of the S1295 residue of LMO7b allowing

interaction with Na,K-ATPase at the cell surface and thus promoting endocytosis of the transporter in AEC (Dada et al. 2015). Moreover, in the hypercapnia-induced Na,K-ATPase downregulation, the activation of JNK requires PKC-ζ-mediated phosphorylation at S129 (Vadász et al. 2012). In line with these previous findings regarding activation of JNK by hypercapnia in ATII cells (Vadász et al. 2012), our current data showed that JNK is strongly phosphorylated by elevated $CO_2$ levels in A549 cells as well.

A recent finding has shed light on the role of JNK1/2 in ENaC regulation. A stimulatory impact of JNK1 on Nedd4-2 activity has been described in polarized kidney epithelial cells and in *Xenopus* oocytes. These results showed that ubiquitination of α-ENaC required JNK1-driven phosphorylation of Nedd4-2 at the T899 residue, located in the HECT domain of the E3 ligase (Hallows et al. 2010). In agreement with that report, our data confirmed that mutation of T899 to alanine reduced ubiquitination of ENaC-β and restored normal cell surface density of the α/β-ENaC complex upon hypercapnia. Similarly, a rescued abundance of ENaC at the cell surface was observed after pretreatment of A549 cells with a specific JNK inhibitor. These results imply a crucial role of JNK in modulating Nedd4-2 activity and confirm that phosphorylation of Nedd4-2 at the T899 residue is an important step in polyubiquitination of β-ENaC which is required for endocytosis of the α/β-ENaC in AEC in response to hypercapnia.

### 5.5 Activity of AMPK-α1 is required for hypercapnia-induced ubiquitination and endocytosis of ENaC

AMPK acts as cellular energy sensor and inhibits energy-consuming processes such as ion transport. This kinase has been described previously as an inhibitor of ENaC, the Na,K-ATPase and CFTR (Hallows et al. 2002; Vadász et al. 2008; Almaça et al. 2009). In agreement with these reports, our results demonstrate an important role of active AMPK in ENaC downregulation. We propose an elevated $CO_2$-induced mechnism, in which ERK1/2 plays a dual role, namely, the kinase directly phoporylates β-ENaC at theT615 residue but also activates AMPK, which in turn promotes JNK1/2-mediated phoporylation of Nedd4-2, thereby leading to endocytosis of the α/β-ENaC complex.

Our data are in line with recently published observations showing that AMPK is an early element of the hypercapnic signaling cascade and that its activation appears to be downstream of ERK1/2

(Welch et al. 2010). Moreover, we showed that treatment of cells with a siRNA against AMPK-α1 or a specific AMPK inhibitor markedly reduces elevated $CO_2$-induced β-ENaC polyubiquitination and subsequent retrieval of the α/β-ENaC complex form the cell surface. Since ENaC endocytosis is dependent on Nedd4-2-mediated β-ENaC polyubiquitination upon hypercapnia, we hypothesized that AMPK regulates ENaC by controlling the Nedd4-2/ENaC-β interaction. Interestingly, enhanced expression of ENaC at the cell surface was reported in the distal airways in AMPK-α1−/− mice (Almaça et al. 2009). In those studies, AMPK inhibited ENaC by increasing its ubiquitination and subsequent endocytosis most likely due to enhancing Nedd4-2 activity. Bhalla and colleagues presented similar findings (Bhalla et al. 2006). In their studies AMPK-driven inhibition of ENaC by Nedd4-2 was prevented by overexpressing of a dominant-negative Nedd4-2 mutant, confirming that Nedd4-2 is a required for AMPK-mediated ENaC downregulation. Moreover, the authors reported that AMPK activation enhanced β-ENaC/Nedd4-2 interaction in human embryonic kidney cells. This is consistent with our co-IP studies in A549 cells in which Nedd4-2 was co-immunoprecipitated with β-ENaC upon hypercapnia.

In addition, $CO_2$ has previously been described as a molecule that impacts intracellular $Ca^{2+}$ concentrations (Briva et al. 2007; Vadász et al. 2008). Of note, CaMKK-β senses alteration in intracellular calcium levels (Hawley et al. 2005) and has been identified as a key kinase activating AMPK-α1 in alveolar epithelial cells in response to hypercapnia and hypoxia (Vadász et al. 2008; Gusarova et al. 2011). These studies showed that active CaMKK-β drives AMPK-α1 phosphorylation promoting Na,K-ATPase endocytosis by PKC-ζ-dependent phosphorylation of the Na,K-ATPase α-subunit at S18. In line with these findings, we demonstrated that pretreatment of A549 cells with a specific CaMKK-β inhibitor abolished the hypercapnia-induced effect of ENaC cell surface endocytosis by preventing AMPK activation. Similar inhibition of ENaC internalization in response to hypercapnia was obtained when A549 cells were pretreated with an ERK (upstream of AMPK) inhibitor. Taken together, these results suggest that the activation of AMPK is an essential step in the hypercapnia-induced ENC downregulation. Importantly, and confirming previously published data (Vadász et al. 2012), our current studies show that AMPK is upstream of JNK in the hypercapnic signaling pathway. Thus, it is most likely that the AMPK-regulated impact on ENaC/Nedd4-2 interaction is mediated by JNK-dependent phosphorylation of Nedd4-2 at T899.

Collectively, our results demonstrate impaired ENaC cell surface abundance upon acute hypercapnia by Nedd4-2-driven polyubiquitination of ENaC-β and subsequent endocytosis of the α/β-ENaC complex as a result of a specific signaling pathway including activation of the ERK/AMPK/JNK axis. Interestingly, these kinases have previously been implicated as negative regulators of Na,K-ATPase (Gusarova et al. 2011; Dada et al. 2015; Vadász et al. 2012), suggesting that at least some key players of the hypercapnic signaling pathway may be common for regulation of both $Na^+$ transporters. Thus, targeting elements of the $CO_2$-induced deleterious signaling pathway may contribute to resolution of lung injury in hypercapnic patients with ARDS leading to better outcomes.

## List of tables

## List of figures

## References

Abriel, H., J Loffing, J. F. Rebhun, J. H. Pratt, L. Schild, J. D. Horisberger, D. Rotin and O. Staub (1999). "Defective regulation of the epithelial Na+ channel by Nedd4 in Liddle's syndrome." J Clin Invest **103**(5): 667-673.

Acute Respiratory Distress Syndrome, N., R. G. Brower, M. A. Matthay, A. Morris, D. Schoenfeld, B. T. Thompson and A. Wheeler (2000). "Ventilation with lower tidal volumes as compared with traditional tidal volumes for acute lung injury and the acute respiratory distress syndrome." N Engl J Med **342**(18): 1301-1308.

Adams, C. M., P. M. Snyder and M. J. Welsh (1997). "Interactions between Subunits of the Human Epithelial Sodium Channel." J Biol Chem **272**(43): 27295-27300.

Adhikari, N. K., R. A. Fowler, S. Bhagwanjee and G. D. Rubenfeld (2010). "Critical care and the global burden of critical illness in adults." Lancet **376**(9749): 1339-1346.

Alli, A. A., H. F. Bao, A. A. Alli, Y. Aldrugh, J. Z. Song, H. P. Ma, L. Yu, O. Al-Khalili and D. C. Eaton (2012). "Phosphatidylinositol phosphate-dependent regulation of Xenopus ENaC by MARCKS protein." Am J Physiol Renal Physiol **303**(6): F800-811.

Almaca, J., P. Kongsuphol, B. Hieke, J. Ousingsawat, B. Viollet, R. Schreiber, M. D. Amaral and K. Kunzelmann (2009). "AMPK controls epithelial Na(+) channels through Nedd4-2 and causes an epithelial phenotype when mutated." Pflugers Arch **458**(4): 713-721.

Althaus, M., W. G. Clauss and M. Fronius (2011). "Amiloride-sensitive sodium channels and pulmonary edema." Pulm Med **2011**: 830320.

Althaus, M., M. Fronius, Y. Buchackert, I. Vadasz, W. G. Clauss, W. Seeger, R. Motterlini and R. E. Morty (2009). "Carbon monoxide rapidly impairs alveolar fluid clearance by inhibiting epithelial sodium channels." Am J Respir Cell Mol Biol **41**(6): 639-650.

Amato, M. B. P., C. S. V. Barbas, D. M. Medeiros, R. B. Magaldi, G. de Paula Pinto Schettino, G. Lorenzi-Filho, R. A. Kairalla, D. Deheinzelin, C. Munoz, R. Oliviera, T. Y. Takagaki and C. R. Ribeiro Carvalho (1998). "Effect of a Protective-Ventil Ation Strategy on Mortality in the Acute Respiratory Distress Syndrome." N Engl J Med **338**(6) 347-354.

Anantharam, A., Y. Tian and L. G. Palmer (2006). "Open probability of the epithelial sodium channel is regulated by intracellular sodium." J Physiol **574**(Pt 2): 333-347.

Asher, C., I. Sinha and H. Garty (2003). "Characterization of the interactions between Nedd4-2, ENaC, and sgk-1 using surface plasmon resonance." Biochem Biophys Acta **1612**(1): 59-64.

Babini, E., H. S. Geisler, M. Siba and S. Grunder (2003). "A new subunit of the epithelial Na+ channel identifies regions involved in Na+ self-inhibition." J Biol Chem **278**(31): 28418-28426.

Bachofen, M. and E. R. Weibel (1977). "Alterations of the gas exchange apparatus in adult respiratory insufficiency associated with septicemia." Am Rev Respir Dis **116**(4): 589-615.

Bachofen, M. and E. R. Weibel (1982). "Structural alterations of lung parenchyma in the adult respiratory distress syndrome." Clin Chest Med **3**(1): 35-56.

Bangel, N., C. Dahlhoff, K. Sobczak, W. M. Weber and K. Kusche-Vihrog (2008). "Upregulated expression of ENaC in human CF nasal epithelium." J Cyst Fibros **7**(3): 197-205.

Baquero, A. F. and T. A. Gilbertson (2011). "Insulin activates epithelial sodium channel (ENaC) via phosphoinositide 3-kinase in mammalian taste receptor cells." Am J Physiol Cell Physiol **300**(4): C860-C871.

Basset, G., C. Crone and G. Saumon (1987). "Significance of active ion transport in transalveolar water absorption: a study on isolated rat lung." J Physiol **384**: 311-324.

Belkin, R. A., N. R. Henig, L. G. Singer, C. Chaparro, R. C. Rubenstein, S. X. Xie, J. Y. Yee, R. M. Kotloff, D. A. Lipson and G. R. Bunin (2006). "Risk factors for death of patients with cystic fibrosis awaiting lung transplantation." Am J Respir Crit Care Med **173**(6): 659-666.

Bellani, G., J. G. Laffey, T. Pham, E. Fan, L. Brochard, A. Esteban, L. Gattinoni, F. van Haren, A. Larsson, D. F. McAuley, M. Ranieri, G. Rubenfeld, B. T. Thompson, H. Wrigge, A. S. Slutsky and A. Pesenti (2016). "Epidemiology, Patterns of Care, and Mortality for Patients With Acute Respiratory Distress Syndrome in Intensive Care Units in 50 Countries." JAMA **315**(8): 788-788.

Bernard, G. R., A. Artigas, K. L. Brigham, J. Carlet, K. Falke, L. Hudson, M. Lamy, J. R. Legall, A. Morris and R. Spragg (1994). "The American-European Consensus Conference on ARDS Definitions,Mechanisms,RelevantOutcomes,andClinicalTrial Coordination." Am J Respir Crit Care Med **149**: 818-824.

Berthiaume, Y., N. C. Staub and M. A. Matthay (1987). "Beta-adrenergic agonists increase lung liquid clearance in anesthetized sheep." J Clin Invest **79**(2): 335-343.

Bhalla, V., D. Daidié, H. Li, A. C. Pao, L. P. LaGrange, J. Wang, A. Vandewalle, J. D. Stockand, O. Staub and D. Pearce (2005). "Serum- and glucocorticoid-regulated kinase 1 regulates ubiquitin ligase neural precursor cell-expressed, developmentally down-regulated protein 4-2 by inducing interaction with 14-3-3." Mol Endocrinol **19**(12): 3073-3084.

Bhalla, V. and K. R. Hallows (2008). "Mechanisms of ENaC regulation and clinical implications." J Am Soc Nephrol **19**: 1845-1854.

Bhalla, V., N. M. Oyster, A. C. Fitch, M. A. Wijngaarden, D. Neumann, U. Schlattner, D. Pearce and K. R. Hallows (2006). "AMP-activated kinase inhibits the epithelial Na + channel through functional regulation of the ubiquitin ligase Nedd4-2." J Biol Chem **281**(36): 26159-26169.

Bhattacharya, J. and M. A. Matthay (2013). "Regulation and Repair of the Alveolar-Capillary Barrier in Acute Lung Injury." Annu Rev Phys **75**(1): 593-615.

Biehl, M., M. G. Kashiouris and O. Gajic (2013). "Ventilator-induced lung injury: minimizing its impact in patients with or at risk for ARDS." Respir Care **58**(6): 927-937.

Blenis, J. (1993). "Signal transduction via the MAP kinases: proceed at your own RSK." Proc Natl Acad Sci USA **90**(13): 5889-5892.

Boase, N. A., G. Y. Rychkov, S. L. Townley, A. Dinudom, E. Candi, A. K. Voss, T. Tsoutsman, C. Semsarian, G. Melino, F. Koentgen, D. I. Cook and S. Kumar (2011). "Respiratory distress and perinatal lethality in Nedd4-2-deficient mice." Nat Commun **2**: 287-287.

Bonny, O., A. Chraibi, J. Loffing, N. F. Jaeger, S. Gründer, J. D. Horisberger and B. C. Rossier (1999). "Functional expression of a pseudohypoaldosteronism type I mutated epithelial Na+ channel lacking the pore-forming region of its α subunit." J Clin Invest **104**(7): 967-974.

Boughter, J. D., Jr. and T. A. Gilbertson (1999). "From Channels to Behavior : An Integrative Model of NaCl Taste." Neuron **22**: 213-215.

Briel, M., M. Meade, A. Mercat, R. G. Brower, D. Talmor, S. D. Walter, A. S. Slutsky, E. Pullenayegum, Q. Zhou, D. Cook, L. Brochard, J. C. M. J.-C. M. Richard, F. Lamontagne, N. Bhatnagar, T. E. Stewart and G. Guyatt (2010). "Higher vs Lower Positive End-Expiratory Pressure in Patients With Acute Lung Injury and Acute Respiratory Distress Syndrome: Systematic Review and Meta-analysis." JAMA **303**(9): 865-873.

Briva, A., I. Vadász, E. Lecuona, L. C. Welch, J. Chen, L. a. Dada, H. E. Trejo, V. Dumasius, Z. S. Azzam, P. M. Myrianthefs, D. Batlle, Y. Gruenbaum and J. I. Sznajder (2007). "High CO2 levels impair alveolar epithelial function independently of pH." PLoS ONE **2**(11): e1238.

Buchäckert, Y., S. Rummel, C. U. Vohwinkel, N. M. Gabrielli, B. a. Grzesik, K. Mayer, S. Herold, R. E. Morty, W. Seeger and I. Vadász (2012). "Megalin mediates transepithelial albumin clearance from the alveolar space of intact rabbit lungs." J Physiol **590**: 5167-5181.

Buchbinder, B. A. (2013). "Impact of hypercapnia on alveolar Na+-transport." Doctoral dissertation.

Butterworth, M. (2010). "Regulation of the epithelial sodium channel (ENaC) by membrane trafficking." Biochim Biophys Acta Mol Basis **1802**(12): 1166-1177.

Butterworth, M. B., R. S. Edinger, H. Ovaa, D. Burg, J. P. Johnson and R. A. Frizzell (2007). "The deubiquitinating enzyme UCH-L3 regulates the apical membrane recycling of the epithelial sodium channel." J Biol Chem **282**(52): 37885-37893.

Butterworth, M. B., R. a. Frizzell, J. P. Johnson, K. W. Peters and R. S. Edinger (2005). "PKA-dependent ENaC trafficking requires the SNARE-binding protein complexin." Am J Physiol Renal Physiol **289**(5): F969-F977.

Canessa, C. M., L. Schild, G. Buell, B. Thorens, I. Gautschi, J. D. Horisberger and B. C. Rossier (1994). "Amiloride-sensitive epithelial Na+ channel is made of three homologous subunits." Nature **367**(6462): 463-467.

Carattino, M. D., R. S. Edinger, H. J. Grieser, R. Wise, D. Neumann, U. Schlattner, J. P. Johnson, T. R. Kleyman and K. R. Hallows (2005). "Epithelial sodium channel inhibition by AMP-activated protein kinase in oocytes and polarized renal epithelial cells." J Biol Chem **280**(18): 17608-17616.

Cargnello, M. and P. P. Roux (2011). "Activation and Function of the MAPKs and Their Substrates, the MAPK-Activated Protein Kinases." Microbiol Mol Biol Rev **75**(1): 50-83.

Chen, J., E. Lecuona, A. Briva, L. C. Welch and J. I. Sznajder (2008). "Carbonic anhydrase II and alveolar fluid reabsorption during hypercapnia." Am J Respir Cell Mol Biol **38**(1): 32-37.

Chen, S. Y., A. Bhargava, L. Mastroberardino, O. C. Meijer, J. Wang, P. Buse, G. L. Firestone, F. Verrey and D. Pearce (1999). "Epithelial sodium channel regulated by aldosterone-induced protein sgk." Proc Natl Acad Sci USA **96**(5): 2514-2519.

Cheng, I. W., M. D. Eisner, B. T. Thompson, L. B. Ware and M. A. Matthay (2005). "Acute effects of tidal volume strategy on hemodynamics, fluid balance, and sedation in acute lung injury." Crit Care Med **33**(1): 63-70.

Chikhani, M., A. Das, M. Haque, W. Wang, D. G. Bates and J. G. Hardman (2016). "High PEEP in acute respiratory distress syndrome: Quantitative evaluation between improved arterial oxygenation and decreased oxygen delivery." Br J Anaesth **117**(5): 650-658.

Chraïbi, A. and J. D. Horisberger (2002). "Na self inhibition of human epithelial Na channel: temperature dependence and effect of extracellular proteases." J Gen Physiol **120**(2): 133-145.

Clerici, C. and C. Plane (2009). "Gene regulation in the adaptive process to hypoxia in lung epithelial cells." Am J Physiol Lung Cell Mol Physiol **296**(3): 267-274.

Cobb, M. H. and E. J. Goldsmith (1995). "How MAP kinases are regulated." J Biol Chem **270**: 14843-14846.

Curley, G., M. M. B. Contreras, A. D. Nichol, B. D. Higgins and J. G. Laffey (2010). "Hypercapnia and acidosis in sepsis: a double-edged sword?" Anesthesiology **112**(2): 462-472.

Czikora, I., A. Alli, H.-f. Bao, D. Kaftan, S. Sridhar, H.-J. Apell, B. Gorshkov, R. White, A. Zimmermann, A. Wendel, M. Pauly-Evers, J. Hamacher, I. Garcia-Gabay, B. Fischer, A. Verin, Z. Bagi, J. F. Pittet, W. Shabbir, R. Lemmens-Gruber, T. Chakraborty, A. Lazrak, M. a. Matthay, D. C. Eaton and R. Lucas (2014). "A Novel TNF-mediated Mechanism of Direct Epithelial Sodium Channel Activation." Am J Respir Crit Care Med. **190**(5): 1-49.

Dada, L. A., E. T. Bittar, L. C. Welch, O. Vagin, N. Deiss-yehiely, A. M. Kelly, M. R. Baker, J. Capri, W. Cohn, J. P. Whitelegge, I. Vadász, Y. Gruenbaum and I. Sznajder (2015). "High CO2 Leads to Na,K-ATPase Endocytosis via c-Jun Amino-Terminal Kinase-Induced LMO7b Phosphorylation " Mol Cell Biol **35**(23): 3962-3973.

Dagenais, A., R. Fréchette, Y. Yamagata, T. Yamagata, J.-F. Carmel, M.-E. Clermont, E. Brochiero, C. Massé and Y. Berthiaume (2004). "Downregulation of ENaC activity and expression by TNF-α in alveolar epithelial cells." Am J Physiol Lung Cell Mol Physiol. **286**(2): L301-L311.

de Wolf, E., J. Cook and N. Dale (2016). "Evolutionary adaptation of the sensitivity of connexin 26 hemichannels to CO2." Proc Biol Sci **284**(1848).

Debonneville, C., S. Y. Flores, E. Kamynina, P. J. Plant, C. Tauxe, M. A. Thomas, C. Münster, A. Chraïbi, J. H. Pratt, J. D. Horisberger, D. Pearce, J. Loffing and O. Staub (2002). "Phosphorylation of Nedd4-2 by Sgk1 regulates epithelial Na+ channel cell surface expression." EMBO J **20**(24): 7052-7059.

Denker, B. M. and S. K. Nigam (1998). "Molecular structure and assembly of the tight junction." Am J Physiol Renal Physiol **274**(1 Pt 2): F1-9.

Downs, C. A., A. Kumar, L. H. Kreiner, N. M. Johnson and M. N. Helms (2013). "$H_2O_2$ regulates lung epithelial sodium channel (ENaC) via ubiquitin-like protein Nedd8." J Biol Chem **288**(12): 8136-8145.

Drummond, H. A., F. M. Abboud and M. J. Welsh (2000). "Localization of β and γ subunits of ENaC in sensory nerve endings in the rat foot pad." Brain Research **884**(1-2): 1-12.

Eaton, A. F., Q. Yue, D. C. Eaton and H.-f. Bao (2014). "ENaC activity and expression is decreased in the lungs of protein kinase C-α knockout mice." Am J Physiol Lung Cell Mol Physiol **307**(5): L374-385.

Eaton, D. C., J. Chen, S. Ramosevac, S. Matalon and L. Jain (2004). "Regulation of Na+ channels in lung alveolar type II epithelial cells." Ann Am Thorac Soc **1**(1): 10-16.

Eaton, D. C., B. Malik, H.-F. Bao, L. Yu and L. Jain (2010). "Regulation of epithelial sodium channel trafficking by ubiquitination." Ann Am Thorac Soc.**7**(7): 54-64.

Edinger, R. S., J. Lebowitz, H. Li, R. Alzamora, H. Wang, J. P. Johnson and K. R. Hallows (2009). "Functional Regulation of the Epithelial Na Channel by IκB Kinase-β Occurs via Phosphorylation of the Ubiquitin Ligase Nedd4-2." J Biol Chem **284**(1): 150-157.

Elbert, K. J., U. F. Schäfer, H. J. Schäfers, K. J. Kim, V. H. Lee and C. M. Lehr (1999). "Monolayers of human alveolar epithelial cells in primary culture for pulmonary absorption and transport studies." Pharm Res **16**(5): 601-608.

Firsov, D., L. Schild, I. Gautschi, A.-M. Mérillat, E. Schneeberger and B. C. Rossier (1996). "Cell surface expression of the epithelial Na channel and a mutant causing Liddle syndrome: A quantitative approach." Proc Natl Acad Sci USA **93**(26): 15370-15375.

Flodby, P., Y. H. Kim, L. L. Beard, D. Gao, Y. Ji, H. Kage, J. M. Liebler, P. Minoo, K. J. Kim, Z. Borok and E. D. Crandall (2016). "Knockout mice reveal a major role for alveolar epithelial type i cells in alveolar fluid clearance." Am J Respir Cell Mol Biol **55**(3): 395-406.

Frank, J., J. Roux, H. Kawakatsu, G. Su, A. Dagenais, Y. Berthiaume, M. Howard, C. M. Canessa, X. Fang, D. Sheppard, M. A. Matthay and J. F. Pittet (2003). "Transforming Growth Factor-β1 Decreases Expression of the Epithelial Sodium Channel αENaC and Alveolar Epithelial Vectorial

Sodium and Fluid Transport via an ERK1/2-dependent Mechanism." J Biol Chem **278**(45): 43939-43950.

Fronius, M., W. G. Clauss and M. Althaus (2012). "Why do we have to move fluid to be able to breathe?" Front Physiol **3**(146): 1-9.

Galietta, L. J. V., P. Pagesy, C. Folli, E. Caci, L. Romio, B. Costes, E. Nicolis, G. Cabrini, M. Goossens, R. Ravazzolo and O. Zegarra-Moran (2002). "IL-4 is a potent modulator of ion transport in the human bronchial epithelium in vitro." J Immunol **168**(2): 839-845.

Gao, S., C. Alarcón, G. Sapkota, S. Rahman, P.-y. Chen, M. J. Macias, H. Erdjument-bromage and P. Tempst (2009). "Ubiquitin ligase Nedd4L targets activated Smad2/3 to limit TGF β signaling." Mol Cell **36**(3): 457-468.

Gates, K. L., H. A. Howell, A. Nair, C. U. Vohwinkel, L. C. Welch, G. J. Beitel, A. R. Hauser, J. I. Sznajder and P. H. S. Sporn (2013). "Hypercapnia impairs lung neutrophil function and increases mortality in murine Pseudomonas pneumonia." Am J Respir Cell Mol Biol **49**(5): 821-828.

Geiser, T. (2003). "Mechanisms of alveolar epithelial repair in acute lung injury-a translational approach." Swiss Med Wkly **133**(43-44): 586-590.

Gille, T., N. Randrianarison-Pellan, A. Goolaerts, N. Dard, Y. Uzunhan, E. Ferrary, E. Hummler, C. Clerici and C. Planès (2014). "Hypoxia-induced inhibition of epithelial Na+ channels in the lung: Role of Nedd4-2 and the ubiquitin-proteasome pathway." Am J Respir Cell Mol Biol **50**(3): 526-537.

Green, W. N. and C. P. Wanamaker (1997). "The role of the cystine loop in acetylcholine receptor assembly." J Biol Chem **272**(33): 20945-20953.

Grunder, S., N. F. Jaeger, I. Gautschi, L. Schild and B. C. Rossier (1999). "Identification of a highly conserved sequence at the N-terminus of the epithelial Na+ channel alpha subunit involved in gating." Pflugers Arch **438**(5): 709-715.

Grzesik, B. A., C. U. Vohwinkel, R. E. Morty, K. Mayer, S. Herold, W. Seeger and I. Vadász (2013). "Efficient gene delivery to primary alveolar epithelial cells by nucleofection." Am J Physiol Lung Cell Mol Physiol **305**(11): L786-794.

Guérin, C., J. Reignier, J.-C. Richard, P. Beuret, A. Gacouin, T. Boulain, E. Mercier, M. Badet, A. Mercat, O. Baudin, M. Clavel, D. Chatellier, S. Jaber, S. Rosselli, J. Mancebo, M. Sirodot, G. Hilbert, C. Bengler, J. Richecoeur, M. Gainnier, F. Bayle, G. Bourdin, V. Leray, R. Girard, L. Baboi and L. Ayzac (2013). "Prone Positioning in Severe Acute Respiratory Distress Syndrome." N Engl J Med **368**(23): 2159-2168.

Gusarova, G. A., H. E. Trejo, L. A. Dada, A. Briva, L. C. Welch, R. B. Hamanaka, G. M. Mutlu, N. S. Chandel, M. Prakriya and J. I. Sznajder (2011). "Hypoxia Leads to Na,K-ATPase Downregulation via Ca2+ Release-Activated Ca2+ Channels and AMPK Activation." Mol Cell Biol **31**(17): 3546-3556.

Gwoździńska, P., B. A. Buchbinder, K. Mayer, S. Herold, R. E. Morty, W. Seeger and I. Vadász (2017). "Hypercapnia Impairs ENaC Cell Surface Stability by Promoting Phosphorylation, Polyubiquitination and Endocytosis of β-ENaC in a Human Alveolar Epithelial Cell Line." Front Immunol **8**(591).

Haerteis, S., B. Krueger, C. Korbmacher and R. Rauh (2009). "The δ-subunit of the epithelial Sodium channel (ENaC) enhances channel activity and alters proteolytic ENaC activation." J Biol Chem **284**(42): 29024-29040.

Hallows, K. R., V. Bhalla, N. M. Oyster, M. A. Wijngaarden, J. K. Lee, H. Li, S. Chandran, X. Xia, Z. Huang, R. J. Chalkley, A. L. Burlingame and D. Pearce (2010). "Phosphopeptide screen uncovers novel phosphorylation sites of Nedd4-2 that potentiate its inhibition of the epithelial Na+ channel." J Biol Chem **285**(28): 21671-21678.

Hallows, K. R., J. E. McCane, B. E. Kemp, L. A. Witters and J. K. Foskett (2002). "Regulation of Channel Gating by AMP-activated Protein Kinase Modulates Cystic Fibrosis Transmembrane Conductance Regulator Activity in Lung Submucosal Cells * CFTR interaction has functional implications in hu." J Biol Chem **278**(2): 998-1004.

Hanukoglu, I. and A. Hanukoglu (2016). "Epithelial sodium channel (ENaC) family: Phylogeny, structure-function, tissue distribution, and associated inherited diseases." Gene **579**: 95-132.

Hawley, S. A., D. A. Pan, K. J. Mustard, L. Ross, J. Bain, A. M. Edelman, B. G. Frenguelli and D. G. Hardie (2005). "Calmodulin-dependent protein kinase kinase β is an alternative upstream kinase for AMP-activated protein kinase." Cell Metab **2**(1): 9-19.

Helenius, I. T., T. Krupinski, D. W. Turnbull, Y. Gruenbaum, N. Silverman, E. A. Johnson, P. H. S. Sporn, J. I. Sznajder and G. J. Beitel (2009). "Elevated CO2 suppresses specific Drosophila innate immune responses and resistance to bacterial infection." Proc Natl Acad Sci USA **106**(44): 18710-18715.

Hendron, E., P. Patel, M. Hausenfluke, N. Gamper, M. S. Shapiro, R. E. Booth and J. D. Stockand (2002). "Identification of cytoplasmic domains within the epithelial Na+ channel reactive at the plasma membrane." J Biol Chem **277**(37): 34480-34488.

Hermanns and et al. (2004). "Lung epithelial cell lines in coculture with human pulmonary microvascular endothelial cells: development of an alveolo-capillary barrier in vitro." Lab Invest **84**(6): 736-752.

Herold, S., N. M. Gabrielli and I. Vadász (2013). "Novel concepts of acute lung injury and alveolar-capillary barrier dysfunction." Am J Physiol Lung Cell Mol Physiol **305**(10): L665-681.

Higgins, B. D., J. Costello, M. Contreras, P. Hassett, D. O' Toole and J. G. Laffey (2009). "Differential effects of buffered hypercapnia versus hypercapnic acidosis on shock and lung injury induced by systemic sepsis." Anesthesiology **111**(6): 1317-1326.

Hollenhorst, M. I., K. Richter and M. Fronius (2011). "Ion transport by pulmonary epithelia." J Biomed Biotechnol **2011**:174306

Hughey, R. P., J. B. Bruns, C. L. Kinlough, K. L. Harkleroad, Q. Tong, M. D. Carattino, J. P. Johnson, J. D. Stockand and T. R. Kleyman (2004). "Epithelial Sodium Channels Are Activated by Furin-dependent Proteolysis." J Biol Chem **279**(18): 18111-18114.

Hughey, R. P., J. B. Bruns, C. L. Kinlough and T. R. Kleyman (2004). "Distinct pools of epithelial sodium channels are expressed at the plasma membrane." J Biol Chem **279**: 48491-48494.

Hummler, E., P. Barker and J. Gatzy (1996). "Early death due to defective neonatal lung liquid clearance in αENaC-deficient mice." Nat Genet **12**(3): 325-328.

Hunter, T. (2007). "The Age of Crosstalk: Phosphorylation, Ubiquitination, and Beyond." Mol Cell **28**(5): 730-738.

Ismailov, I. I., B. K. Berdiev and D. J. Benos (1995). "Biochemical status of renal epithelial Na+ channels determines apparent channel conductance, ion selectivity, and amiloride sensitivity." Biophys J **69**(5): 1789-1800.

Jain, L., X. J. Chen, B. Malik, O. Al-Khalili and D. C. Eaton (1999). "Antisense oligonucleotides against the alpha-subunit of ENaC decrease lung epithelial cation-channel activity." Am J Physiol **276**(6 Pt 1): L1046-1051.

Jaitovich, A., M. Angulo, E. Lecuona, L. a. Dada, L. C. Welch, Y. Cheng, G. Gusarova, E. Ceco, C. Liu, M. Shigemura, E. Barreiro, C. Patterson, G. a. Nader and J. I. Sznajder (2015). "High CO 2 levels cause skeletal muscle atrophy via AMPK, FoxO3a and muscle-specific ring finger protein1 (MuRF1)." J Biol Chem **290**(14): 9183-94

Jeffery, P. K. and L. Reid (1975). "New observations of rat airway epithelium: a quantitative and electron microscopic study." J Anat **120**(Pt 2): 295-320.

Ji, H. L., S. Parker, A. L. Langloh, C. M. Fuller and D. J. Benos (2001). "Point mutations in the post-M2 region of human alpha-ENaC regulate cation selectivity." Am J Physiol Cell Physiol **281**(1): C64-74.

Johnson, E. R. and M. A. Matthay (2010). "Acute lung injury: epidemiology, pathogenesis, and treatment." J Aerosol Med Pulm Drug Deliv **23**(4): 243-252.

Kabra, R., K. K. Knight, R. Zhou and P. M. Snyder (2008). "Nedd4-2 induces endocytosis and degradation of proteolytically cleaved epithelial Na+ channels." J Biol Chem **283**(10): 6033-6039.

Kamynina, E., C. Tauxe and O. Staub (2001). "Distinct characteristics of two human Nedd4 proteins with respect to epithelial Na(+) channel regulation." Am J Physiol Renal Physiol **281**(3): F469-477.

Kashlan, O. B. and T. R. Kleyman (2012). "Epithelial Na + channel regulation by cytoplasmic and extracellular factors." Exp Cell Res **318**(9): 1011-1019.

Kellenberger, S., I. Gautschi, B. C. Rossier and L. Schild (1998). "Mutations causing Liddle syndrome reduce sodium-dependent downregulation of the epithelial sodium channel in the Xenopus oocyte expression system." J Clin Invest **101**(12): 2741-2750.

Kerem, E. and T. Bistritzer (1999). "Pulmonary epithelial sodium-channel dysfunction and excess airway liquid in pseudohypoaldosteronism." N Engl J Med. **341**(3): 156-162.

Kimura, T., H. Kawabe, C. Jiang, W. Zhang, Y.-Y. Xiang, C. Lu, M. W. Salter, N. Brose, W.-Y. Lu and D. Rotin (2011). "Deletion of the ubiquitin ligase Nedd4L in lung epithelia causes cystic fibrosis-like disease." Proc Natl Acad Sci USA **108**(8): 3216-3221.

Knight, K. K., D. R. Olson, R. Zhou and P. M. Snyder (2006). "Liddle's syndrome mutations increase Na+ transport through dual effects on epithelial Na+ channel surface expression and proteolytic cleavage." Proc Natl Acad Sci USA **103**(8): 2805-2808.

Konstas, A. A., D. Mavrelos and C. Korbmacher (2000). "Conservation of pH sensitivity in the epithelial sodium channel (ENaC) with Liddle's syndrome mutation." Pflugers Arch. **441**(2-3): 341-350.

Krause, N. C., H. S. Kutsche, F. Santangelo, E. R. DeLeon, N. P. Dittrich, K. R. Olson and M. Althaus (2016). "Hydrogen sulfide contributes to hypoxic inhibition of airway transepithelial sodium absorption." Am J Physiol Regul Integr Comp Physiol **311**(3): R607-17

Laffey, J. G. and B. P. Kavanagh (1999). "Carbon dioxide and the critically ill-too little of a good thing?" Lancet **354**(9186): 1283-1286.

Lazrak, A., L. Chen, A. Jurkuvenaite, S. F. Doran, G. Liu, Q. Li, J. R. Lancaster and S. Matalon (2012). "Regulation of alveolar epithelial Na + channels by ERK1/2 in chlorine-breathing mice." Am J Respir Cell Mol Biol. **46**(3): 342-354.

Lebowitz, J., R. S. Edinger, B. An, C. J. Perry, S. Onate, T. R. Kleyman and J. P. Johnson (2004). "IκB Kinase-β (IKKβ) Modulation of Epithelial Sodium Channel Activity." J Biol Chem **279**(40): 41985-41990.

Li, T. and H. G. Folkesson (2006). "RNA interference for alpha-ENaC inhibits rat lung fluid absorption in vivo." Am J Physiol Lung Cell Mol Physiol **290**(4): L649-L660.

Lim, K. L., K. C. M. Chew, J. M. M. Tan, C. Wang, K. K. K. Chung, Y. Zhang, Y. Tanaka, W. Smith, S. Engelender, C. a. Ross, V. L. Dawson and T. M. Dawson (2005). "Parkin mediates nonclassical, proteasomal-independent ubiquitination of synphilin-1: implications for Lewy body formation." J Neurosci **25**(8): 2002-2009.

Lu, C., S. Pribanic, A. Debonneville, C. Jiang and D. Rotin (2007). "The PY motif of ENaC, mutated in liddle syndrome, regulates channel internalization, sorting and mobilization from subapical pool." Traffic **8**(9): 1246-1264.

Ly, K., C. J. McIntosh, W. Biasio, Y. Liu, Y. Ke, D. R. Olson, J. H. Miller, R. Page, P. M. Snyder and F. J. McDonald (2013). "Regulation of the delta and alpha epithelial sodium channel (ENaC) by ubiquitination and Nedd8." J Cell Physiol **228**(11): 2190-2201.

Malik, B., Q. Yue, G. Yue, X. J. Chen, S. R. Price, W. E. Mitch and D. C. Eaton (2005). "Role of Nedd4-2 and polyubiquitination in epithelial sodium channel degradation in untransfected renal A6 cells expressing endogenous ENaC subunits." Am J Physiol Renal Physiol **289**(1): F107-116.

Mall, M., B. R. Grubb, J. R. Harkema, W. K. O'Neal and R. C. Boucher (2004). "Increased airway epithelial Na+ absorption produces cystic fibrosis-like lung disease in mice." Nat Med **10**(5): 487-493.

Matalon, S. (1991). "Mechanisms and regulation of ion transport in adult mammalian alveolar type II pneumocytes." Am J Physiol **261**(5 Pt 1): C727-738.

Matalon, S., R. Bartoszewski and J. F. Collawn (2015). "Role of epithelial sodium channels in the regulation of lung fluid homeostasis." Am J Physiol Lung Cell Mol Physiol **309**(11): L1229-38.

Matalon, S. and H. O. Brodovich (1999). "Sodium channels in alveolar epithelial cells: Molecular Characterization, Biophysical Properties and Physiological Significance." Annu Rev Physiol **61**: 627-661.

Matalon, S., A. Lazrak, L. Jain and D. C. Eaton (2002). "Invited review: biophysical properties of sodium channels in lung alveolar epithelial cells." J Appl Physiol **93**(5): 1852-1859.

Matthay, M. A. (2015). "Therapeutic potential of mesenchymal stromal cells for acute respiratory distress syndrome." Ann Am Thorac Soc. **12**(Suppl 1): S54-S57.

Matthay, M. A., R. G. Brower, S. Carson, I. S. Douglas, M. Eisner, D. Hite, S. Holets, R. H. Kallet, K. D. Liu, N. MacIntyre, M. Moss, D. Schoenfeld, J. Steingrub and B. T. Thompson (2011). "Randomized, placebo-controlled clinical trial of an aerosolized beta(2)-agonist for treatment of acute lung injury." Am J Respir Crit Care Med **184**(5): 561-568.

Matthay, M. A., H. G. Folkesson and C. Clerici (2002). "Lung epithelial fluid transport and the resolution of pulmonary edema." Physiol Rev **82**(3): 569-600.

Matthay, M. A. and R. L. Zemans (2011). "The acute respiratory distress syndrome: pathogenesis and treatment." Annu Rev Pathol **6**: 147-163.

May, A., A. Puoti, H. P. Gaeggeler, J. D. Horisberger and B. C. Rossier (1997). "Early effect of aldosterone on the rate of synthesis of the epithelial sodium channel alpha subunit in A6 renal cells." J AM Soc Nephrol **8**(12): 1813-1822.

McAuley, D. F., L. J. M. Cross, U. Hamid, E. Gardner, J. S. Elborn, K. M. Cullen, A. Dushianthan, M. P. W. Grocott, M. A. Matthay and C. M. O'Kane (2017). "Keratinocyte growth factor for the treatment of the acute respiratory distress syndrome (KARE): a randomised, double-blind, placebo-controlled phase 2 trial." Lancet Respir Med **5**(6): 484-491.

McNicholas, C. M. and C. M. Canessa (1997). "Diversity of channels generated by different combinations of epithelial sodium channel subunits." J Gen Physiol **109**(6): 681-692.

Meyrick, B. (1986). "Pathology of the adult respiratory distress syndrome." Crit Care Clin **2**(3): 405-428.

Mutlu, G. M., V. Dumasius, J. Burhop, P. J. McShane, F. J. Meng, L. Welch, A. Dumasius, N. Mohebahmadi, G. Thakuria, K. Hardiman, S. Matalon, S. Hollenberg and P. Factor (2004). "Upregulation of alveolar epithelial active Na+ transport is dependent on beta2-adrenergic receptor signaling." Circ Res **94**(8): 1091-1100.

Mutlu, G. M., P. Factor, D. E. Schwartz and J. I. Sznajder (2002). "Severe status asthmaticus: management with permissive hypercapnia and inhalation anesthesia." Crit Care Med **30**(2): 477-480.

Mutlu, G. M. and J. I. Sznajder (2005). "Mechanisms of pulmonary edema clearance." Am J Physiol Lung Cell Mol Physiol **289**(5):L685-95.

Neuhaus, W., F. Samwer, S. Kunzmann, R. M. Muellenbach, M. Wirth, C. P. Speer, N. Roewer and C. Y. Förster (2012). "Lung endothelial cells strengthen, but brain endothelial cells weaken barrier properties of a human alveolar epithelium cell culture model." Differentiation **84**(4): 294-304.

Nguyen, L. K., W. Kolch and B. N. Kholodenko (2013). "When ubiquitination meets phosphorylation: a systems biology perspective of EGFR/MAPK signalling." J Cell Commun Signal **11**(1): 52-52.

Nichol, A. D., D. F. O'Cronin, K. Howell, F. Naughton, S. O'Brien, J. Boylan, C. O'Connor, D. O'Toole, J. G. Laffey and P. McLoughlin (2009). "Infection-induced lung injury is worsened after renal buffering of hypercapnic acidosis." Crit Care Med **37**(11): 2953-2961.

Nin, N., A. Muriel, O. Peñuelas, L. Brochard, J. A. Lorente, N. D. Ferguson, K. Raymondos, F. Ríos, D. A. Violi, A. W. Thille, M. González, A. J. Villagomez, J. Hurtado, A. R. Davies, B. Du, S. M. Maggiore, L. Soto, G. D'Empaire, D. Matamis, F. Abroug, R. P. Moreno, M. A. Soares, Y. Arabi, F. Sandi, M. Jibaja, P. Amin, Y. Koh, M. A. Kuiper, H. H. Bülow, A. A. Zeggwagh, A. Anzueto, J. I. Sznajder, A. Esteban and V. G. for the (2017). "Severe hypercapnia and outcome of mechanically ventilated patients with moderate or severe acute respiratory distress syndrome." Intensive Care Med **43**(2): 200-208.

Nishio, K., Y. Suzuki, K. Takeshita, T. Aoki, H. Kudo, N. Sato, K. Naoki, N. Miyao, M. Ishii and K. Yamaguchi (2001). "Effects of hypercapnia and hypocapnia on [Ca2+]i mobilization in human pulmonary artery endothelial cells." J Appl Physiol **90**(6): 2094-2100.

Peters, D. M., I. Vadász, L. Wujak, M. Wygrecka, A. Olschewski, C. Becker, S. Herold, R. Papp, K. Mayer, S. Rummel, R. P. Brandes, A. Günther, S. Waldegger, O. Eickelberg, W. Seeger and R. E. Morty (2014). "TGF-β directs trafficking of the epithelial sodium channel ENaC which has implications for ion and fluid transport in acute lung injury." Proc Natl Acad Sci USA **111**(3): E374-383.

Plant, P. J., H. Yeger, O. Staub, P. Howard and D. Rotin (1997). "The C2 domain of the ubiquitin protein ligase Nedd4 mediates Ca2+- dependent plasma membrane localization." J Biol Chem **272**(51): 32329-32336.

Prince, L. S. and M. J. Welsh (1998). "Cell surface expression and biosynthesis of epithelial Na+ channels." Biochem J **336** (Pt 3): 705-710.

Putnam, R. W., J. A. Filosa and N. A. Ritucci (2004). "Cellular mechanisms involved in CO 2 and acid signaling in chemosensitive neurons." Am J Physiol Cell Physiol **287**(339): C1493-C1526.

Raghavendran, K., G. S. Pryhuber, P. R. Chess, B. a. Davidson, P. R. Knight and R. H. Notter (2008). "Pharmacotherapy of acute lung injury and acute respiratory distress syndrome." Curr Med Chem **15**(19): 1911-1924.

Raghavendran, K., D. Willson and R. H. Notter (2011). "Surfactant Therapy for Acute Lung Injury and Acute Respiratory Distress Syndrome." Crit Care Clin **27**: 525-559.

Ranieri, V. M., G. D. Rubenfeld, B. T. Thompson, N. D. Ferguson, E. Caldwell, E. Fan, L. Camporota and A. S. Slutsky (2012). "Acute respiratory distress syndrome: the Berlin Definition." JAMA **307**(23): 2526-2533.

Renard, S., E. Lingueglia, N. Voilley, M. Lazdunski and P. Barbry (1994). "Biochemical analysis of the membrane topology of the amiloride-sensitive Na+ channel." J Biol Chem **269**(17): 12981-12986.

Rossier, B. C. (2002). "Hormonal regulation of the epithelial sodium channel ENaC: N or P(o)?" J Gen Physiol **120**(1): 67-70.

Rotin, D. and S. Kumar (2009). "Physiological functions of the HECT family of ubiquitin ligases." Nat Rev Mol Cell Biol **10**(6): 398-409.

Rotin, D. and O. Staub (2011). "Role of the ubiquitin system in regulating ion transport." Pflugers Arch **461**(1): 1-21.

Rotin, D. and O. Staub (2012). "Nedd4-2 and the regulation of epithelial sodium transport." Front Physiol **3** (212): 1-7.

Roux, J., H. Kawakatsu, B. Gartland, M. Pespeni, D. Sheppard, M. a. Matthay, C. M. Canessa and J.-F. Pittet (2005). "Interleukin-1beta decreases expression of the epithelial sodium channel alpha-subunit in alveolar epithelial cells via a p38 MAPK-dependent signaling pathway." J Biol Chem **280**(19): 18579-18589.

Rubenfeld, G. D. and M. S. Herridge (2007). "Epidemiology and outcomes of acute lung injury." Chest **131**(2): 554-562.

Ryu, J., G. Haddad and W. A. Carlo (2012). "Clinical effectiveness and safety of permissive hypercapnia." Clin Perinatol **39**(3): 603-612.

Salomon, J. J., V. E. Muchitsch, J. C. Gausterer, E. Schwagerus, H. Huwer, N. Daum, C. M. Lehr and C. Ehrhardt (2014). "The cell line NCl-H441 is a useful in vitro model for transport studies of human distal lung epithelial barrier." Mol Pharm **11**(3): 995-1006.

Sambrook J. F.,D. W. Russell (2001). Molecular Cloning: A Laboratory Manual, Volume 1, Cold Spring Harbor Laboratory Press.

Scarpelli, E. M. (2003). "Physiology of the alveolar surface network." Comp Biochem Physiol A Mol Integr Physiol **135**(1): 39-104.

Schild, L. (2010). "The epithelial sodium channel and the control of sodium balance." Biochim Biophys Acta Mol Basis Dis **1802**(12): 1159-1165.

Schild, L., E. Schneeberger, I. Gautschi and D. Firsov (1997). "Identification of amino acid residues in the alpha, beta, and gamma subunits of the epithelial sodium channel (ENaC) involved in amiloride block and ion permeation." J Gen Physiol **109**(1): 15-26.

Schwagerus, E., S. Sladek, S. T. Buckley, N. Armas-Capote, D. A. de la Rosa, B. J. Harvey, H. Fischer, B. Illek, H. Huwer, N. Schneider-Daum, C. M. Lehr and C. Ehrhardt (2015). "Expression and function of the epithelial sodium channel δ-subunit in human respiratory epithelial cells in vitro." Pflugers Arch **467**(11): 2257-73.

Shen, J.-P. and C. U. Cotton (2003). "Epidermal growth factor inhibits amiloride-sensitive sodium absorption in renal collecting duct cells." Am J Physiol Renal Physiol **284**(1): F57-F64.

Shi, H., C. Asher, A. Chigaev, Y. Yung, E. Reuveny, R. Seger and H. Garty (2002). "Interactions of β and γENaC with Nedd4 can be facilitated by an ERK-mediated phosphorylation." J Biol Chem **277**(16): 13539-13547.

Shimkets, R. a., R. P. Lifton and C. M. Canessa (1997). "The activity of the epithelial sodium channel is regulated by clathrin-mediated endocytosis." J Biol Chem **272**(41): 25537-25541.

Shyamsundar, M., D. F. McAuley, R. J. Ingram, D. S. Gibson, D. O'Kane, S. T. McKeown, A. Edwards, C. Taggart, J. S. Elborn, C. S. Calfee, M. A. Matthay and C. M. O'Kane (2014). "Keratinocyte growth factor promotes epithelial survival and resolution in a human model of lung injury." Am J Respir Crit Care Med **189**(12): 1520-1529.

Sigismund, S., S. Confalonieri, a. Ciliberto, S. Polo, G. Scita and P. P. Di Fiore (2012). "Endocytosis and Signaling: Cell Logistics Shape the Eukaryotic Cell Plan." Physiol Rev **92**(1): 273-366.

Snyder, P. M. (2009). "Down-regulating destruction: phosphorylation regulates the E3 ubiquitin ligase Nedd4-2." Sci Signal **2**(79): pe41-pe41.

Snyder, P. M., D. R. Olson, F. J. McDonald and D. B. Bucher (2001). "Multiple WW Domains, but Not the C2 Domain, are Required for Inhibition of the Epithelial Na+ Channel by Human Nedd4." J Biol Chem **276**(30): 28321-28326.

Snyder, P. M., J. C. Steines and D. R. Olson (2004). "Relative Contribution of Nedd4 and Nedd4-2 to ENaC Regulation in Epithelia Determined by RNA Interference." J Biol Chem **279**(6): 5042-5046.

Soundararajan, R., J. Wang, D. Melters and D. Pearce (2010). "Glucocorticoid-induced leucine zipper 1 stimulates the epithelial sodium channel by regulating serum- and glucocorticoid-induced kinase 1 stability and subcellular localization." J Biol Chem **285**(51): 39905-39913.

Sporty, J. L., L. Horálková and C. Ehrhardt (2008). "In vitro cell culture models for the assessment of pulmonary drug disposition." Expert Opin Drug Metab Toxicol **4**(4): 333-345.

Staub, O., I. Gautschi, T. Ishikawa, K. Breitschopf, A. Ciechanover, L. Schild and D. Rotin (1997). "Regulation of stability and function of the epithelial Na+ channel (ENaC) by ubiquitination." EMBO J **16**(21): 6325-6336.

Stockand, J. D., A. Staruschenko, O. Pochynyuk, R. E. Booth and D. U. Silverthorn (2008). "Insight toward epithelial Na+ channel mechanism revealed by the acid-sensing ion channel structure." IUBMB Life **60**(9): 620-628.

Stone, K. C., R. R. Mercer, P. Gehr, B. Stockstill and J. D. Crapo (1992). "Allometric relationships of cell numbers and size in the mammalian lung." Am J Respir Cell Mol Biol **6**(2): 235-243.

Sznajder, J. I. (2001). Alveolar edema must be cleared for the acute respiratory distress syndrome patient to survive. Am J Respir Crit Care Med**163**(6): 1293-1294.

Tan, C. D., I. A. Selvanathar and D. L. Baines (2011). "Cleavage of endogenous γENaC and elevated abundance of αENaC are associated with increased Na + transport in response to apical fluid volume expansion in human H441 airway epithelial cells." Pflugers Arch **462**(3): 431-441.

Taylor, R. W., J. L. Zimmerman, R. P. Dellinger, R. C. Straube, G. J. Criner, K. Davis, K. M. Kelly, T. C. Smith and R. J. Small (2004). "Low-dose inhaled nitric oxide in patients with acute lung injury: a randomized controlled trial." JAMA **291**(13): 1603-1609.

Tiruvoipati, R., D. Pilcher, H. Buscher, J. Botha and M. Bailey (2017). "Effects of Hypercapnia and Hypercapnic Acidosis on Hospital Mortality in Mechanically Ventilated Patients." Crit Care Med **45**(7): e649-e656.

Turner, M. J. (2014). "The Effects of Hypercapnia on CFTR- Dependent HCO3- Secretion in Human Airway Epithelia." J Physiol **594**(6): 1643–1661. .

Vadász, I., L. A. Dada, A. Briva, I. T. Helenius, K. Sharabi, L. C. Welch, A. M. Kelly, B. A. Grzesik, G. R. S. Budinger, J. Liu, W. Seeger, G. J. Beitel, Y. Gruenbaum and J. I. Sznajder (2012). "Evolutionary Conserved Role of c-Jun-N-Terminal Kinase in CO2-Induced Epithelial Dysfunction." PLoS ONE **7**(10)**:** e46696.

Vadász, I., L. A. Dada, A. Briva, H. E. Trejo, L. C. Welch, J. Chen, P. T. Tóth, E. Lecuona, L. a. Witters, P. T. Schumacker, N. S. Chandel, W. Seeger, J. I. Sznajder, I. Vadasz and P. T. Toth

(2008). "AMP-activated protein kinase regulates CO2-induced alveolar epithelial dysfunction in rats and human cells by promoting Na,K-ATPase endocytosis." J Clin Invest **118**(2): 752-762.

Vadász, I., R. D. Hubmayr, N. Nin, P. H. S. Sporn and J. I. Sznajder (2012). "Hypercapnia: A nonpermissive environment for the lung." Am J Respir Cell Mol Biol **46**(4): 417-421.

Vadász, I. and J. I. Sznajder (2017). "Gas exchange disturbances regulate alveolar fluid clearance during acute lung injury." Front Immunol **8**(757): 1-7.

Vadász, I., C. H. Weiss and J. I. Sznajder (2012). "Ubiquitination and proteolysis in acute lung injury." Chest **141**(3): 763-771.

Vallet, V., A. Chraibi, H. P. Gaeggeler, J. D. Horisberger and B. C. Rossier (1997). "An epithelial serine protease activates the amiloride-sensitive sodium channel." Nature **389**(6651): 607-610.

Vohwinkel, C. U., E. Lecuona, H. Sun, N. Sommer, I. Vadász, N. S. Chandel and J. I. Sznajder (2011). "Elevated CO2 levels cause mitochondrial dysfunction and impair cell proliferation." J Biol Chem **286**(43): 37067-37076.

Voilley, N., E. Lingueglia, G. Champigny, M. G. Mattéi, R. Waldmann, M. Lazdunski and P. Barbry (1994). "The lung amiloride-sensitive Na+ channel: biophysical properties, pharmacology, ontogenesis, and molecular cloning." Proc Natl Acad Sci USA **91**(1): 247-251.

Waldmann, R., G. Champigny, F. Bassilana, N. Voilley and M. Lazdunski (1995). "Molecular cloning and functional expression of a novel amiloride-sensitive Na+ channel." J Biol Chem **270**(46): 27411-27414.

Wang, H., L. M. Traub, K. M. Weixel, M. J. Hawryluk, N. Shah, R. S. Edinger, C. J. Perry, L. Kester, M. B. Butterworth, K. W. Peters, T. R. Kleyman, R. A. Frizzell and J. P. Johnson (2006). "Clathrin-mediated endocytosis of the epithelial sodium channel: Role of epsin." J Biol Chem **281**(20): 14129-14135.

Wang, N., K. L. Gates, H. Trejo, S. Favoreto, R. P. Schleimer, J. I. Sznajder, G. J. Beitel and P. H. S. Sporn (2010). "Elevated CO2 selectively inhibits interleukin-6 and tumor necrosis factor expression and decreases phagocytosis in the macrophage." FASEB J **24**(7): 2178-2190.

Ware, L. B. and M. A. Matthay (2001). "Alveolar fluid clearance is impaired in the majority of patients with acute lung injury and the acute respiratory distress syndrome." Am J Respir Crit Care Med. **163**(2): 1376-1383.

Welch, L. C., E. Lecuona, A. Briva, H. E. Trejo, L. A. Dada and J. I. Sznajder (2010). "Extracellular signal-regulated kinase (ERK) participates in the hypercapnia-induced Na,K-ATPase downregulation." FEBS Lett **584**(18): 3985-3989.

Wiedemann, H. P., A. P. Wheeler, G. R. Bernard, B. T. Thompson, D. Hayden, B. deBoisblanc, A. F. Connors, R. D. Hite and A. L. Harabin (2006). "Comparison of two fluid-management strategies in acute lung injury." N Engl J Med **354**(24): 2564-2575.

Wiemuth, D., Y. Ke, M. Rohlfs and F. J. McDonald (2007). "Epithelial sodium channel (ENaC) is multi-ubiquitinated at the cell surface." Biochem J **405**: 147-155.

Wiener-Kronish, J. P., K. H. Albertine, M. A. Matthay, O. Osorio and M. Neuberger (1991). "Differential responses of the endothelial and epithelial barriers of the lung in sheep to Escherichia coli endotoxin." J Clin Invest **88**(3): 864-875.

Wittekindt, O. H. (2017). "Tight junctions in pulmonary epithelia during lung inflammation." Pflugers Arch **469**(1): 135-147.

Wodopia, R., H. S. Ko, J. Billian, R. Wiesner, P. Bärtsch and H. Mairbäurl (2000). "Hypoxia decreases proteins involved in epithelial electrolyte transport in A549 cells and rat lung." Am J Physiol Lung Cell Mol Physiol **279**(6): L1110-1119.

Woods, A., K. Dickerson, R. Heath, S.-P. Hong, M. Momcilovic, S. R. Johnstone, M. Carlson and D. Carling (2005). "Ca2+/calmodulin-dependent protein kinase kinase-beta acts upstream of AMP-activated protein kinase in mammalian cells." Cell Metab **2**(1): 21-33.

Woollhead, A. M., J. W. Scott, D. G. Hardie and D. L. Baines (2005). "Phenformin and 5-aminoimidazole-4-carboxamide-1-beta-D-ribofuranoside (AICAR) activation of AMP-activated protein kinase inhibits transepithelial Na+ transport across H441 lung cells." Am J Physiol Cell Physiol **566**(Pt 3): 781-792.

Wynne, B. M., L. Zou, V. Linck, R. S. Hoover, H. P. Ma and D. C. Eaton (2017). "Regulation of lung epithelial sodium channels by cytokines and chemokines." Front Immunol **8**(766).

Xu, B. E., S. Stippec, A. Lazrak, C. L. Huang and M. H. Cobb (2005). "WNK1 activates SGK1 by a phosphatidylinositol 3-kinase-dependent and non-catalytic mechanism." J Biol Chem **280**(40): 34218-34223.

Yang, L. M., R. Rinke and C. Korbmacher (2006). "Stimulation of the epithelial sodium channel (ENaC) by cAMP involves putative ERK phosphorylation sites in the C termini of the channel's β- and γ-subunit." J Biol Chem **281**(15): 9859-9868.

Yue, G., B. Malik, G. Yue and D. C. Eaton (2002). "Phosphatidylinositol 4,5-bisphosphate (PIP2) stimulates epithelial sodium channel activity in A6 cells." J Biol Chem **277**(14): 11965-11969.

Zhou, R., S. V. Patel and P. M. Snyder (2007). "Nedd4-2 catalyzes ubiquitination and degradation of cell surface ENaC." J Biol Chem **282**(28): 20207-20212.

**Declaration**

I declare that I have completed this dissertation single-handedly without the unauthorized help of a second party and only with the assistance acknowledged therein. I have appropriately acknowledged and referenced all text passages that are derived literally from or are based on the content of published or unpublished work of others, and all information that relates to verbal communications. I have abided by the principles of good scientific conduct laid down in the charter of the Justus Liebig University of Giessen in carrying out the investigations described in the dissertation.

Paulina Gwozdzinska

**Acknowledgements**

I am really thankful to everybody who has supported me through my PhD study and made it an unforgettable experience. First and foremost, I would like to express my gratitude to my supervisors, Prof. Dr. Werner Seeger and Dr. István Vadász for providing fantastic guidance and invaluable advices. Especially to István, for everything he has done for me to complete my PhD. I am also grateful to Prof. Dr. Martin Diener for co-supervision of my PhD studies.

Moreover, I would like to say a huge thank to all of Vadász lab members, especially to Miri, Vitalii and Andres. My thanks must go to Dr. Benno Buchbinder who got me started in the project, sharing with me his knowledge. An extra thank you needs to go as well to Dr. Johanna Salomon from University of Heidelberg, Translational Lung Research Center for sharing with me experience about the electrophysiology. I would like to thank MBML committee: Dr. Rory Morty, Dr. Florian Veit, Dr. Elie El Agha and Dr. Anita Golec for spending their time teaching and inspiring me to be a good scientist. Thank you for your dedication. I am extremely grateful to all my friends in the ECCPS and BFS, especially to Mira, Irina, Ivonne and Elsa for friendship, constant support and for being amazing company throughout the past four years.

Finally, I would like to thank my parents, Ela and Pawel and my husband, Konrad for their support and encouragement. Even if I try, my words are not enough to express my gratefulness for their patience and believe. This thesis is dedicated to my grandmother, Longina, who was one of the most important people in my life.

## Curriculum Vitae

The curriculum vitae was removed from the electronic version of the paper.